PARALLEL SESSION ON MULTI-PARTICLE PRODUCTION AND INCLUSIVE REACTIONS

NEW RESULTS FROM FERMILAB ON HADRON PRODUCTION IN INCLUSIVE HADRON-HADRON INTERACTIONS

E.W.Beier
University of Pensylvania, U.S.A.

In this report I will discuss recent results from FNAL from three experiments on single particle inclusive hadron-hadron interactions. All the experiments measure the cross sections for the reactions

$$a + p \rightarrow c + X \ ,$$

where a and c are charged hadrons $(\pi^{\pm}, K^{\pm}, p^{\pm})$ and X represents undetected particles.

A Fermilab-Northeastern-Northern-Illinois collaboration[1] has studied the processes

$$pp \rightarrow \left\{ \begin{matrix} \pi^{\pm} \\ K^{\pm} \end{matrix} \right\} + X$$

at incident momenta of 200 and 400 GeV/c. The spectrometer utilizes two half quadrupoles and multiwire proportional chambers to measure the momentum and angle of the secondary particle, and scintillation and Cherenkov counters to measure the secondary particle type. The kinematic region covered by the spectrometer is

$$-1.0 \leq X_{\parallel} \leq 0$$

$$0.3 \leq P_{\perp} \leq 1.0 \ \text{GeV/c} \ .$$

The objective of the experiment is to measure the single particle invariant cross section, $E \frac{d^3\sigma}{d^3p}$ at fixed S and especially at large X, and to study the S dependence at large X.

The cross sections for π^+ and π^- production by 200 and 400 GeV/c protons is shown in Fig.1a as a function of the radial scaling variable $X_R = (X_{\parallel}^2 + X_{\perp}^2)$ at fixed $P_{\perp}$ =0.5 GeV/c. The absolute normalization of this preliminary result is not yet available, but the relative normalization is correct to ±10 per cent. In fig.1b the ratio of these cross sections at 200 and 400 GeV/c is displayed. Although the cross sections vary by almost four decades over the range of X_R, it is seen that scaling holds to about ±10 per cent up to $X_R \simeq$ ≃ 0.9.The authors report further that for $K^{\pm}$ production scaling is valid to within ± 20 per cent to $X_R \simeq 0.8$.

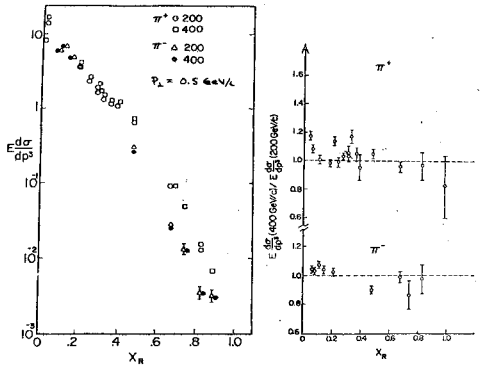

Fig.1a,b

The University of Pennsylvania group[2] with which I am associated has measured the cross sections for the reactions

$$\left\{ \begin{matrix} \pi^{\pm} \\ K^{\pm} \\ p^{\pm} \end{matrix} \right\} + p \rightarrow \left\{ \begin{matrix} \pi^{\pm} \\ K^{\pm} \\ p^{\pm} \end{matrix} \right\} + X$$

as a function of S over a fixed region of phase space in the fragmentation region of the target proton. The spectrometer consists of a small dipole magnet and multiwire proportional chambers to measure the momentum and angle of the secondary particle and scintillation and Cherenkov counters to measure the particle type. The spectrometer measures particles in fixed angle and momentum intervals in the laboratory corresponding approximately to $P_{\perp} \simeq$ 0.3 GeV/c and $y_{LAB} \simeq$ 0.6, 0.4 and 0.2 for produced π, K and p respectively. Incident momenta of 4.6, 8,10, 12, 15, 20 and 24 GeV/c were measured at Brookhaven and incident momenta of 150 and 250 GeV/c were measured at Fermilab.

The objective of the experiment is to fit the measured cross sections to the form $A + B s^{1/2}$ or $A + B s^{-1/2} + C s^{-1}$ as suggested by Mueller-Regge theory, and then to extrapolate to $s^{-1/2}=0$ to test the factorization of the Pomeron trajectory. Pomeron factorization requires that for incident particle types a and a':

$$\frac{E \frac{d^3\sigma}{d^3p}(ab \rightarrow c)}{E \frac{d^3\sigma}{d^3p}(a'b \rightarrow c)} \overset{s \rightarrow \infty}{=} \frac{\sigma_{tot}(ab)}{\sigma_{tot}(a'b)} \ .$$

The measured cross sections, integrated over the acceptance of the spectrometer, are shown for π^-, π^+, K^+ and p production in Fig.2.

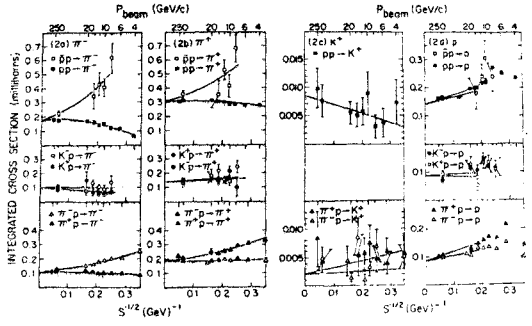

Fig. 2

The ratios of the intercepts at $S^{-1/2}=0$ are given in Table 1 where the quantity $\Delta\sigma$ is the invariant cross section integrated over the spectrometer acceptance. We conclude from Table 1 that Pomeron factorization holds quite well.

Table 1

	Particle type $C=\pi^-$	$C=\pi^+$	$C=p$	$\frac{\sigma_{tot}(aC)}{\sigma_{tot}(a'C)}$ Diffractive part
$\frac{\Delta\sigma(\bar{p}p\to C)}{\Delta\sigma(pp\to C)}$	0.63±0.03	0.62±0.03	0.62±0.03	0.61±0.03
$\frac{\Delta\sigma(Kp\to C)}{\Delta\sigma(pp\to C)}$	0.60±0.06	0.45±0.04	0.61±0.08	0.53±0.02

The Fermilab single Arm Spectrometer[3] Group has measured inelastic diffractive scattering in conjunction with their measurements of elastic scattering. The reaction studied is $a+p\to a+X$, where $a=\pi^\pm, K^\pm$ and $p^\pm$. The high resolution spectrometer covered the kinematic range

$$0.7 \le x_{\parallel} \le 1.0$$

$$0.05 \le |t| \le 0.7$$

and the incident momenta ranged from 50 to 175 GeV/c.

This experiment has tested scaling by comparing the invariant cross sections for $pp\to pX$ at 70 and 175 GeV/c as a function of $x_{\parallel}$ at $|t|=0.3$. Over the range $0.75 \le x_{\parallel} \le 0.97$ they find that scaling holds at a level of sensitivity of 10 per cent.

At high energy and x near unity, Regge theory suggests that the process $a+p\to a+X$ is dominated by Pomeron exchange, leading to the relation

$$M_x^2 \frac{d^2\sigma}{dt\,dM_x^2} = \frac{1}{16\pi s_0^2}\left|\beta_{aa\mathbb{P}}(t)\right|^2 \sigma_{tot}^{\mathbb{P}p}(M_x^2,t)$$

where M_x is the mass of the system X, $s_0=1$ GeV^2 is the Regge scale factor, $\beta_{aa\mathbb{P}}$ is the coupling between the incident hadron a and the exchanged Pomeron, and $\sigma_{tot}^{\mathbb{P}p}(M_x^2,t)$ is the Pomeron-proton total cross section. At large M_x^2 $\sigma_{tot}^{\mathbb{P}p}$ should become independent of M_x^2, and the expression above should thus be independent of M_x^2. Figure 3a shows the quantity $M_x^2 \frac{d^2\sigma}{dt\,dM_x^2}$ plotted as a function of M_x^2 for $\bar{p}p$ and pp scattering at different average values of t and with data at 140 and 175 GeV/c combined. One observes resonance production at $M_x^2 \sim 1600$ MeV/c and no dependence on M_x^2 between 4 and 9 (GeV/c^2)^2.

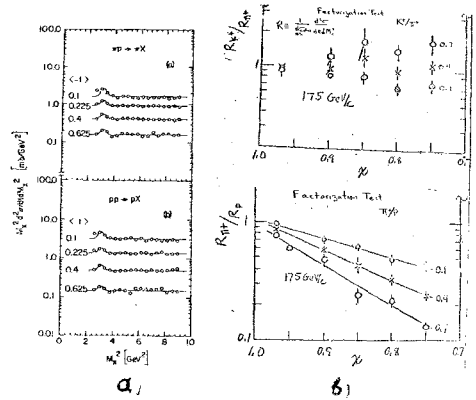

a) b)

Fig. 3

Using the same phenomenology, the elastic differential cross section $a+p\to a+p$ can be written

$$\left.\frac{d\sigma}{dt}\right|_{elast} = \frac{1}{16\pi s_0^4}\left|\beta_{aa\mathbb{P}}(t)\right|^2\left|\beta_{pp\mathbb{P}}(t)\right|^2.$$

The implied factorization of the Regge residues requires that

$$R = \frac{M_x^2 \frac{d^2\sigma}{dt\,dM_x^2}}{\left.\frac{d\sigma}{dt}\right|_{elast}} = \frac{\sigma_{tot}^{\mathbb{P}p}(M_x^2,t)}{\sqrt{16\pi\left(\frac{d\sigma}{dt}\right)_{pp\to pp}}}$$

be independent of incident particle type a. In Fig.3b R_{K^+}/R_{π^+} and R_{π^+}/R_p are plotted as a function of X for $-t$ =0.1; 0.4 and 0.7. One observes that as $X \to 1$, factorization holds for all particle types and values of t, but for X significantly different from 1 the ratio depends significantly on particle type and t. For the mass range $4 \leq M_X^2 \leq 9$ $(GeV/c^2)^2$, or $0.975 \leq X \leq 0.995$, the triple Regge formalism adequately describes the high energy data, and the "Pomeron-proton" total cross section

$$\sigma_{tot}^{Pp}(t) = 2.9 \exp(-1.04t + 0.35t^2)\ mb$$

is obtained. Defining the triple Pomeron coupling constant at $t=0$, by

$$\tau_0 = \sqrt{\sigma_{tot}^{PP}} \cdot \frac{M_X^2 \frac{d^2\sigma}{dt dM_X^2}}{\frac{d\sigma}{dt}\Big|_{elast.}}$$

the values of τ_0 for all six particle types are in statistical agreement. The average value of τ_0 obtained from the $\pi^{\pm}$ and p data is $\langle\tau_0\rangle = 0.80 \pm 0.03\ GeV^{-1}$.

References

1. R.Kammerud et al. 285/A2-53.
2. E.W.Beier et al. 402/A2-58.
3. Fermilab Single Arm. Spectrometer Group "Inelastic Diffractive Scattering at Fermilab. Energies" to be published.

МНОЖЕСТВЕННОЕ РОЖДЕНИЕ ЧАСТИЦ В $\bar{P}P$ -ВЗАИМОДЕЙСТВИЯХ

И.М.Граменицкий

ОИЯИ, Дубна

Одной из важных характеристик неупругих взаимодействий являются топологические сечения и параметры, характеризующие множественность. Топологические сечения для $\bar{p}p$-взаимодействий известны вплоть до импульса 100 ГэВ/с. Зависимость средней множественности $\langle n_{ch}\rangle$ от энергии при $P_{лаб} \geq 5$ ГэВ/с хорошо описывается соотношением вида $\langle n_{ch}\rangle = (0{,}69 \pm 0{,}19) + (1{,}05 \pm 0{,}05) \ln s$ /I/. Меньше информации о поведении $\langle n_{ch}\rangle$ имеется для $\bar{p}n$ -взаимодействий, однако, существующие данные свидетельствуют о том, что $\langle n_{ch}\rangle_{\bar{p}n} < \langle n_{ch}\rangle_{\bar{p}p}$ (рис.I)/2/.

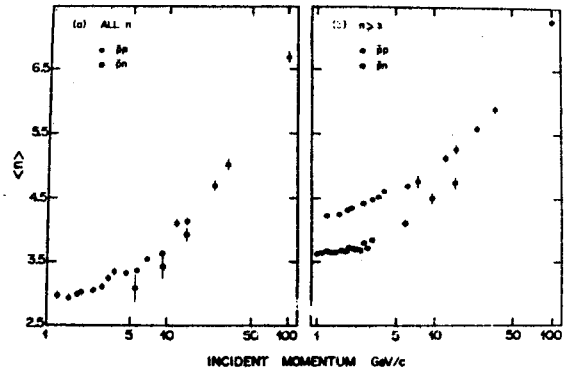

Рис.I

Исследование корреляционных явлений может дать информацию о механизме взаимодействия. Анализ корреляций по множественности заряженных частиц, вылетающих в переднюю и заднюю полусферы, дает оценку сечения дифракционной диссоциации. Распределение по множественности "вперед-назад"/3,4/ определяется как $P(n_f, n_b) = \sigma(n_f, n_b)/\sigma_{in}$, где n_f и n_b - число частиц в передней и задней полусферах, соответственно. Разделив это дискретное распределение на четную (n_f, n_b - четные) и нечетную (n_f, n_b -нечетные) части, можно приближенно оценить нижний предел сечения дифракционной диссоциации $\sigma_d/\sigma_{in} = P_{odd} - P_{even}$.

Для $\bar{p}p$ -взаимодействий при 22,4 ГэВ/с[5] при дополнительных предположениях, вытекающих из простой двухкомпонентной модели, получено $\sigma_{ann}/\sigma_{in} = 0,11\pm0,03$, что согласуется с ранее полученными данными по анализу спектра недостающих масс[6]. Зависимость среднего заряда $\langle Q \rangle = (n_+ - n_-)/n_{tot}$ для передней и задней полусферы как функция p_T для двух интервалов быстрот при 22,4 ГэВ/с[7] представлена на рис.2. Можно

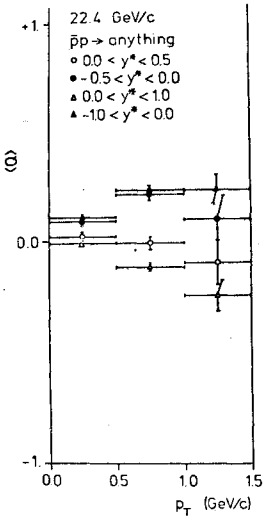

Рис.2

видеть, что наблюдается увеличение (уменьшение) с p_T среднего заряда в задней (передней) полусферах. Аналогичный эффект наблюдается также для pp- и π^-p -взаимодействий, причем увеличение зарядовой асимметрии с ростом p_T в $\bar{p}p$- больше, чем в pp- и меньше, чем в π^-p -взаимодействиях.

Изучение двухчастичных корреляций при 22,4 ГэВ/с[8] проводилось с помощью корреляционной функции $C(y_1, y_2)$, представленной в виде разложения по полуинклюзивным процессам

$$C^{ij}(y_1,y_2) = \sum \omega_N C^{ij}_N(y_1,y_2) + \sum \omega_N (\rho^i_N(y_1) - \rho^j_N(y_1)) \times (\rho^i_N(y_2) - \rho^j_N(y_2)), \quad (I)$$

где $C^{ij}_N(y_1,y_2)$ - корреляционная функция для событий с данной множественностью N :

$$C^{ij}_N(y_1,y_2) = \rho^{ij}_N(y_1,y_2) - \frac{n^i - \delta_{ij}}{n} \rho^i_N(y_1)\rho^j_N(y_2) \quad (2)$$

и $\omega_N = \sigma_N/\Sigma\sigma_N$, $\rho_N(y) = \frac{1}{\sigma_N} d\sigma_N/dy$, n^i - число частиц сорта i .

Разложение (I) позволяет оценить верхний предел суммарных короткодействующих корреляций $C^{ij}_{SR} = \sum \omega_N C^{ij}_N(y_1,y_2)$. Корреляционная функция $C(y_1, y_2)$, изображенная на рис.3, в зависимости от $y_1 = y_2$ имеет ярко выраженный пик при $y_1 = y_2 = 0$, который, однако, связан с суперпозицией состояний с различным числом частиц. Корреляционная функция C_{SR} , показанная на том же рисунке, также имеет пик при $y_1 = y_2 = 0$, но существенно меньшей величины. Там же для сравнения приведены данные для pp при 69 ГэВ/с (кресты) и K^-p при 32 ГэВ/с (точки). Возможно, что наблюдаемый в C_{SR} эффект связан с кинематическими корреляциями.

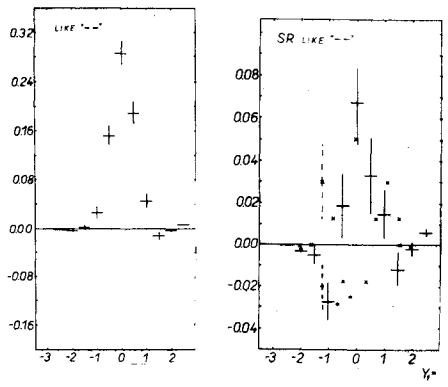

Рис.3

Азимутальные корреляции исследовались для реакций $\bar{p}p \to 2\pi^+2\pi^-$, $2\pi^+2\pi^-\pi^0$ и $2\pi^+2\pi^-(m\pi^0)$ при 5,7 ГэВ/с[9]. В распределениях по азимутальному углу $\varphi = \arccos[(p_{x1}p_{x2})/|p_1||p_2|]$ пар пионов одинакового и разного знака наблюдается заметное различие, особенно при уменьшении разности продольных и поперечных импульсов (рис.4). Аналогичный эффект, значительно ярче выраженный, наблюдается также при 22,4 ГэВ/с в инклюзивных реакциях[10]. Коэффициент асимметрии для тождественных и нетождественных пар равен $B_L = 0,002\pm0,02$ и $B_{uL} = 0,140\pm0,01$, соответственно. Наблюдаемый эффект может быть связан с влиянием интерференции в парах тождественных частиц.

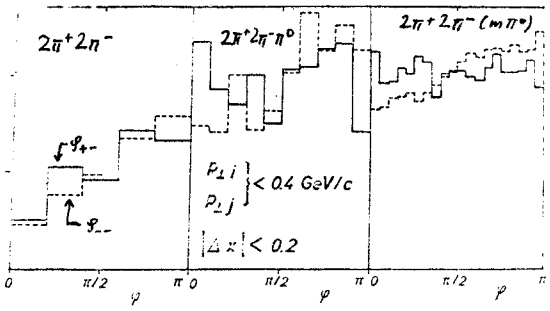

Рис.4

Выделение эксклюзивных каналов, в том числе аннигиляционных, легко осуществляемое при сравнительно небольших энергиях, становится крайне затруднительным при импульсах $p \gtrsim 10$ ГэВ/с. В работе[11] приведены данные по оценке сечений различных каналов в $\bar{p}p$-взаимодействиях при 9,1 ГэВ/с. Особое внимание в работе уделено разделению неоднозначных событий и выделению аннигиляционного канала. Последнее особенно трудно в связи с большим количеством нейтральных частиц, возникающих при аннигиляции. Для определения доли событий с разным числом нейтральных частиц применялся метод подгонки распределений по квадрату недостающей массы.

В результате анализа были определены сечения различных каналов реакций. Полное сечение аннигиляции в пионы оказалось равным $13{,}2\pm0{,}5$ мбн при $\sigma_{tot} = 57{,}5\pm73$ мбн. Были определены также сечения рождения резонансов ρ^0, ω^0 и изобары Δ^{++} $(\bar{\Delta}^{++})$. Инклюзивные сечения рождения ρ^0 и Δ^{++} приведены в табл.I.

Таблица I

Конечное состояние	$\rho^0+\ldots$	ρ^0 + пионы	$\Delta^{++}+\ldots$
Сечение (мбн)	$7{,}0\pm1{,}0$	$6{,}5\pm1{,}5$	$5{,}35\pm0{,}14$

Можно видеть, что относительный вклад ρ-мезонов в аннигиляционном канале очень велик.

Сечение процесса $\bar{p}p\to\Delta^{++}\bar{\Delta}^{++}$ равно $0{,}9\pm0{,}1$ мбн, т.е. составляет 35% от сечения реакции $\bar{p}p\to\bar{p}p\pi^+\pi^-$. Следует отметить, что эта доля падает с энергией и при 32 ГэВ/с составляет $\sim 15\%$[12].

Определение сечения рождения K^0-, Λ -$\bar{\Lambda}$ и π^0-мезонов исследовалось при импульсах 4,6, 9,1, 12, 22,4 и 32 ГэВ/с[13-15].

Инклюзивные сечения рождения этих частиц приведены в табл.2.

Таблица 2

P (ГэВ/с)	4,6	9,1	12	22,4	32
$K^0+\bar{K}^0$	$3{,}8\pm0{,}18$	$4{,}4\pm0{,}26$	$4{,}08\pm0{,}12$	$4{,}48\pm0{,}4$	$6{,}1\pm0{,}6$
Λ	$0{,}61\pm0{,}05$	$0{,}31\pm0{,}1$	$0{,}17\pm0{,}08$	$1{,}23\pm0{,}18$	$1{,}6\pm0{,}2$
$\bar{\Lambda}$			$1{,}03\pm0{,}06$	$0{,}92\pm0{,}15$	$1{,}4\pm0{,}2$
π^0	73 ± 3	78 ± 4		59 ± 4	68 ± 5

Были построены инвариантные сечения для инклюзивных процессов с рождением V^0-частиц. Инвариантная функция $F(x)$ для реакции $\bar{p}p\to\Lambda+X$ при разных энергиях приведена на рис.5. Ошибки

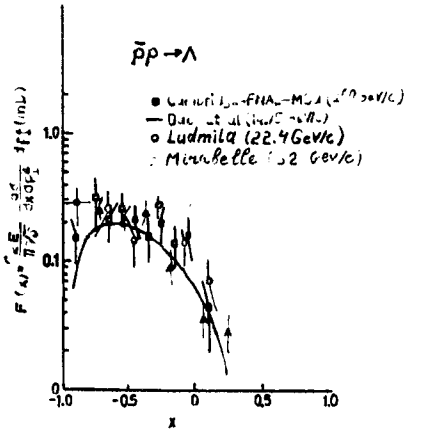

Рис.5

в полученных данных слишком велики, чтобы сделать определенные выводы об энергетической зависимости $F(x)$.

Литература

1. L.N.Abesalashvili et al. Phys.Lett.,52B,236 (1974).
2. H.Braun et al. Submitted paper to the Conference. 376/2A-95.
3. D.R.Suider. ANL/IHEP 7326 (1973).
4. H.Grassler et al. Nucl.Phys., B90 461 (1975).
5. E.G.Boos et al. Submitted paper to the Conference. 201/2A - 25.

6. E.G.Boos et al. Preprint JINR, E1-9781,Dubna, 1976.
7. E.G.Boos et al. Submitted paper to the Conference 903/A4 - 8.
8. E.G.Boos et al. Submitted paper to the Conference 161/A2 - 9 .
9. H.W.Atherton et al. Submitted paper to the Conference 400/2A - 60.
10. E.G.Boos et al. Submitted paper to the Conference 686/2A - 64.
11. P.S.Gregory et al. Submitted paper to the Conference 683/2A - 102.
12. M.A.Jabiol et al. Submitted paper to the Conference 1036/A1 - 9 .
13. M.T.Kegan et al. Submitted paper to the Conference 682/2A - 63.
14. O.Bertrand et al. Submitted paper to the Conference 722/2A - 67.
15. J.Manton et al. Submitted paper to the Conference 1035/2A - 90.

ИНКЛЮЗИВНОЕ ОБРАЗОВАНИЕ РЕЗОНАНСОВ И ДВУХЧАСТИЧНЫЕ КОРРЕЛЯЦИИ В $\pi^- N$-ВЗАИМОДЕЙСТВИЯХ ПРИ p = 40 ГЭВ/С

В.Г.Гришин
Объединенный институт ядерных исследований, Дубна

В настоящем докладе представлена часть результатов по исследованию инклюзивного рождения резонансов и двухчастичных корреляций вторичных частиц в $\pi^- p$-взаимодействиях при p = 40 ГэВ/с, полученные большой группой физиков ОИЯИ и институтов стран-участниц ОИЯИ[I-4]. Основное внимание в докладе будет уделено вопросу определения вероятности образования ρ^0-мезонов и изменению наших представлений о двухчастичных азимутальных корреляциях вторичных пионов с учетом рождения резонансов. Экспериментальный материал, около 11000 неупругих $\pi^- p$-взаимодействий, был получен с помощью двухметровой пропановой пузырьковой камеры, облученной на серпуховском ускорителе.

I. Сечение рождения ρ^0-мезонов в $\pi^- p$-взаимодействиях, определенное общепринятым методом по спектру эффективных масс $(\pi^+\pi^-)$-мезонов

Основным источником информации о рождении ρ^0-мезонов является спектр эффективных масс пар $\pi^+\pi^-$-мезонов. На рис. I приведено инклю-

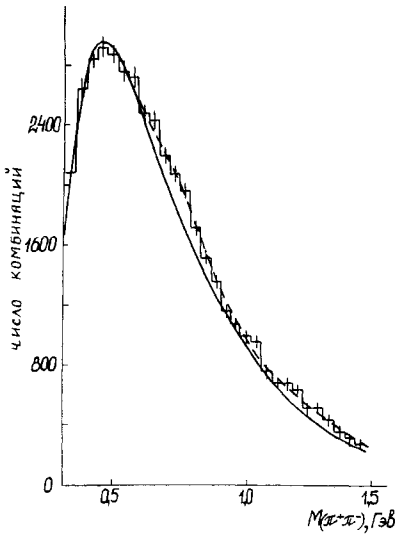

Рис. I

зивное распределение $M(\pi^+\pi^-)$ для π^-p-взаимодействий при p = 40 ГэВ/с. Сплошная линия - фоновая кривая и пунктирная - аппроксимирующая функция:

$$F(M) = (1-\alpha_\rho-\beta_f)\,\Phi(M) + \alpha_\rho\,Б.В._\rho(M) + \beta_f\,Б.В._f(M),$$

где α_ρ и β_f - относительные вклады резонансов $\rho^0\to\pi^+\pi^-$ и $f\to\pi^+\pi^-$, $\Phi(M)$ - фоновое распределение, нормированное на единицу. Функции Брейта-Вигнера (Б.В.) брались при M_0 = 770 МэВ, Γ_0 = 150 МэВ, ℓ = 1 для ρ^0-мезона и 1270 МэВ, 170 МэВ, ℓ = 2 для f-мезона. Мы также учитывали искажение функций Б.В. из-за экспериментальных погрешностей в измерении $M(\pi^+\pi^-)$. Правильность учета этих погрешностей была проверена по распределению $M(K_1^0)$, которое было определено по распадным $\pi^\pm$-мезонам в этом же эксперименте/1/.

Фоновая кривая $\Phi(M)$ бралась в виде

$$\Phi(M) = K(M_1)^\alpha \exp(-bM_1 + cM_1^2),$$

где $M_1 = M(\pi^+\pi^-) - 2m_\pi$, K - нормировочный коэффициент и a, b, c - подбираемые параметры.

В результате такого анализа было получено, что

$$\sigma(\rho^0) = (5{,}8\pm1{,}4)\ \text{мбн}.$$

В этом случае доля π^+-мезонов, образованных при распаде $\rho^0\to\pi^+\pi^-$ от всех π^+-мезонов, составляет $\approx(15\pm4)\%$ и практически не меняется в интервале 16-200 ГэВ для π^-p-взаимодействий.

Однако следует отметить, что при $E\gtrsim20$ ГэВ "сигнал" от ρ^0-мезона в спектрах $M(\pi^+\pi^-)$ составляет всего лишь (10÷20)%. Поэтому от выбора фоновой кривой, особенно в области резонанса, существенно зависит величина сечения – $\sigma(\rho^0)$. В связи с этим мы исследовали влияние учета отражения распада $\omega\to\pi^+\pi^-\pi^0$ на определение величины $\sigma(\rho^0)$.

2. Учет влияния образования ω-мезонов на спектр $M(\pi^+\pi^-)$ и определение сечений рождения ρ^0 и ω-мезонов

В случае образования ω-мезонов продукты их распадов $\omega\to\pi^+\pi^-\pi^0$ дают вклад в спектр $M(\pi^+\pi^-)$ в интервале масс от $2m_\pi$ до $(m_\omega - m_{\pi^0})$, т.е. вблизи ρ^0-резонанса. Учет распадных пар $(\pi^+\pi^-)$ от ω-мезонов приводит к следующему виду аппроксимирующей функции:

$$F(M) = (1-\alpha_\rho-\beta_f-\gamma_\omega)\,\Phi(M) + \alpha_\rho\,Б.В._\rho(M) + \beta_f\,Б.В._f(M) + \gamma_\omega\,L_\omega(M),$$

где $L_\omega(M)$ была вычислена с учетом матричного элемента распада $\omega\to3\pi$. В результате аппроксимации экспериментального спектра $M(\pi^+\pi^-)$ функцией $F(M)$ было получено: $\sigma(\rho^0)$ = 13,3±1,4 мбн, $\sigma(\omega)$ = 10,0±1,1 мбн и $\sigma(f)$ = 1,3±0,8 мбн при $\overline{\chi^2}$ = 1,37. В этом случае доля π^+-мезонов, образованных в результате распадов $\rho^0\to\pi^+\pi^-$ и $\omega\to\pi^+\pi^-\pi^0$ от всех вторичных π^+, составляет $\Delta\approx(50\pm5)\%$! Если предположить, что $\sigma(\rho^+) = \sigma(\rho^0)$, и учесть образование Δ^{++}-изобары ($\sigma\approx1$ мбн) и f-мезонов, то $\Delta\approx70\%$!

Таким образом, проведенное исследование показывает, что заметное рождение ω^0-мезонов может существенно изменить полученные ранее данные по $\sigma(\rho^0)$. В связи с этим мы попытались оценить $\sigma(\omega)$ по спектрам эффективных масс $(\pi^+\pi^-\pi^0)$-систем, где π^0-мезоны восстанавливались по эффективной массе двух гамма-квантов, зарегистрированных в пропановой пузырьковой камере. Однако статистика невелика ($\approx$ 700 π^0-мезонов), и поэтому отсюда можно сделать лишь качественное заключение, что $\sigma(\omega)$ = (4÷10) мбн.

Таким образом, традиционный метод определения сечений образования резонансов при $E\gtrsim20$ ГэВ из-за большого числа "ложных" комбинаций становится неэффективным. Он, по-видимому, дает только нижнюю границу $\sigma(\rho^0)$.

3. Азимутальные корреляции

Изучение двухчастичных азимутальных корреляций в π^-p-взаимодействиях при p = 40 ГэВ/с показало, что коэффициент асимметрии

$$B = [N(\varphi\gtrsim\pi/2) - N(\varphi<\pi/2)]/N_{tot}$$

может быть тем параметром, который позволит определять сечения рождения резонансов в инклюзивных процессах при высоких энергиях. ($N(\varphi\gtrsim\frac{\pi}{2})$ - число пар пионов с углом $\varphi\gtrsim\pi/2$). На рис. 2

приведены зависимости B от $M(\pi\pi)$ при различных ограничениях на разность быстрот и модулей поперечных импульсов пионов. Из рисунка видно,

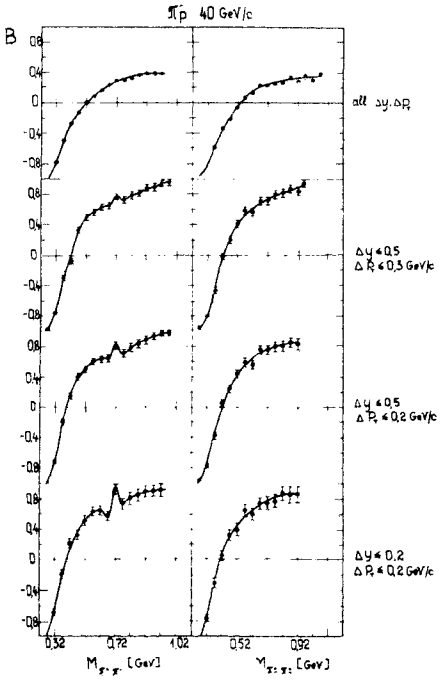

Рис. 2

что при $\Delta y \leq 0{,}2$ и $\Delta p_\perp \leq 0{,}2$ ГэВ/с для $\pi^+\pi^-$-пар имеется четкий сигнал, связанный с ρ^0-мезоном. В то же время, в распределениях по $M(\pi^\pm\pi^\pm)$ при тех же ограничениях он отсутствует. Таким образом, параметр $B(M(\pi\pi))$ является более чувствительным индикатором резонансов, чем традиционное распределение по $M(\pi\pi)$.

В последние годы было обнаружено различие в поведении $dN/d\varphi$ для тождественных и разных пар пионов. Оно часто связывается с эффектом тождественности. Однако учет рождения резонансов может существенно уменьшить это различие. На рис. 3 приведены отношения вероятностей образования $(\pi^\pm\pi^\pm)$-пар к $(\pi^+\pi^-)$-парам. На рис. 4 построены те же распределения, но при этом были исключены пары $(\pi^+\pi^-)$-мезонов с $M = M(\rho^0) \pm 80$ МэВ. Как видно, различие в поведении $dN/d\varphi$ практически исчезло.

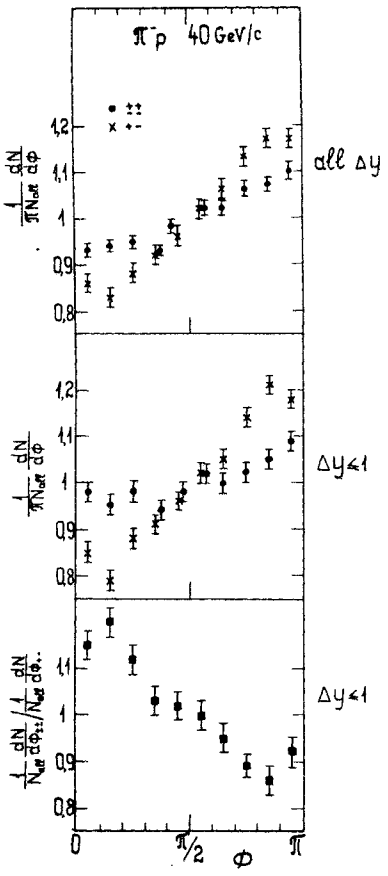

Рис. 3

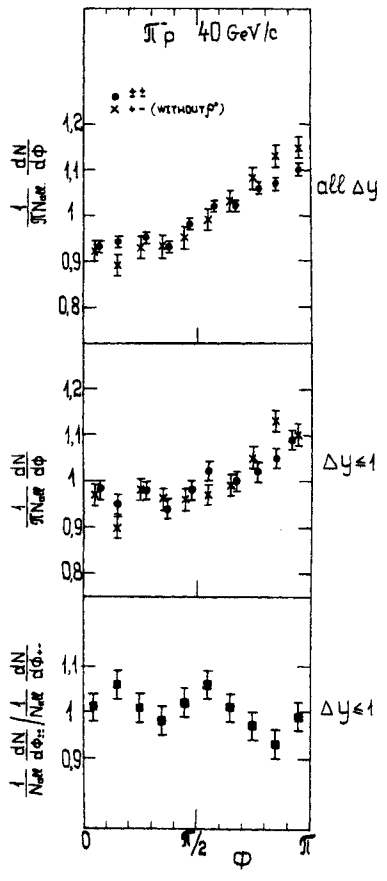

Рис. 4

Литература

1. Н.Ангелов, К.П.Вишневская, В.Г.Гришин и др. Препринт ОИЯИ, I-9536, Дубна, 1976.
2. Н.Ангелов, К.П.Вишневская, В.Г.Гришин и др. "Исследование рождения резонансов в π^-p - взаимодействиях при 40 ГэВ/с". Доклад, представленный на XVШ Международную конференцию по физике высоких энергий (Тбилиси, I5-2I июля, 1976).
3. Н.Ангелов, К.П.Вишневская, В.Г.Гришин и др. "Исследование эффектов тождественности и влияния рождения ρ^o-мезонов на корреляции частиц в π^-p -взаимодействиях при p =40 ГэВ/с". Доклад, представленный на XVШ Международную конференцию по физике высоких энергий (Тбилиси, I5-2I июля, 1976).
4. Н.Ангелов, К.П.Вишневская, В.Г.Гришин и др. "Изучение двухчастичных корреляций гамма-квантов и заряженных частиц в π^-p-взаимодействиях при p = 40 ГэВ/с". Доклад, представленный на XVШ Международную конференцию по физике высоких энергий (Тбилиси, I5-2I июля, 1976).

INCLUSIVE PARTICLE AND RESONANCE PRODUCTION

Aachen-Berlin-Bonn-CERN-Cracow-London-Vienna-Warsaw Collaboration

P.Schmid

CERN, Geneva, Switzerland

This talk summarises work on inclusive resonance production done by the Aachen-Berlin-Bonn-CERN-Cracow-London-Vienna-Warsaw Collaboration during the past year [1]. It is based on about 1.1 million events coming from the following bubble chamber experiments: π^+p at 8, 16 and 23 GeV/c, π^-p at 16 GeV/c and K^-p at 10 and 16 GeV/c. The resonances ρ^o, f, η, ω, K^*_{890}, K^*_{1420}, Δ^{++} and $\Sigma^{\pm}_{1385}$ are studied. Results are presented on

- separation of fragmentation and central production of secondary particles;
- universality of transverse momentum spectra;
- direct particle production and contributions from resonance decays.

The energy dependence of total production cross sections of resonances is discussed separately by P. Chliapnikov at this Conference.

SEPARATION OF FRAGMENTATION AND CENTRAL PRODUCTION OF SECONDARY PARTICLES

Longitudinal momentum spectra of ρ^o production in π^+p and π^-p interactions at 16 GeV/c are very similar. They differ, however, from the corresponding spectra in pp interactions at 24 GeV/c as seen in fig. 1.

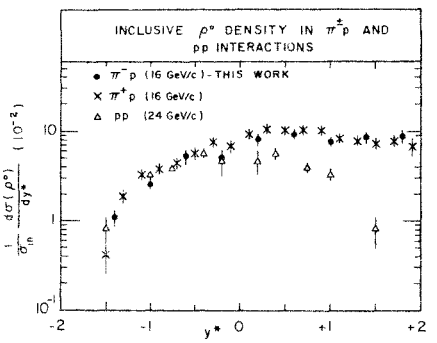

Fig.I- Comparison of the c.m. rapidity distribution of ρ^o in I6 GeV/c π^-p interactions with the same in I6 GeV/c π^+p (Ib) and 24 GeV/c pp interactions (6).

Whereas the spectra coincide for $y < 0$, ρ production is much stronger in the forward direction for πp than it is for pp interactions. The difference can be interpreted as being due to different beam fragmentation. A quantitative estimate of beam fragmentation and central components can be obtained by comparing invariant cross sections for ρ^o production in π^+p with K^*_{890} production in K^-p interactions at 16 GeV/c (fig. 2). As K^*_{890} is mainly produced by kaon fragmentation, the difference of the two spectra may be considered as an estimate of the central component of ρ production. Using the cross sections

$$\sigma_{\rho^o}(\pi^+p) = 4.7 \pm 0.4 \text{ mb}$$

$$\sigma_{K^{*o}}(K^-p) = 3.3 \pm 0.4 \text{ mb}$$

at 16 GeV/c the following estimates have been obtained [1]:

$$\sigma^F_{K^{*o}} = \sigma^{\infty}_{\rho^o} = 3.1 \pm 0.4 \text{ mb}$$

$$\sigma^C_{\rho^o} = 1.6 \pm 0.5 \text{ mb}$$

$$\sigma^C_{K^{*o}} = 0.2 \text{ mb}$$

where F and C stand for fragmentation and central production, respectively. These estimates are consistent with the interpretation of fig. 2 as given above.

Similarly spectra for the production of Σ^+_{1385} and Σ^-_{1385} may be compared in K^-p interactions at 16 GeV/c (fig. 3). If Σ^+ and Σ^- are produced by a "central" process, they should have the same cross section, as the total charge of the initial state is zero.

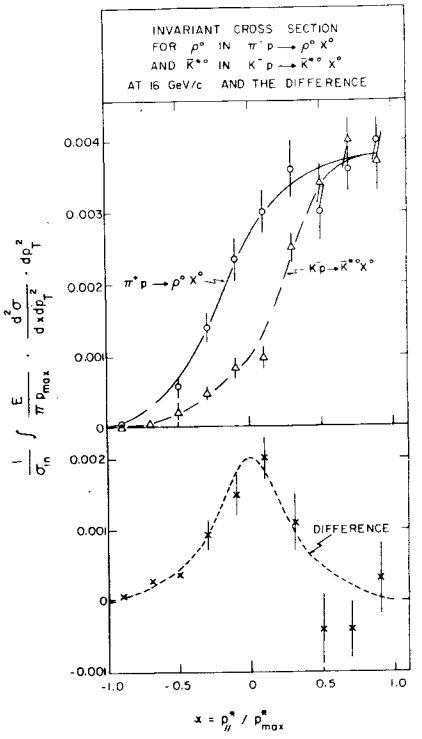

Fig.2 Comparison of the invariant x-distributions of ρ^0 in π^-p and K^{*0}_{890} in K^-p interactions at 16 GeV/c (Ib)

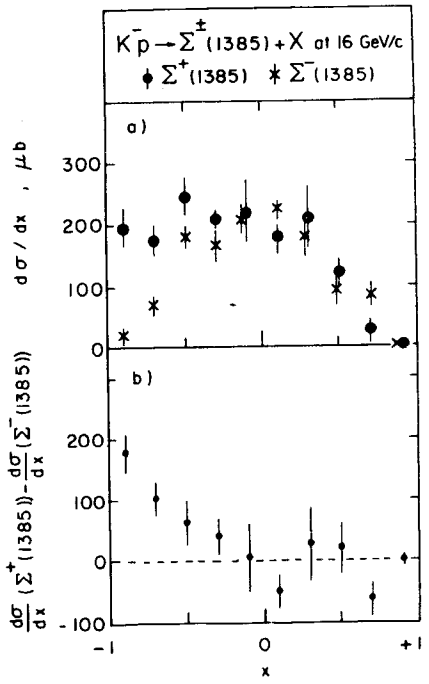

Fig.3 Comparison of $d\sigma$ / dx for $\Sigma^+(1385)$ and $\Sigma^-(1385)$ production at 16 GeV/c K^-p interaction (Ie).

In the proton fragmentation region Σ^- production should be small as it requires double charge exchange, whereas Σ^+ production is allowed. Indeed the difference of two spectra is very suggestive of a fragmentation component. With the cross sections $\sigma_{\Sigma^{*+}}(K^-p) = 0.41 \pm 0.05$ mb and $\sigma_{\Sigma^{*-}}(K^-p) = 0.27 \pm 0.04$ mb at 10 GeV/c (Ie) one arrives at fragmentation and central components of

$$\sigma^{F}_{\Sigma^*} = 0.14 \pm 0.07 \text{ mb}$$
$$\sigma^{C}_{\Sigma^*} = 0.27 \pm 0.04 \text{ mb}$$

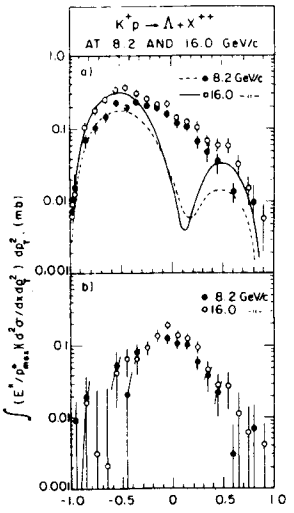

A different technique has been used by the Birmingham- Brussels-CERN- Mons Collaboration to separate fragmentation and central production of Λ's in K^+p interactions at 8 and 16 GeV/c (2). Contributions from beam and target fragmentation have been obtained by fitting triple-Regge expressions to the distributions of large |x| and by extrapolating them to small |x| (Fig.4(a)). The central component of Σ production is obtained by subtracting the sum of the two fragmentation components from the overall spectrum (Fig.4(b)).

Fig.4 a) Invariant x distribution for Λ production K^+p interactions at 8.2 GeV. The curves represent fits of triple Regge expressions to the fragmentation regions.
b) Difference between data and fragmentation components of fig.4(a) representing the central component of Λ production.

2. UNIVERSALITY OF TRANSVERSE SPECTRA

Inclusive p_T^2 distributions of produced particles have been found to depend on the mass of the particle (3). Spectra for heavy particles are approximately exponential between $p_T^2 = 0$ and 2 (GeV/c). For ligth particles like pions and kaons the spectra have a much steeper slope at small p_T^2 which gradually decreases to about the same slope as for heavy particles above p_T^2 1 (GeV/c). Apart from some structure at very small p_T^2, resonances turn out to have spectra with an exponential fall-off out to about 2(GeV/c)^2 with slopes similar to the ones of heavy particles. Some resonance spectra are shown in Fig.5(a,b,c) and compared to spectra of pions and kaons, respectively.

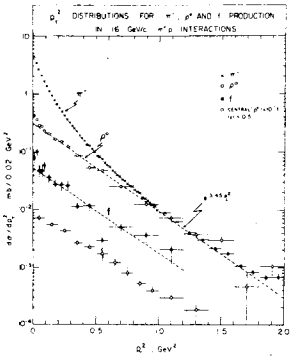

Fig.5 p_T^2 distributions for

a) π^-,ρ^0 and f production in π^+n interaction at 16 GeV/c (Ia).

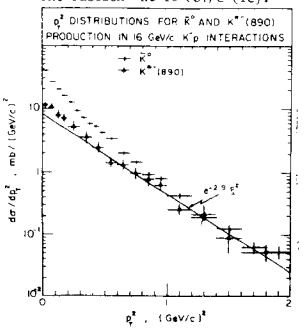

b) K^0 and K^{*-}_{890} production in K^-n interaction at 16 GeV/c (Ic).

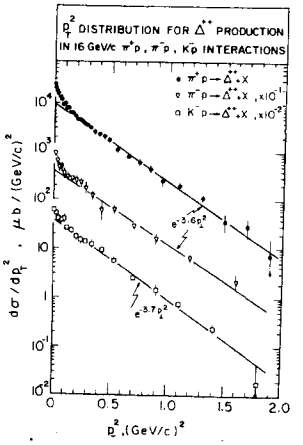

c) Δ^{++} production in π^+p, π^-p and K^-p inetraction at 16 GeV/c (Id).

A surprisingly similar slope is found for all resonances studied inclusively independent of the initial state over a large range of lab. momenta (6 - 200 GeV/c, see Table I). Moreover the same slope is found for "quasi"-inclusive $p_\perp^2$ distributions of η and ω production [1f] (fig. 6).

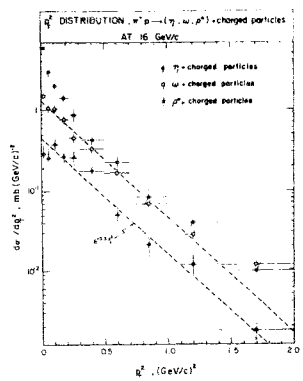

Fig. 6 $p_\perp^2$ distributions for the inclusive reactions $\pi^+ p \to (\eta, \omega, \rho^0)$ + charged particles at 16 GeV/c [1f].

TABLE I

Slopes of $p_\perp^2$ distributions for inclusive resonance production.

Resonance Produced	Initial State	Incident Momentum (GeV/c)	Slope of $d\sigma/dp_\perp^2$ $(GeV/c)^{-2}$	Reference
ρ^0	$\pi^+ p$	6	3.9 ± 0.4	[5]
		16	3.45 ± 0.1	[1a]
		22	3.0 ± 0.6	[5]
	$\pi^- p$	16	2.95 ± 0.2	[1b]
	pp	12	3.6 ± 0.4	[6]
		24	3.6 ± 0.4	[6]
		147	2.7 ± 0.5	[7]
		205	3.0 ± 1.0	[8]
f^0	$\pi^+ p$	16	3.45 ± 0.3	[1a]
ω	$\pi^+ p$	16	3.3 ± 0.15	[1f]
	pp	12	3.4 ± 0.2	[6]
		24	3.7 ± 0.3	[6]
η	$\pi^+ p$	16	3.3 ± 0.3	[1f]
K^{*-}_{890}	$K^- p$	16	2.9 ± 0.2	[1c]
$\bar{K}^{*0}_{890}$	$K^- p$	16	3.15 ± 0.2	[1c]
K^{*+}_{890}	pp	12	3.4 ± 0.4	[6]
		24	2.8 ± 0.3	[6]
Δ^{++}	$\pi^+ p$	16	3.6 ± 0.2	[1d]
	$\pi^- p$	16	3.6 ± 0.2	
	$K^- p$	16	3.7 ± 0.2	
Σ^+_{1385}	$\pi^+ p$	16	3.6 ± 0.15	[9]
	$K^- p$	4.2	3.7 ± 0.2	[10]
		10	3.4 ± 0.3	[9]
		16	3.4 ± 0.25	[9]
Σ^-_{1385}	$\pi^+ p$	16	3.8 ± 0.5	[9]
	$K^- p$	4.2	3.9 ± 0.3	[10]
		10	3.3 ± 0.4	[9]
		16	2.9 ± 0.3	[9]

This combined evidence leads to the conjecture of universality of the slope of $p_\perp^2$ spectra of directly produced particles. "Second order" effects like

- systematic differences of slopes for certain beams or produced particles

or

- a slow decrease of slopes with increasing energy cannot be established with presently available data.

Slope universality will be used in the following as a method of estimating production cross sections.

The first example concerns η and ω production in $\pi^+ p$ interactions at 16 GeV/c [1f]. With bubble chamber data these resonances can only be observed when all other particles in the final state are charged (or observed V^0s). To compare them to ρ production, ρ's should be studied in similar "quasi"-inclusive reactions, i.e. produced with charged particles only. The ratio of the production cross section in the $p_\perp^2$ range where all three resonances have exponential distributions with almost identical slopes is found to be

$$\eta : \omega : \rho = 0.3 : 0.8 : 1.$$

Based on slope universality and on the similarity of x and y distributions [1f], these ratios are assumed to be true also for the fully inclusive case and the following cross sections for η and ω production are obtained:

$$\sigma_\eta = 1.5 \pm 0.3 \text{ mb}$$

$$\sigma_\omega = 4.0 \pm 0.6 \text{ mb}$$

3. DIRECT PARTICLE PRODUCTION AND CONTRIBUTIONS FROM RESONANCE DECAYS

As cross sections for resonance production are large, many of the final particles observed are in fact decay products. With some plausible assumptions [1h] it is straightforward to calculate the contribution of the important resonances, the cross sections of which have been measured at 16 GeV/c, to the final particle yield (Table II). Almost half of the production cross section of the particles listed in Table II can be accounted for by known resonances. As possible contributions from broad or high mass resonances are difficult to measure, the numbers obtained can be used to get upper bounds for the fraction of directly produced particles.

TABLE II

Particle	% from resonance		in interaction
K^η	∿ 45%	K^*_{890}	$K^- p$
	3%	K^*_{1420}	
Λ	∿ 40%†	Σ_{1385}	$K^- p$, $\pi^+ p$
π^-	∿ 25%	$\rho^0 \rho^-$	$\pi^+ p$
	2.5%	f	
	15%	ω	
	2%	η	
	∿ 45%		

† This percentage holds for true Λs, i.e. after subtracting Σ^0s from the observed Λ yield.

An experimental technique has been developed to establish differential spectra of decay products which can then be subtracted from the overall particle spectra. Such an analysis has been done for negative pions produced in $\pi^+ p$ interactions and for neutral kaons in $K^- p$ interactions both at 16 GeV/c [1g]. As expected from pure kinematics, fig. 7(a) shows that decay pions are

the more peaked at small $p_\perp^2$ the smaller the Q-value of the resonance and the heavier the mass recoiling against the pion. Summing up the contributions of all meson resonances studied (fig. 7(b)), the particular form of the $p_\perp^2$ spectrum of pions can well be reproduced. Because of the heavy recoiling mass, pions coming from baryon resonances are expected to contribute even more to the peak at small $p_\perp^2$.

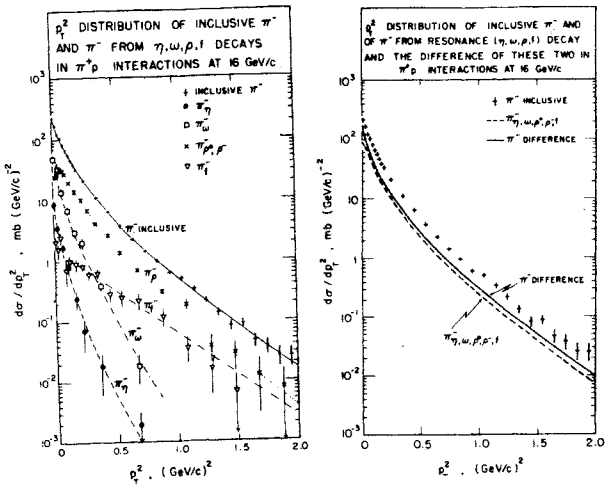

Fig. 7 $p_\perp^2$ distributions of π^- production in π^+p interaction at 16 GeV/c [1f].

a) Inclusive π^- distribution and spectra of π^-s coming from η, ω, ρ and f resonances

b) Inclusive π^- distributions, sum of all π^-s from (η, ω, ρ, f) decay (broken line) and difference of the two distributions (full line).

Having shown that pions at small $p_\perp^2$ mainly come from resonance decays, one can try to get another upper bound on direct pion production using the conjecture of slope universality. As seen in fig. 4(a) the $p_\perp^2$ spectrum of pions is compatible with the exponential ρ spectrum above $p_\perp^2 \sim 0.8$ GeV^2 where decay-pions are expected to play a less important role. Extrapolating the exponential spectrum at large $p_\perp^2$ down to $p_\perp^2 = 0$, one obtains an upper bound for direct pion production of 20% of the total pion yield. Taking into account the large $p_\perp^2$ tail of decay-pions one arrives at a best estimate of about 10%. In Table III we compare the production cross cross sections for meson resonances and the estimate for directly produced pions with quark model predictions by Anisovitch and Shekhter [4]. Although the predictions are only valid for a large number of produced quarks, i.e. high energies, the quantitative agreement between data and predictions is surprisingly good for resonances not containing strange quarks. The predictions for ϕ and η production, however, are off by one order of magnitude which may indicate some dynamical mechanism like the Zweig-Iizuka rule for suppressing these states.

TABLE III

Comparison of particle ratios in 16 GeV/c π^+p interactions with quark model predictions [4].

PARTICLE RATIO	QUARK MODEL PREDICTION	"EXPERIMENTAL" RESULT
ω/ρ	1	0.8 ± 0.2
η/ω	11/18 = 0.14	0.39 ± 0.03
π^-_D/ρ^0	1/3 = 0.33	∿ 0.5 - 1.0
π^-_D/ρ^-_{ALL}	1/14 = 0.07	< 0.5 best estimate ∿ 0.1
ϕ/ρ^0	1/9 = 0.11	< 0.025
η'/η	19/11 = 1.7	∿ 0.05 - 0.10

I would like to thank the Birmingham-Brussels-CERN-Mons Collaboration for allowing me to include unpublished results. I am especially grateful to Drs. V. T. Cocconi, M. J. Counihan, H. G. Kirk, P. K. Malhotra, F. Mandl, D. R. O. Morrison and H. Saarikko for their assistance in preparing this talk.

REFERENCES

[1a] M. Deutschmann et al., Nucl. Phys. B103 (1976) 426.

[1b] J. Bartke et al., Nucl. Phys., B107 (1976) 93.

[1c] Inclusive Production of $\bar{K}^*(890)$ and $\bar{K}^*(1420)$ in K^-p Interactions at 10 and 16 GeV/c, Aachen-Berlin-CERN-London-Vienna Collaboration, H. G. Kirk et al., CERN/EP/PHYS 76-13.

[1d] Inclusive $\Delta^{++}(1236)$ Production in π^+p, π^-p and K^-p Interactions at 16 GeV/c, Aachen-Berlin-Bonn-CERN-Cracow-Heidelberg-London-Vienna-Warsaw Collaboration.

[1e] Inclusive Production of $\Sigma^\pm(1385)$ in K^-p Interactions at 10 and 16 GeV/c, Aachen-Berlin-CERN-London-Vienna Collaboration.

[1f] Eta and Omega Meson Production in Medium Energy $\pi^\pm p$ and K^-p Collisions, Aachen-Berlin-Bonn-CERN-Cracow-London-Vienna-Warsaw Collaboration, CERN/EP/PHYS 76-28.

[1g] A Study of Indirect Pion Production in π^+p Interactions at 16 GeV/c, Aachen-Berlin-Bonn-CERN-Cracow-Heidelberg-Warsaw Collaboration, CERN/EP/PHYS 76-27.

[1h] Inclusive Yields and Transverse Spectra of the Mesons Comparison with the Quark Model and the Problem of "Direct" Pion Production, Aachen-Berlin-Bonn-CERN-Cracow-London-Vienna-Warsaw Collaboration, CERN/EP/PHYS 76-30.

[2] The Reactions $K^+p \to \Lambda X^{++}$ and $K^+p \to \bar{\Lambda} X^{++}$ at Incident Momenta of 8.2 and 16 GeV/c, Birmingham-Brussels-CERN-Mons Collaboration, P. V. Chliapnikov et al., CERN/EP/PHYS 76-11.

[3] See e.g. Experimental Review of Strong Interactions at High Energy, D. R. O. Morrison, Lectures at the Fifth Hawaii Topical Conference in Particle Physics, 1973.

[4] V. V. Anisovitch and V. M. Shekhter, Nucl. Phys. B (73) 455.

[5] H. A. Gordon et al., Phys. Letters 34B (75) 284.

[6] V. Blobel et al., Phys. Letters 48B (74) 73.

[7] D. Fong et al., Phys. Letters 60B (75) 124.

[8] R. Singer et al., Phys. Letters 60B (76) 385.

[9] Aachen-Berlin-Bonn-CERN-Cracow-London-Vienna-Warsaw Collaboration, F. Mandl, private communication.

[10] Study of $\Sigma^\pm(1385)$ Inclusive Production in K^-p Interactions at 4.2 GeV/c, Amsterdam-CERN-Nijmegen-Oxford Collaboration, CERN/EP/PHYS 76-23.

ASSOCIATED CORRELATION EFFECTS IN π^-p-INTERACTIONS AT 40 GeV/c

L.N.Abesalashvili, N.S.Amaglobeli, N.K.Koutsidi, T.G.Makharadze, R.G.Salukvadze, L.A.Slepchenko, Yu.V.Thevzadze, M.S.Chargeishvili

High Energy Nuclear Physics Problem Laboratory, Tbilisi St.University, USSR

Results of an experimental study of semi-inclusive reactions in π^-p interactions at 40 GeV/c are presented in this paper. The work was done within the framework of the 2-m JINR propane bubble chamber international collaboration[1]. The results reported are based on the analysis of ~10400 inelastic interactions. Data processing was described elsewhere[2].

The distribution of an associated multiplicity as a function of transverse momentum of the trigger $\pi^\pm$-meson from reaction

$$\pi^-p \to \pi^\pm + (n-1)_{ch} + \ldots \qquad (1)$$

is shown in fig.1. Data from π^-n-collisions (on quasi-free neutrons of the carbon nucleus) are also given for comparison.

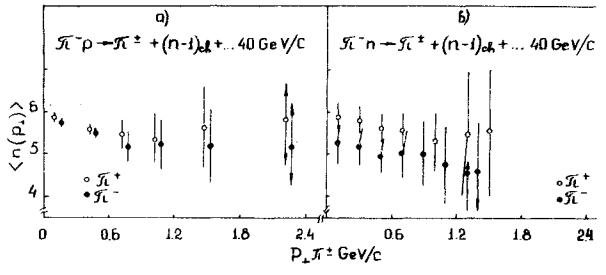

Fig.1.The associated charged multiplicity as a function of transverse momentum of the trigger $\pi^\pm$-mesons.

A weak dependence of the associated multiplicity on $p_\perp$ is seen for low $p_\perp$ region ($p_\perp \lesssim 0.5$ GeV/c), whereas $\langle n(p_\perp)\rangle$ is nearly constant for higher $p_\perp$. The experimental results were approximated by the expression

$$\langle n(p_\perp)\rangle = a + b/p_\perp \qquad (2)$$

deduced within the framework of the diffraction excitation model for semi-inclusive reactions[3,4]. Small values of parameter b (e.g, for π^--mesons $b = 0.08 \pm 0.02$) point a rather weak correlations between n and $p_\perp$.

However it turns out that such behaviour of the $\langle n(p_\perp)\rangle$ is the result of averaging over some different dynamical effects that manifest themselves in different phase-space regions; that we see in fig.2, where the associated multiplicity dependence on $p_\perp$ is shown for different kinematical regions of trigger $\pi^\pm$-mesons. Note

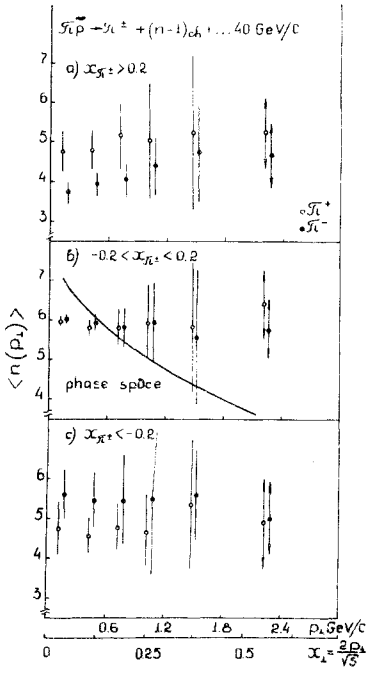

Fig.2. The same dependence in different phase space regions of the trigger particle.

the following main features: i) the $\langle n(p_\perp)\rangle$ values in fragmentation regions - fig.2a) and 2c) are lower than in the central region - fig.2b) because of the diffraction-type mechanisms of the particle production; II) an approximate constancy of the $\langle n(p_\perp)\rangle$- e.g., in the central region - is the result of the influence of the process dynamics - the fact clearly seen when comparing the experimental data with Monte-Carlo generated events[5] - curve in the fig.2b); III) the associated multiplicity for the trigger π^--mesons from beam fragmentation region shows tendency to increase.

Further analysis of the $\langle n(p_\perp)\rangle$ for fast π^--mesons reveals that particles produced in the central region are responsible for this rise of the $\langle n(p_\perp)\rangle$ - fig. 3b).

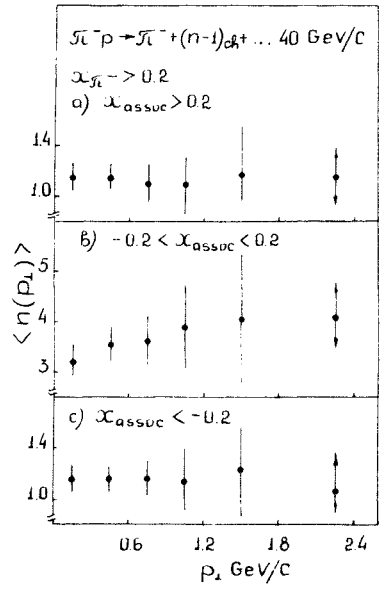

Fig.3. The same dependence for trigger π^- in the beam fragmentation region; associated particles in different phase space regions.

So in this case we can't explain the rise of the $\langle n(p_\perp) \rangle$ for forward emitted π^--mesons by means of the model of beam particle excitation in the course of its interaction with the target hadron constituents[6].

When taking two subsets of associated particles: those having the same direction of the $\vec{p}_\perp$ as the trigger particle and the ones with the opposite direction, the different behaviour of the $\langle n(p_\perp) \rangle$ is seen - fig.4. Whereas the associated multiplicity decreases in the same hemisphere it has a tendency to rise in the opposite one - while correlations of a kinematical origin produce a fall of the $\langle n(p_\perp) \rangle$ in both hemispheres-curves in the fig.4.

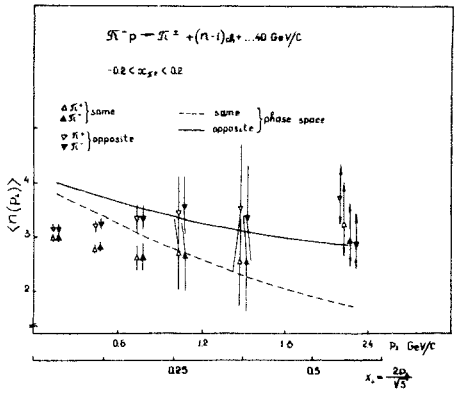

Fig.4. The same dependence for $\pi^\pm$-mesons from the central region in the same and opposite hemispheres.

We have studied further the dependence of the average transverse momentum of associated particles on the value of $p_\perp$ of the trigger particle. Our data show an increase in the $\langle p_\perp \rangle_{ass}$ with the increase in the $p_{\perp\, trig}$ value- fig.5 - which is well approximated by a linear dependence

$$\langle p_\perp \rangle_{ass} = a_1 + b_1 \cdot p_{\perp\, trig} \qquad (3)$$

(e.g. for π^+-mesons $\chi^2/N = 5.86$, $a_1 = 0.354 \pm 0.001$, $b_1 = 0.028 \pm 0.003$).

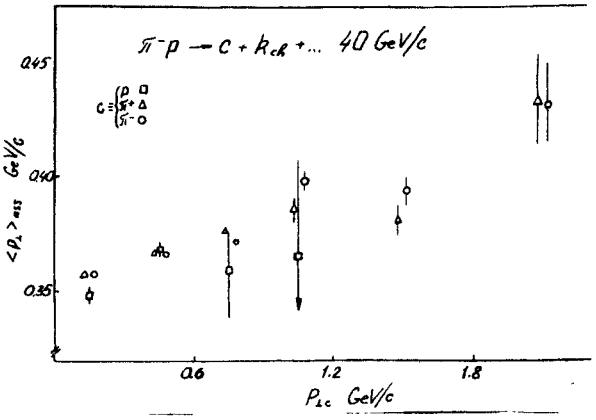

Fig.5. The average transverse momentum of associated particles as a function of the $p_\perp$ of the trigger particle.

When analysing the average associated $p_\perp$ in different azimuthal cones we see that in the cones with opening angle $\varphi > 90^\circ$ $\langle p_\perp \rangle_{ass}$ increases when increasing $p_\perp$ of the trigger the more the closer is φ to 180° - fig.6. However $\langle p_\perp \rangle_{ass}$ increases also for particles in the narrow cone on the same side ($\varphi < 30^\circ$), whereas it decreases in two other cones. It agrees rather well with the big correlations observed at the ISR for high $p_\perp$ particles in the cases of $\varphi \approx 0^\circ$ and $\varphi \approx 180^\circ$[7].

Note in conclusion that the results reported here point at the associated productions of particles with $p_\perp$ greater than the average one and the data do not contradict "jet-type" models.

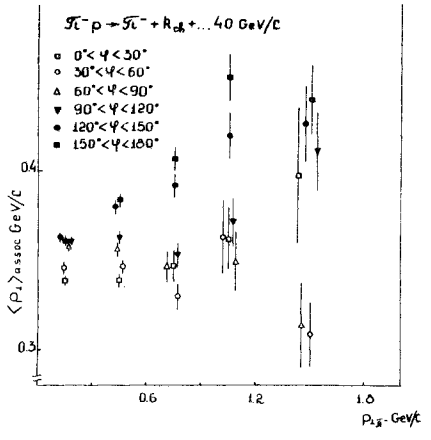

Fig.6. The same dependence in different azimuthal cones for the trigger π^--meson.

The authors are grateful to the staff of the 2-metre chamber international collaboration and to the group of physicists and laboratory assistants of the High Energy Nuclear Physics Problem Laboratory of the Tbilisi State University.

References

1. Nguen Din Ty, V.N.Penev et al. JINR, 13-5942, Dubna, 1973.
2. A.N.Abdurakhimov, N.S.Angelov et al. JINR, 1-6967, Dubna, 1973.
3. L.N.Abesalashvili, N.S.Amaglobeli et al.Sov. J.of Nucl.Phys., 23, 782 (1976); JINR, 1-9406, Dubna, 1975.
4. J.S.Darbaidze, L.A.Slepchenko. Bull. of the Acad. of Sci.Georg. SSR, 79, 61 (1975).
5. S.N.Komarova, G.I.Kopylov et al. JINR, 1-8501, Dubna, 1974.
6. L.J.Gutay, A.T.Laasen et al. Lett.al Nuovo Cim., 16, 49 (1976).
7. F.W.Busser et al. Phys.Lett., 51B, 306 (1974); Nucl.Phys., B106, 1 (1976).

INVESTIGATION OF SOME INCLUSIVE DISTRIBUTIONS OF Λ^0-HYPERONS AND K^0_1-MESONS IN π^-C^{12} INTERACTIONS AT 40 GEV/C

L.N.Abesalashvili, N.S.Amaglobeli, L.T.Akhobadze, D.V.Gersamia, M.A.Dasaeva, T.L.Kchvachadze, N.S.Koutsidi, R.G.Salukvadze, Yu.Thevzadze, M.S.Chargeishvili

Tbilisi State University, USSR

In this paper we present results on the investigation of some inclusive spectra of Λ^0-hyperons and K^0_1-mesons produced in π^-C and π^-C^{12} interactions at 40 GeV/c. (Symbol π^-C applies to the π^--meson interactions with carbon without accounting pion interactions with quasifree nucleons).

As an experimental material for physical investigation were used events selected from the films of 2m JINR propane chamber, obtained in π^--meson beam at the Serpukhov accelerator. Questions concerning the measuring of πp-events and section definition of their production are considered in papers /1/ and /2/. Distributions for π^-C and π^-C^{12} interactions are compared with corresponding distributions for $\pi^- p$ collisions.

Momentum Characteristics of Λ^0-Hyperons and K^0_1-Mesons

In Fig.1 normalised momentum distributions of Λ^0 and K^0_1 particles are presented for π^-C^{12}, π^-C and $\pi^- p$ interactions. Comparison of distributions for $\pi^- p$ and π^-C collisions makes it possible to examine the influence of nucleus over the considered distributions. It may be seen that in π^-C interactions the part of slow particles is slightly higher and there is a tendency of decreasing the number of particles with maximal momenta. An average momenta of Λ^0 and K^0_1-particles in π^-C interactions are less than in $\pi^- p$ collisions (see Table I). Momentum distributions of Λ^0 and K^0_1-particles for π^-C^{12} interactions within the range of errors coincide with corresponding distributions for $\pi^- p$ collisions.

In Table I the average characteristics of Λ^0-hyperons and K^0_1-mesons produced in $\pi^- p$, π^-C and π^-C^{12} interactions are given.

Table 1

		$\langle p_{lab} \rangle$	$\langle p_{11\,cm} \rangle$	$\langle p_\perp \rangle$	B	χ^2/N
$\pi^- p$	Λ^0	3,67±0,22	3,58±0,22	0,489± 0,016	3,21±0,57	2,4/5
	K^0	5,43±0,20	5,38±0,20	0,452±0,012	4,19±0,47	1,7/6
$\pi^- C$	Λ^0	3,36±0,18	3,26±0,18	0,490±0,014	3,49±0,43	2,3/5
	K_1^0	4,68±0,16	4,48±0,15	0,465±0,010	3,68±0,38	7,2/6
$\pi^- C^{12}$	Λ^0	3,52±0,13	3,43±0,13	0,478±0,010	3.7I±0,39	3.3/5
	K_1^0	5,01±0,12	4,90±0.11	0,469±0,007	3,28±0,42	8,3/6

In Table I one may see that in $\pi^- C$ interactions meanly slower neutral strange particles are produced than in pion-nucleon interactions. The average values of transverse momenta of Λ^0-hyperons in $\pi^- C^{12}$, $\pi^- C$ and $\pi^- p$ collisions coinside. One may say the same of K_1^0-mesons transverse momenta. These facts show that transverse momenta do not depend on the nature of colliding particles.

One-Particle Inclusive Distributions of Λ^0 Hyperons and K_1^0-Mesons

The behaviour of normalized invariant differential sections $\frac{E\,d^2\sigma}{dp_{11}\,dp_\perp^2}$ in lab.system for Λ^0-hyperons and K_1^0-mesons from $\pi^- C^{12}$, $\pi^- C$, $\pi^- p$ interactions was investigated. Integration by square of transverse and longitudinal momentum leads to the functions.

$$H_1(p_{11}) = \frac{1}{\sigma_{in}} \int \frac{E\,d^2\sigma}{dp_{11}\,dp_\perp^2}\, dp_\perp^2$$

$$H_2(p_\perp^2) = \frac{1}{\sigma_{in}} \int E^{-1} d^2\sigma / dp_{11}\, dp_\perp^2\, dp_{11}$$

Functions $H_1(p_{11})$ for Λ^0-hyperons and K_1^0-mesons in lab.system of coordinates are given in Fig.2. For comparison the relations of these values are given too:

$$R = \frac{H_1(p_{11})_{\pi^- C}}{H_1(p_{11})_{\pi^- p}}$$

It may be seen that $H_1(p_{11})$ for $\pi^- C$ and $\pi^- p$ interactions slightly differs in the region of low value of longitudinal momentum in the case of Λ^0-hyperons and K_1^0-mesons as well. Our experimental distributions by square of transverse momentum in $\pi^- p$, $\pi^- C$ and $\pi^- C^{12}$ interactions up to 1 $(GeV/c)^2$ are shown in Fig.3. (One may see that functions $H_2(p_\perp^2)$ for Λ^0 and K_1^0 particles in $\pi^- C^{12}$, $\pi^- C$ and $\pi^- p$ collisions coinside within the range of errors. Functions $H_2(p_\perp^2)$ for Λ^0-hyperons and K_1^0-mesons in the given interactions were fitted by the exponent of the form $H_2(p_\perp^2) = A e^{-B p_\perp^2}$.

The results of fitting are given in Table I. Coefficient B is the same for $H_2^{\Lambda^0}(p_\perp^2)$ and $H_2^{K^0}(p_\perp^2)$.

From the comparison of different distributions of Λ^0-hyperons and K_1^0-mesons from $\pi^- p$ and $\pi^- C$ interactions one may conclude that carbon nucleus unsubstentially change the momentum and angle characteristics of Λ^0 and K_1^0-particles. The influence of carbon nucleus is observed as a displacement of momentum spectra of Λ^0 and K_1^0 particles to the smaller values. Secondary interactions in Carbon nucleus play, apparently, unimportant role in the production of Λ^0 and K_1^0-particles.

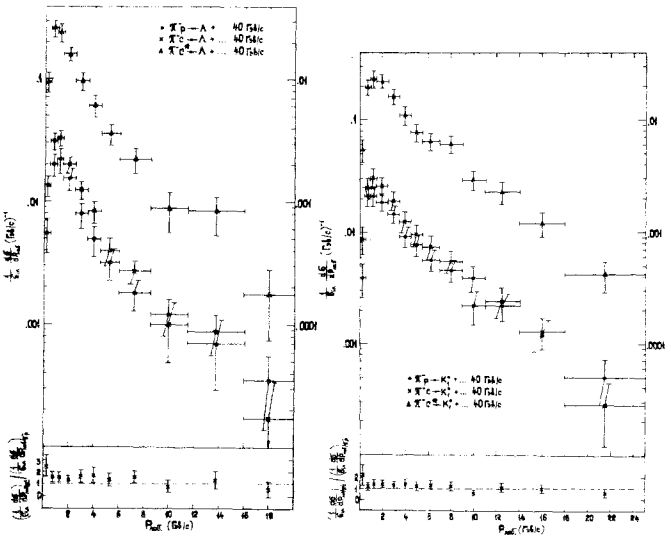

Fig.1.

Normalized momentum distribution of Λ^0 hyperon and K_1^0-mesons in lab. system.

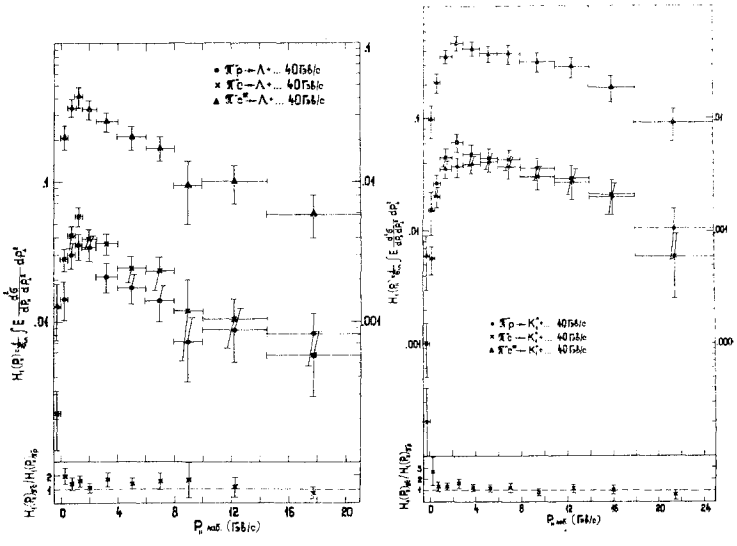

Fig.2.

Distribution of the function $H_1(P_{II})$ to P_{II} for Λ^0 -hyperons and K^0_1- mesons.

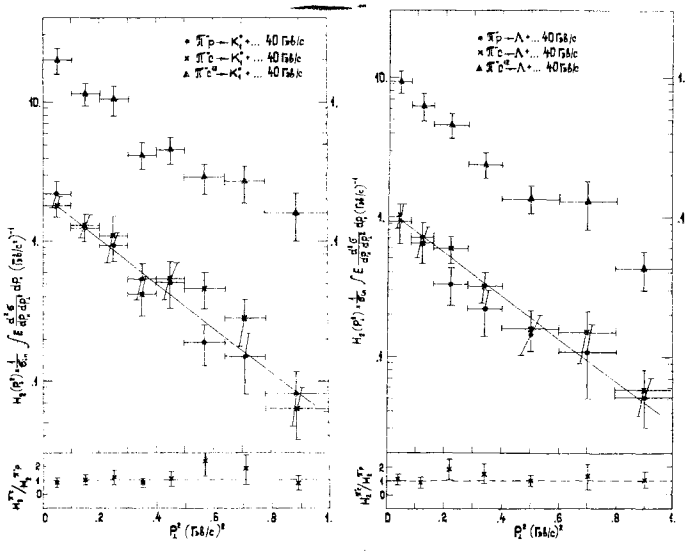

Fig.3.

Dependence of the function $H_2(P^2)$ on P^2 for Λ^0-hyperons and K^0_1-mesons.
Straight line - the result of approximation of experimental data from interactions.

References

1. Budapest-Bucharest-Dubna-Cracow-Hanoi-Sofia-Tashkent-Tbilisi-Ulan Bator- Collaboration. JINR P1-7267, Dubna,1973; Journal of Nucl. Phys.(USSR),17,1251(1973);Nucl.Phys.,B79,57 (1974).
2. N.Angelov, C.P.Vishnevskaia,V.G.Grishin et al. JINR,P1-9209,Dubna,1975; Nucl.Phys.,(USSR), (in print).

TWO-PARTICLE CORRELATIONS

E.P.Kistenev

IHEP, Serpukhov, USSR

Progress in correlation studies reached in recent years makes it obvious that a real understanding of the phenomena responsible for the structure observed in correlations is impossible without precise separation of the production mechanisms playing a dominant role in different regions of the phase space. For this reason this talk will be devoted mainly to those results which provide information about the interplay between the correlations and production dynamics.

1. Longitudinal Correlations in the Central Region

The correlations are usually studied in terms of correlation functions. The most popular definitions are the following:

$$C_n^*(\vec{P}_1,\vec{P}_2)=\frac{1}{n^i(n^j-\delta^{ij})}\rho_n^{ij}(\vec{P}_1,\vec{P}_2)-\frac{1}{n^i n^j}\rho_n^i(\vec{P}_1)\rho_n^j(\vec{P}_2),$$

$$R_n^*(\vec{P}_1,\vec{P}_2)=C_n^*(\vec{P}_1,\vec{P}_2)\,/\,\left(\frac{1}{n^i n^j}\rho_n^i(\vec{P}_1)\rho_n^j(\vec{P}_2)\right),$$

where $\rho_n(\vec{P})=\frac{1}{\sigma_n}\frac{d\sigma_n}{d\vec{P}}$, $\rho_n^{ij}(P_1,P_2)=\frac{1}{\sigma_n}\frac{d\sigma_n}{d\vec{P}_1 d\vec{P}_2}$

are one and two particle densities, i, j - types of the particles in the pair.

The inclusive correlation function can be defined in a similar way and rewritten in terms of the components of semiinclusive processes

$$C_n^*(\vec{P}_1,\vec{P}_2)=\sum_n \omega_n C_n^*(\vec{P}_1,\vec{P}_2)+\sum_n \omega_n(\rho^i(\vec{P}_1)-\rho_n^i(\vec{P}_1))(\rho^j(\vec{P}_2)-\rho_n^j(\vec{P}_2)),$$

where $\omega_n=\sigma_n/\sigma_{inel.}$

The first term in this equation is the sum of the semiinclusive correlation functions taken with the weights proportional to the topological cross sections.The second term is a crossing term which originates from the mixing of the semiinclusive spectra depending on the multiplicity.The last term does not contain any information about the dynamical correlations among the produced particles[1].

The semiinclusive correlations are presented to the conference for $\pi^- p$ [2-6], pp [7], $\bar{p}p$ [8] and ph [9] interactions in the energy range 5-400 GeV/c. General structure of such correlations is illustrated in fig. 1 where the values of the semiinclusive correlation functions $C_n^*(y_1, y_2)$ are plotted against the $\frac{1}{2}(y_1 - y_2)$ for a fixed value of $\frac{1}{2}(y_1 + y_2) = 0$ [7] (y_1 and y_2 - rapidities of the particles in pair).

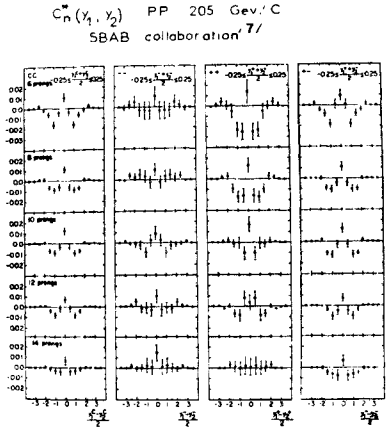

Fig. 1

a) The observed correlations are of short range and the function $C_n^*(y_1, y_2)$ decreases sharply from its value at $y_1 = y_2 = 0$.

b) The values in the central bin are of compatible size for all the charge combinations.

In the framework of the simple cluster emission model the shape of the semiinclusive correlation function can be parametrized in the form [10]

$$C_n^*(y_1, y_2) = \frac{\langle K(K-1)\rangle}{\langle K\rangle (n-1)} \left(F(y_1, y_2) - \frac{1}{n(n-1)} \rho_n(y_1)\rho_n(y_2) \right),$$

where K - is the cluster multiplicity, $F(y_1, y_2)$ - two particle density within the cluster. New data of SBAB collaboration [7] support the conclusion from PSB experiment [11] that the clusters are entities with multiplicity independent characteristics. As seen from data of fig. 2 where the values of $\langle K(K-1)\rangle / \langle K\rangle$ are functions of the scaled multiplicity $n/\langle n\rangle$ the multiplicity distribution within a cluster is broader than a δ -function ($\langle K(K-1)\rangle / \langle K\rangle = K_0 - 1$) and narrower than a Poisson-like distribution ($\langle K(K-1)\rangle / \langle K\rangle \simeq \langle K\rangle (n-1)/\langle n\rangle$. The small values of $\langle K(K-1)\rangle / \langle K\rangle$ in the figure imply an average number of charged particles $\langle K\rangle \leq 2$ which means that well known resonances, such as vector or tensor bosons could play a dominant role in the picture observed.

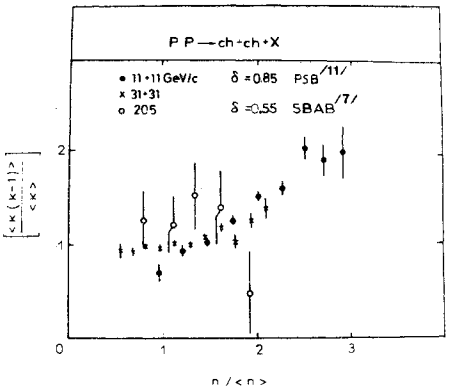

Fig. 2

The effect of ρ^0 -production on longitudinal correlations was investigated by the BFGMOP collaboration in $\pi^- p$ interactions at 11.2 GeV/c [6] (fig. 3).

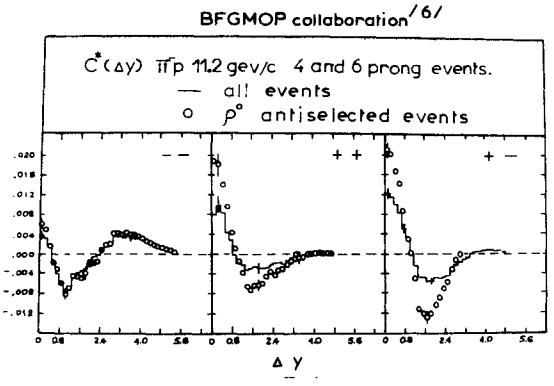

Fig. 3

The ρ^0 -meson leads to the effect of forcing apart the π -pairs reducing the short range correlations in $\pi^+\pi^+$ and $\pi^+\pi^-$ systems. This conclusion coincides with a prediction made by E.Levin and M.Ryskin in the context of multiperipheral model considering the alignment of the resonances in the final state [12].

The French-Soviet Union pp -collaboration at 69 GeV/c previously reported the existence of the maxima in semiinclusive correlation function $C_n^*(y_1 = y_2)$ at $y_1 = y_2 = \pm 1$ for both

$\pi^-\pi^-$ and $\pi^+\pi^-$ combinations[13]. The corresponding data are now available also in pp interactions at 205 GeV/c[7], K^-p at 32 GeV/c[14] and $\bar{p}p$ at 22.4 GeV/c[8]. The compilation of the proton data for multiplicity $n=10$ is shown in fig. 4. Positive correlations are present

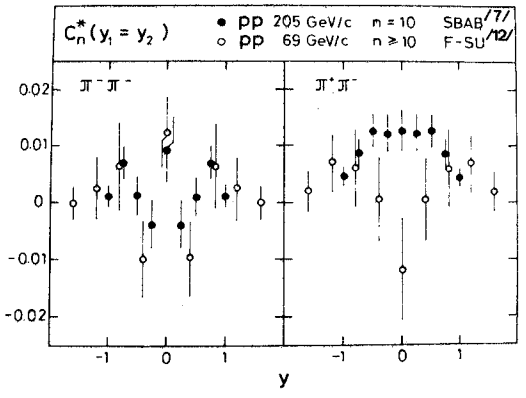

Fig. 4

in all data. The same structure as at 69 GeV/c is seen in the 205 GeV/c data for $\pi^-\pi^-$ pairs. One of the possible explanation for the maxima in $C_n^*(y_1=y_2)$ at $y_1=y_2=\pm 1$ could be the anisotropy of the resonance decay if they are produced in aligned state. The central maximum at $y_1=y_2=0$ can be a manifestation of the second order interference effect (see for example the minirapporteur talk of M. Podgoretsky at this conference).

The data for $\pi^+\pi^-$ combinations are contradictory, The dip at $y_1=y_2=0$ seen in the 69 GeV/c data is absent at 205 GeV/c. More precise data are still needed to study this effect in detail.

2. Joint Angular-Momentum Correlations

The existence of the angular correlations can be partly explained by the negative sign in the right-hand part of the corresponding inclusive sum rule which can be written for identical particles as follows

$$\int (\vec{P}_{t1}\vec{P}_{t2})\rho(\vec{P}_1,\vec{P}_2)\frac{d^3P_1}{E_1}\frac{d^3P_2}{E_2} = -\int P_t^2\rho(\vec{P})\frac{d^3P}{E}$$

which means that wide open pairs are favoured over narrow ones.

Compilation of the data for azimuthal asymmetry defined as $B=[N(\varphi>\frac{\pi}{2})-N(\varphi<\frac{\pi}{2})]/N_{tot}$ is shown in fig.5[6] (φ is the opening angle in transverse momentum plane).

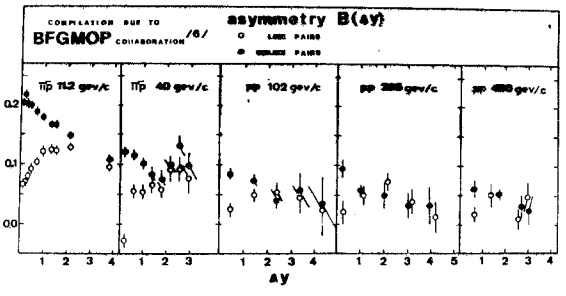

Fig. 5

Comparison for the different energies and initial states suggests that at least for small values of the rapidity difference Δy the asymmetry B for like and unlike particles have consistently a similar behaviour. Higher multiplicity and consequently more neutral particles results in a decrease of asymmetry with energy as is seen from this figure.

The constructive interference which exists in the pairs of like particles[15] can explain the difference between the azimuthal correlations for like and unlike pairs only in the threshold region $M_{\pi\pi}\simeq 2m_\pi$ where the energy-momentum vectors of the particles in pair are almost equal. Outside this region the resonance production can contribute to the observed difference in the correlations. The corresponding data are now available from a number of experiments. Fig. 6 shows the results obtained in π^-p experiments at 40 GeV/c[16] (a) and 11.2 GeV/c[6] (b).

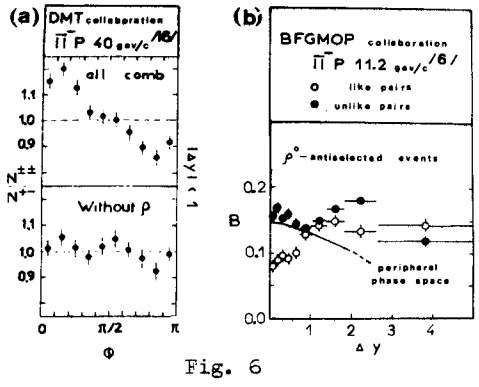

Fig. 6

When ρ -like combinations are excluded from the data no clear distinction between the distributions of the opening angle in transverse momentum plane for like and unlike pion pairs is left in π^-p data at 40 GeV/c[16] (fig.6a).

The elimination of the events with a $\pi^+\pi^-$ couple in the ρ-region from the total sample makes the experimental data for unlike pairs consistent within the errors with statistical model prediction (fig. 6b). The situation is different for like pairs where the decrease of the asymmetry at small Δy still exists

Let us summarize now the conclusions of these two sections.

The data presented to the conference support the existence of the positive short-range correlations in rapidity space for both like and unlike charge combinations. The dependence of the semiinclusive correlation function on Δy can be parametrized in the framework of the independent cluster emission model with cluster multiplicity $\langle K \rangle \leq 2$ which means that the resonances could play a dominant role in the longitudinal correlations, even if no quantitative connection has yet been established.

The angular correlations observed in the $\pi\pi$ systems are mainly of the kinematical origin. The difference between the like and unlike charge pairs apart from the threshold region where the interference effects could be essential can be explained by the resonance production.

References

1. V.V.Ammosov et al. French-Soviet Union Collaboration, preprint IHEP M-16, Serpukhov, 1975.
2. Notre Dame-Duke-Canada-Iowa-Maryland-Michigan Collaboration, conference paper 1023/A2-103.
3. I.Ya.Chasnikov et al. Alma-Ata, USSR, conference paper 166/A2-4.
4. N.Angelov et al. JINR, Dubna conference paper 157/A2-12.
5. Dubna-Košice-Minsk-Tbilisi Collaboration, conference paper 810/A2-79.
6. Bologna-Firenze-Genova-Milano-Oxford-Pavia Collaboration, conference paper 1202/A2-160.
7. Stony Brook-Argonne-Batavia Collaboration, conference paper 738/A2-106.
8. Alma-Ata-Dubna-Helsinki-Košice-Moscow-Prague Collaboration, conference paper 161/A2-9.
9. Strasbourg-Rehovot Collaboration, conference paper 375/A2-38.
10. E.L.Berger. Nucl.Phys., B85, 61 (1975).
11. S.R.Amendolia et al. Nuovo Cim., 31, 17 (1976).
12. E.M.Levin, M.G.Ryskin, conference paper 83/A3-3.
13. V.V.Ammosov et al. French-Soviet Union Collaboration, preprint IHEP M-21, Serpukhov, 1975.
14. V.V.Babintsev et al. French-Soviet Union and CERN-Soviet Union Collaboration, preprint IHEP M-24, Serpukhov, 1975.
15. G.I.Kopylov, M.I.Podgoretsly. JINR, Dubna, conference paper 1007/A2-120.
16. Dubna-Moscow-Tbilisi Collaboration, conference paper 205/A2-108.

RECENT RESULTS ON 32 GEV/C $K^{\pm}p$ AND $\bar{p}p$ INTERACTIONS IN THE MIRABELLEE BUBBLE CHAMBER

Presented by R.Barloutaud, DPhPE,CEV-Saclay, France

This report is intended to be a summary of the recent results obtained by the France-Soviet Union and CERN-Soviet Union Collaborations* with the 4.6 m. MIRABELLE hydrogen bubble chamber exposed at the Serpukhov accelerator to RF separated K^+, K^- and $\bar{p}$ beams at 32 GeV/c. These results are based on the analysis of 100K, 80K and 12K pictures of K^+, K^- and $\bar{p}$ experiments respectively.

All events including V^o and e^+e^- pairs have been doubly scanned, measured on manual or automatic devices and submitted to 4C kinematical fits. Therefore, both inclusive and exclusive studies have been carried out on these samples. Four communications[1-4] for the K^+p , five for the K^-p [5-9] and two for the $\bar{p}p$[10-11] experiments were reported.

In this brief sketch of the results given in these papers, the data on the similar final states obtained with the different beams will be presented together allowing a useful comparison between the K^+p, K^-p and $\bar{p}p$ interactions.

I. INCLUSIVE STUDIES

1.1. Particle Multiplicities

The π^o average multiplicity $\langle n_{\pi^o} \rangle$ assumed to be equal to $\langle n_\gamma \rangle / 2$ is almost identical in the three experiment (1.89±0.05),(1.96±0.05) and (1.80±0.15) for K^+p, K^-p and $\bar{p}p$ interactions respectively as well as its topological dependence shown in fig.1. The shape of the $\langle n_{\pi^o} \rangle$ dependence is also quite compatible with the results obtained in $\pi^{\pm}p$ and pp interactions[12]. In the K^-p experiment the average multiplicity of each type of produced particle has been evaluated by using the equations of charge, strangeness and baryonic number conservation and some general hypothesis on the production of K^o, K^+ and antibaryons. In particular, the average multiplicity of π^+ and π^- are found to be quite compatible with the π^o multiplicity ($\langle n_{\pi^+} \rangle$ = =1.87±0.07, $\langle n_{\pi^-} \rangle$=1.96±0.10). The multiplicity distribution of π^+ and π^- has also been derived. It is presented in fig.2 and differs significantly from the charged particle multiplicity distribution since more than 20% of these particles

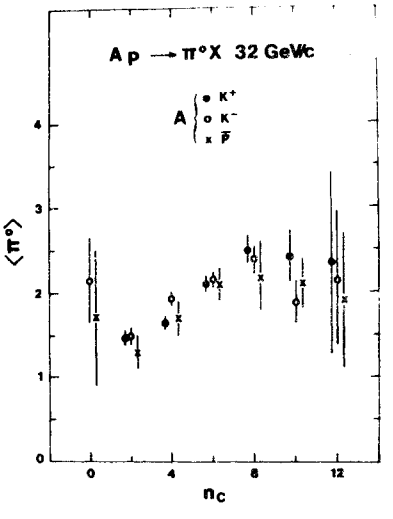

Fig.1. π^o average multiplicity as a function of the charged topology.

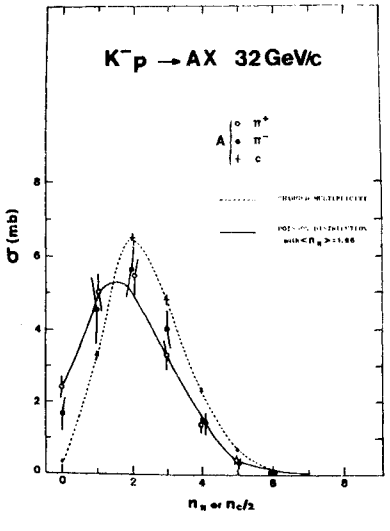

Fig.2. $\pi^{\pm}$ cross section as a function of the $\pi^{\pm}$ multiplicity and topological cross section (dashed curve). The full curve is a Poisson distribution.

* The laboratories involved in the Collaborations are: Bruxelles, Mons, Paris, Saclay and Serpukhov for the K^+p experiment; Aachen,Berlin, CERN, Saclay, Serpukhov and Vienna for the K^-p experiment; Bruxelles, Mons, Saclay and Serpukhov for the $\bar{p}p$-experiment.

are not pions. The dispersion D and the correlation coefficient f_2 have been determined for π^+, π^- and π^o multiplicity distributions; in the π^o case, the average value of the number of produced $\gamma\gamma$ pairs has been used. A general agreement is found within the experimental errors between these coefficients for $\pi^\pm$ and π^o. In particular, f_2 is compatible with zero for $\pi^\pm$ and π^o, and the $\pi^\pm$ distributions are compatible with a Poisson distribution as seen in figure 2.

1.2. Associated Charged Multiplicities in K^-p Interactions

The average charged particle multiplicity $\langle n_x \rangle$ of the system X associated to π^+, π^- (for $X_{\pi^-} < 0$, K^n, Λ and identified protons ($p_p < 1.2$ GeV/c) has been calculated as a function of M_x^2. Below $M_x^2 \simeq 40$ GeV^2, i.e. mainly in the fragmentation region of the incident particle, the M_x^2 dependence of $\langle n_x \rangle$ is well described by the logarithmic law $\langle n_x \rangle = \alpha + \beta \ln M_x^2$ with a coefficient β which is about the same as the one describing the dependence of the total multiplicity in the K^-p interaction. Above 40 GeV^2 the β coefficient increases strongly especially for $\pi^\pm$ and K^n inclusive reactions, indicating that the values of $\langle n_x \rangle$ found in the central region are larger than expected by the law describing the S dependence of the charged multiplicity. A similar phenomenon has been seen also in K^+p interactions[13].

1.3. $K^n = K^o + \bar{K}^o$ Production

The inclusive cross sections for the reactions

$$A + p \rightarrow K^n + X$$

are (7.6±0.2), (9.8±0.25) and (6.3±0.6) mb for $A = K^+$, K^- and $\bar{p}$ respectively. Their comparison with lower energy data shows a small increase for $K^\pm p$ interactions and a more rapid rise for $\bar{p}p$ interactions. Using the cross sections for the reactions $K^-p \rightarrow \Lambda K^n + X$ and $K^\pm p \rightarrow K^n K^n + X$ and some simple hypothesis on the K and $\bar{K}$ charge distributions among the possible final states, the percentage K^c/K^n ($\bar{K}^o/K^n$) in $K^+(K^-)p$ interactions has been evaluated to be 10% (13%). As it is impossible to separate accurately the two strangeness components of the K^n, this value has to be kept in mind before interpreting quantitatively the K^n production properties in $K^\pm p$ interactions.

The invariant cross section for K^n productions are presented as a function of X in fig.3.

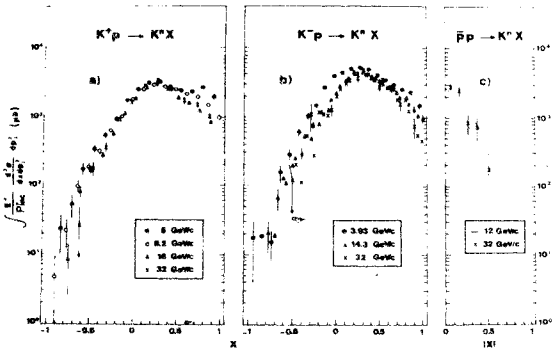

Fig.3. Invariant cross section as a function of X.

These distributions are quite similar for K^+p and K^-p interactions and they do not show any strong variation with the data obtained at 16 or 14.3 GeV/c. In the $\bar{p}p$ interactions in which the symmetrical K^n distribution has been folded around $X=0$ the errors are still too large to draw any firm conclusion.

A systematic study of the approach to scaling in K^+p interactions has led to the following conclusions:

a) in the K^+ fragmentation region, no energy variation is found between 16 and 32 GeV/c for all sets of inclusive variables;

b) scaling is not observed in the proton fragmentation region where its approach is described by an S^{-1} behaviour, suggesting the contribution of ϕ exchange (strangeness annihilation);

c) in the central region the decrease of the structure function found at low energy is not observed between 16 and 32 GeV/c (see fig.4).

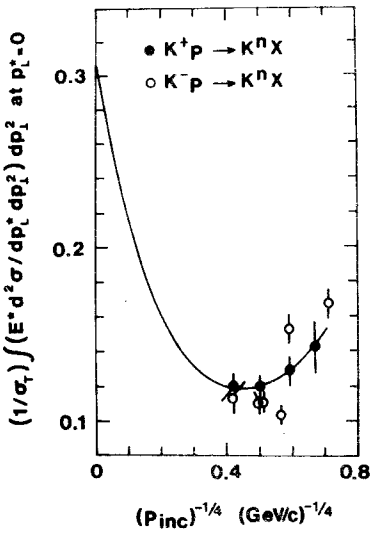

Fig.4. Invariant cross sections at $X=0$ normalized to the total cross section, as a function of $(P_{inc})^{-1/4}$.

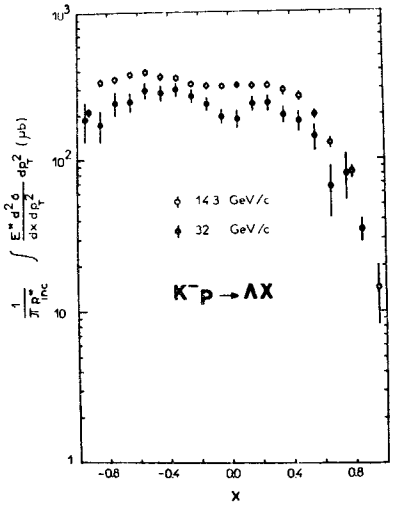

Fig.5. Invariant cross section as a function of x .

The same behaviour is found in K^-p interactions. A general fit of the structure function to all K^+p available experimental data in the interval $|x| < 0.1$ to a double Regge model including PR ($s^{-1/4}$ dependence) and RR ($s^{-1/2}$ dependence) terms is also shown (curve of fig.4); it predicts a rise of the structure function at $X=0$ above ~ 30 GeV/c and its asymptotic value.

1.4. Λ Production

The inclusive production cross section for Λ (and Σ^0) amounts to (0.8 ± 0.08), (2.35 ± 0.08) and (1.7 ± 0.3) mb in K^+p , K^-p and $\bar{p}p$ interactions respectively. A strong increase with incident momentum of the K^+p and $\bar{p}p$ cross sections is observed, while for K^-p there is a definite flattening in the decrease found at lower energy.

In K^-p interactions where the Λ are copiously produced a detailed analysis has been done of the different processes contributing to their production. In particular, the dip which develops near $X=0$ at 32 GeV/c in the invariant cross section (fig.5) can be qualitatively explained by the simultaneous decrease of the hypercharge annihilation processes $(K^-p \to \Lambda + n\pi)$ which has a rather flat X dependence, and the increase of two other processes. The firts one, $(K^-p \to \Lambda K\bar{K} + X)$ occurs mainly in the proton fragmentation region; from the $K^-p \to \Lambda K^n + X$ cross section it is found to contribute to about 50% of the whole Λ cross section. The second one $(K^-p \to \Lambda N\bar{N} + X)$ plays a role in the $X>0$ region. Its relative intensity is estimated from the $K^-p \to \Lambda + p + X$ cross section derived from the events where a Λ and an identified proton are found; it amounts to $\sim$ 13% of the total cross section. This leaves only 37% for the contribution of the hypercharge annihilation, for which the cross section decreases with incident momentum as $P_{inc}^{-0.7}$ between 4 and 32 GeV/c.

1.5. $K^{*\pm}_{890}$ Production

The production of K^{*+}_{890} and K^{*-}_{890} resonances is very important in the K^+p and K^-p -interactions respectively. It is visible on fig.6 where the $K^n\pi^+$ and $K^n\pi^-$ mass distributions are shown. These distributions fitted with a Breit-Wigner function and a suitable background have led to the

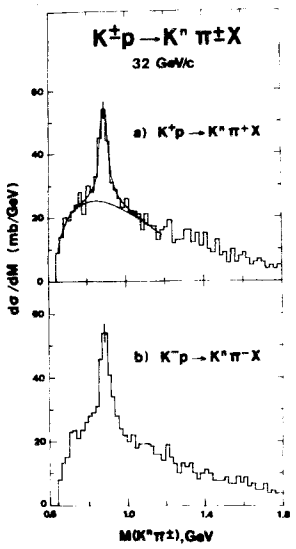

Fig.6. Invariant mass distributions.

following cross sections: $\sigma(K^{*+})$ =(3.4±0.4)mb and $\sigma(K^{*-})$ =(3.9±0.5) mb. Taking into account the proportion of $\bar{K}^0(K^0)$ previously found in $K^+p(K^-p)$ interactions, this means that about one third of the $K^0(\bar{K}^0)$ come from the $K^{*+}(K^{*-})$ decays. Comparing these data with lower energy ones one does not see any obvious energy dependence, although the variation could be compatible with that observed for $K^0(\bar{K}^0)$. The structure functions which have been calculated as a function of X (fig.7) are comparable for K^{*+} and K^{*-} and do not display (for K^{*-}) any significant energy dependence when compared to 10 and 14.3 GeV/c data. Finally the density matrix of these vector

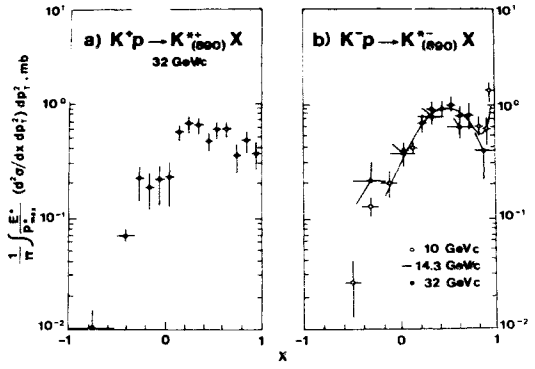

Fig.7. Invariant cross section as a function of X.

resonances have been calculated in the $K^{\pm}$ fragmentation region in the G.J.frame. They show a small amount of alignment and lead to a proportion of ~ 70% of unnatural parity exchange between the incident $K^{\pm}$ and the $K^{*\pm}$ in the region on $M_X^2/s < 0.5$ and $|t_{KK^*}| < 1$ GeV^2.

II. EXCLUSIVE STUDIES

2.1. $K^{\pm}p$ Elastic Scattering

Results have been presented at this Conference on K^-p elastic scattering: the total cross section (2.54±0.10 mb) and the differential cross section are in very good agreement with the data obtained in a counter experiment (14) at 25 and 40 GeV/c. The fig.8 presents the differential cross section; the full line is a fit

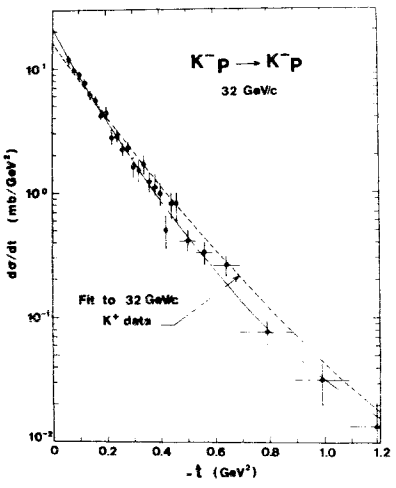

Fig.8. Differential cross section $d\sigma/dt$ for K^-p elastic scattering; the full curve is a Ae^{Bt+Ct^2} fit to the data, and the dashed curve is the fit to K^+p elastic scattering at 32 GeV/c[15].

to Ae^{Bt+Ct^2}. The dashed curve is the fit obtained in the K^+p elastic scattering at 32 GeV/c (15). A first cross over between the two fitted distributions is found at $|t_0|$=(0.16±0.05) GeV^2, which is in agreement with the values found at lower energy (16) and recently in the 50-175 GeV energy range (17). A second cross over located around 1.2 GeV^2 and also reported at 14 GeV (16) can also be guessed from the 32 GeV/c data.

2.2. Reactions $Ap \to Ap + n(\pi^+\pi^-)$ where $A = K^+, K^-, \bar{p}$

The cross sections of these reactions have been measured, they are summarized in table.1. The energy dependence of the four-body reactions $(n=1)$ shows a steeper decrease for K^+ and $\bar{p}$ incident particles than for K^-, which can be explained by a larger amount of 3 and 2 body non diffractive processes (as $K^*\Delta^{++}$ or $\overline{\Delta^{++}}\Delta^{++}$) present in these final states. The general behaviour of the outgoing particles is illustrated in 4,6 and 8 body reactions in fig.9, where the

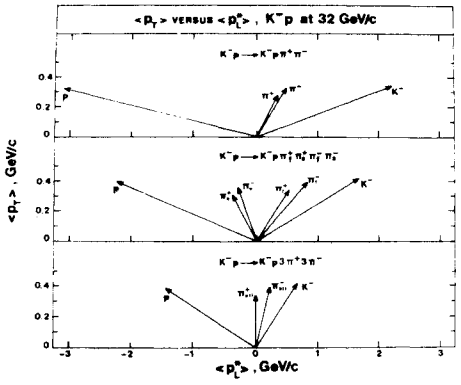

Fig.9. Average direction in the C.M.system of the particles emitted in 4,6 and 8 body reactions.

average C.M. directions is indicated for each kind of particle. The leading effect of p and K^- is, as expected, strongly reduced when the number of pions increases.

2.3. Diffraction Dissociation in 4 Body Reactions

A simple way to present the clustering effects in the four body reactions is to plot the π^+ C.M. rapidity versus the π^- C.M.rapidity as done in fig.10 for the K^+, K^- and $\bar{p}$ reactions. The populations of the sectors where y_{π^+} has the same sign as y_{π^-} is larger than that of the two other sectors especially in $K\bar{p}\,\pi^+\pi^-$ final state where the $K^-\pi^+\pi^-$ and the $p\pi^+\pi^-$ threshold enhancements dominate the reaction. In $K^+p\,\pi^+\pi^-$ and $\bar{p}p\,\pi^+\pi^-$ final states, the sectors $y_{\pi^-}>0$ and $y_{\pi^+}<0$ have still an important population which is dominated by non-diffractive production of Δ^{++} and K^{*0}_{890}, Δ^{++} and $\overline{\Delta^{++}}$ respectively. The cross sections of the $K^\pm\pi^+\pi^-(Q^\pm)$ and $p\pi^+\pi^-$ diffractive enhancements defined as $M_{K^\pm\pi^+\pi^-}<1,5$ GeV and $M_{p\pi^+\pi^-}<2.5$ GeV are presented in table II. The ratios of these cross sections to the elastic $K^\pm p$ and $\bar{p}p$ ones, given also in table II, are equal within experimental errors in agreement with the factorization requirements.

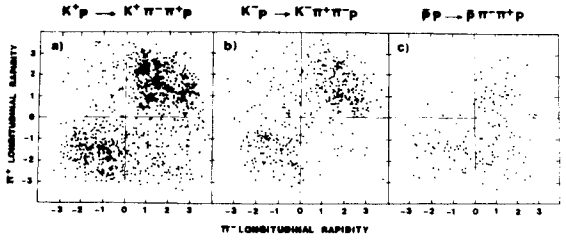

Fig.10. Scattered plot of the y_{π^+} versus y_{π^-} C.M. rapidity in the 4 body reactions.

2.4. Principal Axis Analysis in the Reactions $K^+p \to K^+p\pi^+\pi^-$ and $K^+p \to K^+p\,2\pi^+2\pi^-$

An analysis of these two reactions has been carried out by this method. The distributions of $\cos\alpha$, where α is the generalized scattering angle defined in the principal axis formalism, have a slope, for the 4 and 6 body reactions of (205 ± 10) and (175 ± 25), which is comparable to that obtained in elastic scattering at 32 GeV/c (195 ± 9). Moreover for these two reactions the outgoing particles are concentrated around a principal plane revealing a certain amount of planarity. Although these observations are difficult to interpret quantitatively, it is interesting to see that some alignment subsists in the 6 body event at this energy.

I would like to thank Dr. P.Granet for the important part he took in the preparation of this report.

Table I

Cross sections in mb for the reactions $K^{\pm}p \to K^{\pm}p + n(\pi^+\pi^-)$ and $\bar{p}p \to \bar{p}p + n(\pi^+\pi^-)$

	K^+p	K^-p	$\bar{p}p$
n=1	0.62±0.05	0.61±0.04	1.40±0.12
n=2	0.15±0.01	0.14±0.01	0.33±0.06
n=3	0.050±0.006	0.060±0.008	0.14±0.04

Table II

Cross sections and ratios σ/σ_{ee} for the diffractive enhancements defined as $M_{K\pi\pi} < 1.5$ GeV and $M_{p\pi\pi} < 2.5$ GeV in 4 body reactions

Final state	$pQ^+ \to K^+\pi^+\pi^-$	$pQ^- \to K^-\pi^+\pi^-$	$N^{*+}K^+ \to p\pi^+\pi^-$	$N^{*+}K^- \to p\pi^+\pi^-$	$N^{*+}\bar{p} \to p\pi^+\pi^-$
	230±20	235±20	160±20	177±20	480±80
	(9±1)%	(9.6±1)%	(6.7±1.3)%	(7.0±1.5)%	(5.8±1)%

References

1. P.V.Chliapnikov et al.Study of Inclusive Reaction $K^+p \to K^h + X$ at 32 GeV/c. 1167/A2-127.
2. M.De Beer et al. Inclusive K^{*+}_{890} Production in K^+p Interactions at 32 GeV/c.1168/A2-128.
3. J.Saudraix et al. General Features of the Reaction $K^+p \to K^+p\pi^+\pi^-$ at 32 GeV/c.1165/A1-121.
4. I.V.Ajienko et al. An Analysis of K^+pInteractions at 32 GeV/c in Terms of "Principal Axis" Variables.1162/A1-50.
5. C.Cochet et al. Particle Multiplicities in K^-p Interactions at 32 GeV/c.1034/A2-89.
6. V.V.Babintsev et al. A Study of the Associated Multiplicities in K^-p Interactions at 32 GeV/c. 204/A2-35.
7. Yu.J.Arestov et al. Study of Λ Production Processes in K^-p Interactions at 32 GeV/c.207/A2-37.
8. U.Gensch et al. Inclusive Resonance Production in K^-p Interactions at 32 GeV/c.206/A2-36.
9. A.Givernaud et al. Cross Features of the Dominant Exclusive Reactions in K^-p Interactions at 32 GeV/c.38/A1-37.
10. J.Hanton et al.Inclusive Production of Strange Particles and π^0_s in $\bar{p}p$ Interactions at 32 GeV GeV/c. 1035/A2-90.
11. M.A.Jabłol et al. Cross Sections and General Features of the 4C Channels in $\bar{p}p$ Interactions at 32 GeV/c.1036/A1-9.
12. F.T.Dao and J.Whitmore. P.L.46B(1973)252.
13. France-Soviet Union and CERN-Soviet Union Collaboration,to be published in Nuclear Physics.
14. Y.M.Antipov et al. N.P.B57(1973)333.
15. Y.Cranet et al.P.L.62B(1976)350.
16. G.Brandenburg et al. P.L.58B(1975)367.
17. R.L.Anderson et al. Fermilab preprint 76/47.

ЭКСПЕРИМЕНТАЛЬНЫЕ ДАННЫЕ ОБ ИЗМЕРЕНИИ РАЗМЕРОВ ОБЛАСТИ ВЗАИМОДЕЙСТВИЯ. ЭФФЕКТ ТОЖДЕСТВЕННОСТИ

М.И.Подгорецкий
Объединенный институт ядерных исследований, Дубна

I. Экспериментальные работы, представленные на конференцию, вместе с опубликованными ранее, содержат информацию о взаимодействиях $\pi^{\pm}p, \pi^{-}C, pp, \bar{p}p$ и $\bar{p}n$ в интервале импульсов от I до 200 ГэВ/с.

Возможность корреляционного измерения размеров источника впервые была продемонстрирована в связи с т.н. эффектом Гольдхабера (см./I/ и последующие экспериментальные работы; на конференции - доклады/2-4/). Однако принципиальные основы корреляционного метода в его современном понимании разработаны в течение последних пяти лет/5-8/. Основная идея, взятая из астрономии/6,9/, имеет своим исходным пунктом классические работы Г.С.Горелика/10,11/, установившего наличие интерференционных свойств света, испускаемого независимыми источниками. Применительно к пионам эта идея достаточно широко обсуждена в указанной выше литературе. Речь идет о бозе-симметризации амплитуды регистрации двух тождественных пионов, испущенных в разные моменты времени и из разных мест излучающего объема. В результате возникают интерференционные корреляции, повышающие вероятность регистрации тождественных пионов с близкими импульсами.

Соответствующие формулы модельно зависимы, но имеют общую структуру. Если, например, источники "включаются" одновременно и расположены на поверхности сферы радиуса R, а их время жизни $\tau \gg R/c$, то вероятность наблюдения пионов с импульсами $\vec{p}_1$ и $\vec{p}_2$

$$W = W_0(1+\Delta),\ \Delta = \frac{[2J_1(q_\perp R)/q_\perp R]^2}{1+(q_0\tau)^2} \simeq \frac{\exp[-\frac{1}{4}q_\perp^2 R^2]}{1+(q_0\tau)^2}. \quad (I)$$

Здесь $q_0 = E_1 - E_2$, $\vec{q} = \vec{p}_1 - \vec{p}_2$, $\vec{q}_\perp$ - проекция $\vec{q}$ на плоскость, перпендикулярную $\vec{\beta} = \frac{\vec{p}_1 + \vec{p}_2}{2}$. Множитель W_0 соответствует фоновому распределению без интерференции. Обычно для экспериментального определения W_0 используют пары $\pi^+\pi^-$, хотя такой выбор требует еще специального обсуждения.

Наблюдая корреляции пар $\pi^+\pi^+$ и $\pi^-\pi^-$, можно с помощью (I) измерить параметры R и τ. Можно также определить форму излучающей области, если сопоставить результаты для пар, вылетающих в разных направлениях.

В общем случае физический смысл величины τ довольно сложен. Она слагается из среднего времени жизни источников τ_1, разброса моментов "включения" источников τ_2 и "продольного времени" $\tau_3 = \frac{R}{V}$, где V - скорость отбираемых пионов.

При современном состоянии эксперимента можно надеяться измерить только некоторую комбинированную эффективную величину τ. В отношении величины R следует подчеркнуть, что она связана с расстоянием между источниками, поставляющими тождественные пионы с близкими импульсами. В статистических схемах это совпадает с полными размерами излучающей области, но в мультипериферических моделях R, вероятно, характеризует расстояние между соседними узлами диаграмм. Заметим еще, что если пионы рождаются не непосредственно, а в результате распада достаточно долгоживущих резонансов, величины R и τ определяются пробегом и временем жизни этих резонансов.

Высказывались опасения, что $\pi\pi$-взаимодействия в конечном состоянии могут существенно исказить нарисованную картину. Оценки, проведенные в/21/, показали, что это не так.

2. Экспериментальные результаты получены в работах/2,12-18/, где приведены спектры $q_\perp$ для различных значений q_0 и спектры q_0 для различных значений $q_\perp$. Параметры R и τ измерялись путем сопоставления двумерных распределений по $q_\perp$ и q_0 с выражениями типа (I); фоном в большинстве случаев служили пары $\pi^+\pi^-$. На рис. I и 2 приведены для примера некоторые из полученных распределений (рис. I из/2/, рис. 2 из/18/). Из совокупности указанных работ с несомненностью следует как само существование интерференционных корреляций тождественных частиц, так и двумерный характер этого эффекта.

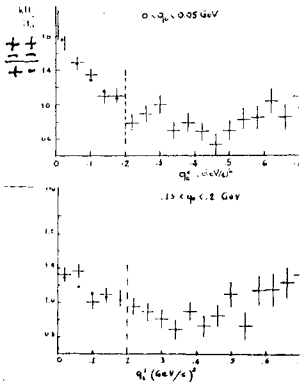

Рис. I

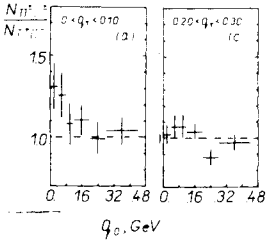

Рис. 2

В таблице дана сводка полученных результатов. По ряду обстоятельств их следует пока что считать предварительными. Отметим, в частности, что в большинстве случаев отношение $\frac{W(0,0)}{W(\infty,\infty)} < 2$, т.е. не согласуется с формулами типа (I). Это может быть связано со многими

Таблица

№ работы	Реакция	Импульс, ГэВ/с	R, Фм	$c\tau$, Фм
/2/	$\bar{p}n \to 3\pi^-2\pi^+n$	I,0+I,6	$I,29\pm0,06$	$I,47^{+0,I8}_{-0,I6}$
/I2/	$K^+p \to K^+p2\pi^+2\pi^-$	8,25	$0,8\pm0,08$	$\sim I,0$
/I3/	$pp \to p\pi\pi\ldots, n_c \geq 6$	28,5	$I,3\pm0,I$	$0,3\pm0,4$
/I4/	$\pi^\pm p \to \pi^\pm p 2\pi^+2\pi^-$ $\to \pi^\pm p 3\pi^+3\pi^-$	4+25	$I,0^{+0,4}_{-0,2}$	$0,7^{+0,6}_{-0,3}$
/I5/	$\pi^-p \to \pi\pi\ldots, n_c \geq 6$ $\pi^-C \to \pi\pi\ldots, n_c \geq 6$	40	$I,3\pm0,3$ $5,I\pm I,5$	$0,5\pm0,4$ $2,0\pm2,2$
/I6/	$\pi^-p \to p2\pi^+3\pi^-X^0$ $\to p2\pi^+3\pi^-$ $\to n3\pi^+3\pi^-$	II,2	$I,04\pm0,I$	$0,4I\pm0,I5$
/I7/	$\pi^-C \to p\pi^-\pi^-\pi^+\ldots$	3,7	$2,6\pm I,2$	$0,76\pm0,47$
/I8/	$\bar{p}p \to \pi\pi\ldots, n_c \geq 6$	22,4	$3,I\pm0,4$	$3,3\pm I,4$

причинами; не исключено, что существенную роль играют особенности использованного фона. Для пар $\pi^+\pi^-$ интерференционные корреляции отсутствуют в рамках простейших статистических моделей, но они могут иметь место для мультипериферических схем и даже для таких статистических моделей, в которых мезоны образуются в результате распада промежуточных резонансов. Это может понизить отношение $W(0,0)/W(\infty,\infty)$ и несколько изменить параметры R и τ. Из сказанного ясна важность специального изучения и сопоставления различных способов конструирования фона /I2,I5,I7/. Не исключено, что в некоторых случаях окажется целесообразным применять процедуры "перемешивания" вторичных частиц, описанные в /I9/.

Во всех работах величина τ оказалась довольно малой ($c\tau \lesssim R$). Поскольку одна из компонент τ имеет чисто геометрическую природу /6,I9/, истинное время жизни еще меньше, что плохо согласуется с наивными статистическими представлениями. Следует, впрочем, иметь в виду, что измеряемое значение τ зависит от скорости источника. Кроме того, ошибки в определении энергии также могут привести к фиктивному уменьшению величины τ.

Из работ /I4-I6/, по-видимому, следует, что в $\pi^\pm p$ -взаимодействиях при $n_c \geq 6$ величина $R \sim 1$ Фм и мало зависит от знака и энергии первичных частиц в интервале от 4 до 40 ГэВ/с. Интересно, что такое же значение R получено также для взаимодействий K^+p при 8,25 ГэВ/с /I2/ и pp при 28,5 ГэВ/с /I3/. Иначе ведут себя аннигиляционные процессы. При импульсе (I+I,6) ГэВ/с величина R примерно такая же, как для πp- и pp -взаимодействий /2/. Однако с увеличением энергии R сильно растет /I8/. Вместе с тем параметры удара в процессах с аннигиляцией, по-видимому, в несколько раз меньше, чем в процессах без аннигиляции /20/. Причины этих различий пока что неизвестны.

Следует подчеркнуть, что "корреляционные размеры" не должны обязательно совпадать с размерами, определяемыми из анализа поперечных импульсов вторичных частиц или с помощью данных по упругому рассеянию. В каждом из этих случаев мы получаем информацию о различных сторонах сильных взаимодействий. Поэтому все указанные подходы надо считать не конкурирующими, а дополняющими друг друга.

С связи с исследованиями в области релятивистской ядерной физики интересны корреляции тождественных частиц, образующихся во взаимодействиях с участием ядер. В настоящее время известны такие результаты по $\pi\pi$ -корреляциям в π^-C -взаимодействиях при 3,7 ГэВ/с /I7/ и 40 ГэВ/с /I5/. В обеих работах отмечается сильное увеличение R по сравнению с πp -взаимодействиями. Интересно было бы выяснить, как

ведут себя $\pi^+\pi^-$-корреляции (а также корреляции между быстрыми протонами) при переходе к более тяжелым ядрам.

Выше уже отмечалось, что корреляционный анализ, в принципе, позволяет получить представление о форме излучающей области. Такие попытки были предприняты при изучении π^+p -взаимодействий[14] и $\bar{p}p$ -взаимодействий[15]. В обеих работах получены указания на отступления от сферы, однако в первом случае речь идет об эллипсоиде, сжатом в направлении движения первичных частиц, а во втором случае - о вытянутом эллипсоиде. Дальнейшее изучение этого вопроса представляет несомненный интерес.

Корреляции тождественных частиц имеют, по-видимому, непосредственное отношение к азимутальным корреляциям и к корреляциям поперечных импульсов, но этот вопрос выходит за рамки моей темы. Недостаток времени не позволяет также обсудить методы определения параметра удара и сопоставить их с корреляционным методом.

Итоговый вывод таков: изучение корреляций тождественных частиц может дать новые важные сведения о свойствах сильных взаимодействий, если удастся существенно повысить точность экспериментальных данных. Вероятно, это обстоятельство потребует более широкого использования электронных методик, хотя пузырьковые камеры тоже не сказали еще здесь своего последнего слова.

Литература

I. G.Goldhaber, S.Goldhaber et al., Phys.Rev., 120, 300 (1960).
2. G.Borreani, F.Marchetto et al., 112/A2-66.
3. N.N.Biswas, J.M.Bishop et al. 1022/A2-107.
4. A.Quareni-Vigundelli, G.Di Caporiacco et al., 1202/A2-132.
5. Б.Г.Гришин, Г.И.Копылов, М.И.Подгорецкий. ЯФ, I3, III6 (I97I).
6. Г.И.Копылов, М.И.Подгорецкий. ЖЭТФ, 69, 4I4 (I975); см. также литературу, цитированную в этой статье.
7. E.V.Shuryak. Phys.Lett., 44B, 387 (1973).
8. G.Cocconi. Phys.Lett., 49B, 459 (1974).
9. R.Hanbury Brown, R.Q.Twiss. Phil.Mag., 45, 663 (1954).
I0. Г.С.Горелик. ДАН СССР, 58, 45 (I947).
II. Г.С.Горелик. ДАН СССР, 83, 549 (I952).
I2. F.Grard, V.P.Henry et al. Nucl.Phys., 102B, 221 (1976).
I3. J.Canter, F.T.Dao et al. BNL-20516 (1975).
I4. M.Deutschmann, R.Honecker et al. Nucl.Phys., 103 B, 198 (1976).
I5. N.Angelov, L.A.Didenko et al. 205/A2-108.
I6. E.Calligarich, G.Cecchet et al. Lett. Nuovo Cim., 16, 129 (1976).
I7. Ю.Д.Баюков, В.Б.Гаврилов и др. ИТЭФ-70 (I976).
I8. А.А.Локтионов, К.С.Такибаев и др. I60/A2-I0.
I9. G.I.Korylov, M.I.Podgoretsky. Commun. JINR, E2-9285, Dubna, 1975.
20. H.Braun, P.Fischer et al. 377/A2-109.
2I. Г.И.Копылов. 939/A2-II9.

MULTIPLE PRODUCTION ABOVE 10^{14} eV

N.N.Roinishvili
Institute of Physics of the Academy of Sciences of GSSR, Tbilisi

1. Introduction

There are 5 contributions presented to the Conference concerning multiple production above 10^{14} eV.

i. The main problem discussed in all of them is the following. Are the experimental data at very high energy ($\sim 10^{15}$ eV) in agreement with extrapolations of data obtained at the accelerators ($\sim 10^{12}$ eV)?

In most of them the answer is more or less, but negative.

ii. All the papers presented used an indirect method of evaluating results.

As it is at present impossible to investigate individual hadron-hadron interactions their arguments are based on properties of nuclear-electromagnetic cascades (NEC) induced by a high energy hadron in the atmosphere or in solid substance.

iii. Depending on lower energy limit of detected particles two kinds of phenomena are observed.

1. Extensive air showres (EAS) are NEC at the age when they are almost in equilibrium of their development. Main component of EAS are electrons, muons and hadrons, the number of which is about 10^5-10^6. Suitable arrangement for their detection covers km^2. Threshold energy $E_{th} \sim 1$MeV.

2. γ and hadron families are young NEC in which a number of first step of generations is detected. Main component of the families are photons, electrons and hadrons. Suitable arrangements are the so-called x-ray emultion chambers ($E_{th} \sim$ (1-2) TeV).

2. EAS Results

EAS data are analysed in two contributions, presented by Moscow State University[1] and the English-Polish group[2].

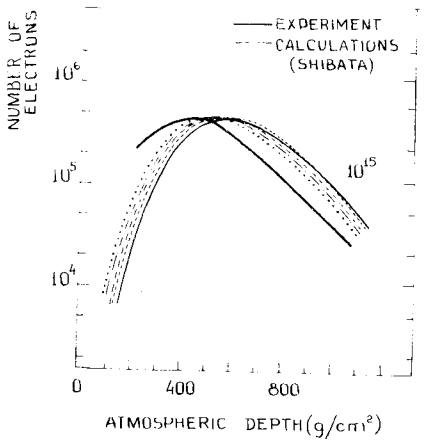

Fig.1 shows the average cascade curve of EAS at 10^{15} eV[2]. Full line denotes experimental data, dotted lines, various extrapolations of accelerator data.

As is seen, EAS develops more rapidly than it is expected.

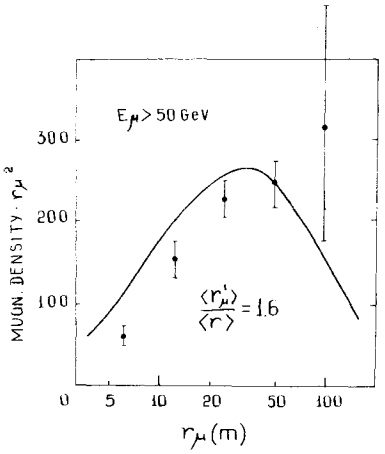

Fig.2.(MSU result, presented by the English-Polish group) Lateral distribution of the high energy muons. The figure proves that the fast development of EAS relates to the hadronic component as well.

Another piece of information comes from correlations between various components of EAS[1].

The authors of both the contributions are analysing a number of possible reasons of such disagreement:

change of chemical composition of primary cosmic ray,

increase of nucleon-antinucleon pair production and others.

They came to the conclusion that the best explanation is based on the assumption: the

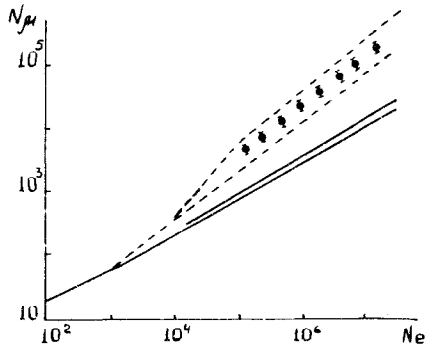

Fig.3. Multiplicity of muons in showers with given number of electrons is by an order of magnitude higher than expected.

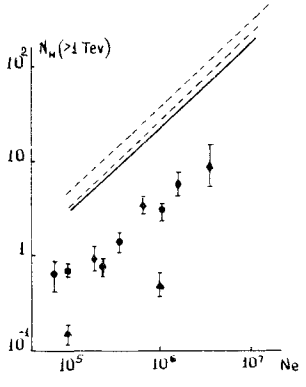

Fig.4. Multiplicity of hadrons is by an order of magnitude lower than expected.

average multiplicity increases as $\langle n \rangle \sim E^{1/4}$ or even more rapidly above 10^{14} eV.

3. Families Results

During the last three years 7 Soviet and 2 Polish institutes exposed x-ray emulsion chambers with total area ~ 1000 m^2 in Pamir mountains (Pamir collaboration)[3]. Two reports concerning the work are presented. The experimental one is based on analyses of 230 families with total energy $\Sigma E \geq 30$ TeV ($E_0 \gg 10^{14}$ eV). The second report presents NEC calculations of checked various models having inclusive spectra like that obtained on the accelerators[4].

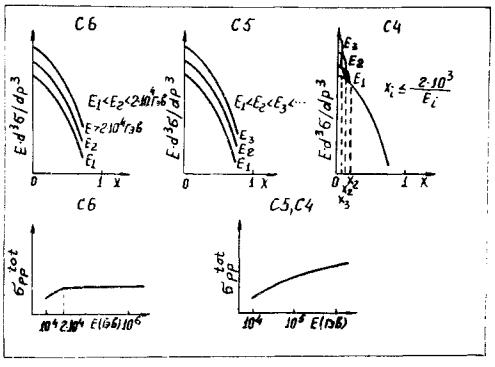

Fig.5 shows a typical property of used models.

In C6 σ_{tot} rise only till 10^{14} eV. According to it inclusive spectra of pions change in the whole region of x from 0 to 1.

In C5 and C4 $\sigma_{tot} = (3.6 \ln E_0 + 40.7)$ mb

In C5 inclusive spectra changed as in C6, and in C4 only the pionisation region violates the scaling.

It is shown in the report that the flux of hadrons and photons obtained by Pamir collaboration can be explained better by C4 model.

The most direct result is presented in the experimental paper of Pamir collaboration[3] (Fig.6). It is integral distribution of f' variable normalised to one family. f' is an analog of x-variables for nuclear electronic cascade. It is the fraction to total energy carried out by given photons $f' = E/\Sigma' E$. In this analysis f'_{min} is independent of $\Sigma' E$ and equal to 0.04.

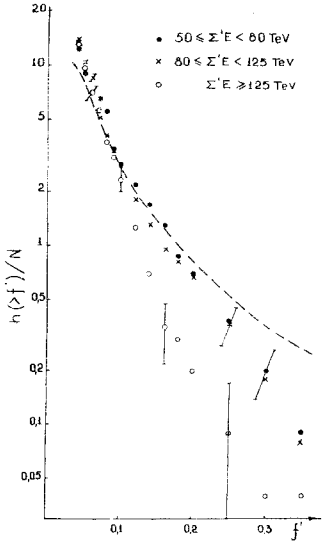

Fig.6

It can be shown that if scaling holds in fragmentation region then f' spectra do not depend on the ΣE .

As one can see from Fig.6, starting from 10^{14} eV f' spectra indicate that it is not the fact. Unfortunately, statistics is still poor. In the nearest future better statistics will be available in Pamir experiment.

§4. Results Obtained by NEC in Solid Substances

The serious change of elementary act at 10^{14} eV is presented by Lebedev Physical Institute[5]. By means of ionization calorimeter in Tian Shan mountains, the authors were studying NEC properties in lead. They observed that

i. The fraction of the energy of primary hadron transferred to π^0 ($K_{\Sigma^0} \simeq 17\%$) is independent of the energy until 30 TeV.

ii. An attenuation length which at lower energy is equal to $3\lambda_{int}$ sharply increases at E $\sim 10^{14}$ eV (Fig.7).

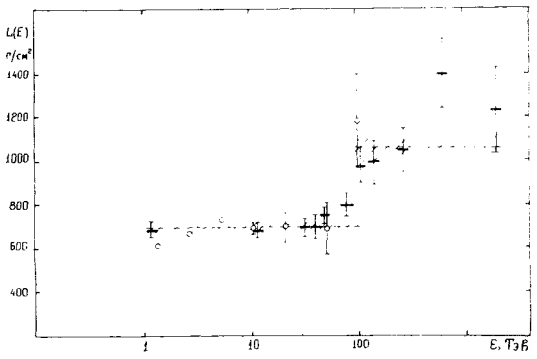

Fig.7

One of the simplest explanation of the result is the production of a new unstable particle with $\sigma_{in}(\alpha K)$ 2 or 3 times less than σ_{in}^{hh} (or K^{hh}).

References

Papers contributed to the conference.

1. S.N.Vernov et al. 778/A2-110.
2. J.Olejniczak et al. 194/A2-29.
3. V.K.Budilov et al. 169/A2-1.
4. A.M.Dunaevsky et al. 803/A2-84.
5. V.P.Pavljuchenko et al. 168/A2-2.

INCLUSIVE REACTIONS AT MEDIUM ENERGIES

W.Kittel

University of Nijmegen, Netherlands

Two interesting questions studied in inclusive reactions at medium energies are those of inclusive resonance production and strange baryon production. The first has been treated by P.Schmid[1], so I can concentrate on strange baryon production.

At medium energies, the inclusive $K^-p \to \Lambda^c X^c$ cross section decreases like about $p_{LAB}^{-0.5}$, while the $K^-p \to K^0\Lambda^c$ cross section increases slightly[2]. The $\pi^-p \to \Lambda^0 X^0$ structure function shows approximate scaling for $X \gtrsim -0.8$ between 5 and 205 GeV/c, while it grows by a factor 3 at $X \simeq 0$ for $\pi^-p \to K^0 X^0$ in the same energy range[3].

A high statistics measurement of the Λ^0 polarization P in $K^-p \to \Lambda^0$ + pions at 4.2 GeV/c[4] shows (fig.1) that P is positive for $X \lesssim -0.5$

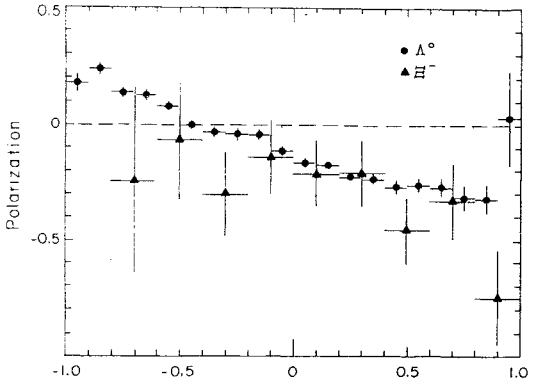

Fig.1. Polarization of the Λ^0 and Ξ^- from $K^-p \to \Lambda^0 X^0$ and $K^-p \to \Xi^- X^+$ at 4.2 GeV/c.

and negative above in this reaction. From comparison to higher energies[5] we deduce that P decreases with energy for $X \lesssim -0.5$ while it is constant for $X \gtrsim -0.5$. The Ξ^- polarization from $K^-p \to \Xi^- X^+$ at 4.2 GeV/c[6] is given in the same figure. It compares well with that of the Λ^0 in the region where the Ξ^- structure function is large ($X \gtrsim -0.5$).

On the other hand, the polarization of Λ^0's produced in $\pi^-p \to \Lambda^0 X^0$ at 8 GeV/c[7] vanishes for $0 < X \leq 0.6$ and rises to $P = 1$ for $X \to 1$. In $\bar{p}p \to \Lambda^0 X^0$ studied at 5.7 GeV/c[4] the Λ^0 polarization is small or negative for $X < 0$; a similar behaviour is found for Λ^0's from $K^-p \to \Lambda^0 + K\bar{K} +$

pions at 4.2 GeV[4]. These observations are in qualitative agreement with the similarities or differences of the triple-Regge diagrams possibly contributing to the above reactions.

Quantitative results can be obtained for the effective trajectories in triple-Regge diagrams, even at energies where the conditions for the triple-Regge expansion are not satisfied. In agreement with the observed polarization, the p-trajectory was shown to dominate $K^- \xrightarrow{p} \Lambda^0$ beam fragmentation at 4.2 GeV/c[8]. For $p \xrightarrow{K^-} \Lambda^0$ target fragmentation at 4.2 GeV/c the effective trajectory lies between the K and K^* trajectory[8], for $K^+ \xrightarrow{p} \Lambda^0$ at 8.2 and 16 GeV/c[9] the data are consistent with the K trajectory (fig.2).

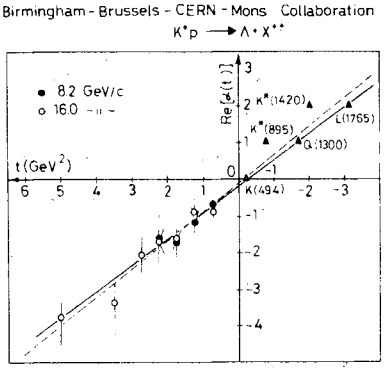

Fig.2. Effective trajectory points for $K^+ p \to \Lambda^0 X^{++}$ target fragmentation. The dashed line is a fit through the data at 8.2 and 16.0 GeV/c, the solid line is the trajectory drawn through the K, Q and L positions.

At medium energies, the mass distribution of X is dominated by resonance production. This can be described by the triple-Regge expansion only in an average sense[10]. For target fragmentation $p \xrightarrow{K^-} \Lambda^0$ at 4.2 GeV/c, the off-shell forward $K\bar{K}$ and $K^*\bar{K}$ scattering amplitude is written as a sum of Veneziano four-point amplitudes plus diffractive terms[11]. Leaving 11 coupling constants as free parameters gives the fit to the m_X distribution shown in fig.3 for various t intervals. Five of these eleven couplings determine the target fragmentation $p \xrightarrow{K^-} \Sigma^+$. The m_X distribution for this reaction is reproduced without further fitting, also for various t intervals.

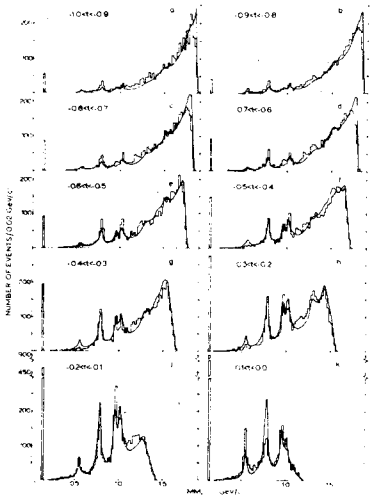

Fig.3. Missing mass produced against the Λ^0 in $K^- p \to \Lambda^0 X^0$ target fragmentation at 4.2 GeV/c for ten $t_{p\Lambda}$ intervals between -1,0 and 0,0 GeV^2. The curves are from the fit described in the text.

The inclusive Σ (1385) cross section falls for $\Sigma^+(1385)$ production at medium energies and is constant for $\Sigma^-(1385)$ production[12]. While $\Sigma^-(1385)$ is predominantly produced around $X=0$, $\Sigma^+(1385)$ has a leading particle peak around $X \simeq -0.8$, in particular at 4.2 GeV/c. The decay distribution of $\Sigma^+(1385)$ is in agreement with prediction of the additive quark model.

References

1. P.Schmid."Inclusive Part. and Resonance Spectra - an Attempt to Separate Directly Produced Particles from Decay Products" Invited talk in this session.
2. ANL-Brussels-Kansas-Michigan-Tufts Collaboration, B.Musgrave et al. "Inclusive V^0-Production in $K^- p$ Interaction at 6.5 GeV/c". Paper 366/A2-59.
3. Dubna-Tbilisi-Kosice-Erevan-Minsk-Collaboration, Yu.A.Budagov et al."Inclusive Λ^0 and K^0-Production in $\pi^- p$ and $\pi^- C$ Interactions at 5 GeV/c". Paper 811 / A2-82.
4. Amsterdam-CERN-Nijmegen-Oxford Collaboration "Study of Λ -Polarization in 4.2 GeV/c $K^- p$ and 5.7 GeV/c $\bar{p}p$ Interactions. Paper 272/A2-50.
5. I.Bartsch et al. Nucl.Phys., B40, 103 (1972); S.U.Chung et al. Phys.Rev., D11, 1010 (1975); M.Abramowicz et al. Nucl.Phys., B105, 222 (1976).
6. Amsterdam-CERN-Nijmegen-Oxford Collaboration "A Study of Inclusive Ξ^- Production from $K^- p$ Interactions at 4.2 GeV/c" paper 276/A2-51.

7. Freiburg-Saclay-Zurich Collaboration, "Preliminary Results on Incl. Forward Λ -Production in $\pi^{\pm}p$ and $K^{-}p$ Interactions at 8 and 12 GeV/c" Paper at this Conference.
8. R.Blokzijl et al. Nucl.Phys., B48, 401 (1975).
9. CERN-Birmingham-Brussels-Mons Collaboration, P.V.Chliapnikov et al. "The Reactions $K^{+}p \to \Lambda X^{++}$ and $K^{+}p \to \bar{\Lambda} X^{++}$ at Incident Momenta of 8.2 and 16.0 GeV/c", paper 1060/A2-75.
10. Chan Hong-Mo, H.I.Miettinen and R.G.Roberts. Nucl.Phys., B54, 411 (1973).
11. Amsterdam-CERN-Nijmegen-Oxford Collaboration, R.Blokzijl et al. Dual Analysis of Target Fragmentation in $K^{-}p \to \Lambda X$ and $K^{-}p \to \Sigma^{\mp} X$ at 4.2 GeV/c" paper 279/A2-78.
12. Aachen-Berlin-CERN-London-Vienna Collaboration, "Inclusive Production of $\Sigma^{\mp}$ (1385) in $K^{-}p$ Interactions at 10 and 16 GeV/c", paper 144/A2-111.
I.D.Aljolhin et al. "Σ^{*}(1385) and K^{*} Resonance Production in $\pi^{-}p$ Interactions at 4.35 and 4.85 GeV/c", paper 190/A2-23.
Amsterdam-CERN-Nijmegen-Oxford Collaboration, "Study of $\Sigma^{\mp}$(1385) Inclusive Production in $K^{-}p$ Interactions at 4,2 GeV/c", paper 278/A2-52.

INCLUSIVE π^{o} AND γ PRODUCTION IN PION-PROTON INTERACTIONS AT 5 GEV

Yu.A.Budagov, L.Šándor

JINR, Dubna

One meter JINR propane bubble chamber collaboration (Dubna-Košice-Tbilisi-Yerevan-Minsk) studied the inclusive neutral particle production ($\pi^{o}, \gamma, \Lambda^{o}, K^{o}$) in 5 GeV pion-nucleon interactions. Some results are presented in this report and compared with high energy experimental data.

Previously we have measured the cross sections of many different exclusive reactions $\pi^{-}p \to$ $(0,2,4)$ charged particles + $(1,2,3,4,5)\pi^{o}$ and $\pi^{-}p \to (0,2,4)$ charged particles + $(\geq 1\nu^{o}) + (\geq 1\pi^{o})$. Together with the data of other groups they form almost a complete set of 5 GeV $\pi^{-}p$ -scattering partial cross sections[1]. This allowed one to obtain new data on the multiparticle production.

The π^{o} multiplicity distribution at 5 GeV is close to Poisson form with $f_2^{\omega} = -0.07 \pm 0.10$; at 40 GeV this distribution becomes wider[2].

The analysis of the total multiplicity $n = n_{+} + n_{-} + n_{o} + 1$ distribution for the reaction $\pi^{-}p \to n_{+}\pi^{+} + n_{-}\pi^{-} + n_{o}\pi^{o} + N$ at our energy and at 10, 16, 40 GeV (other groups measurements) shows[3] that the logarithm of the integrated probability of $\geq n$ particle production $F(n)$ is a linear function of the reduced multiplicity squared: $F(n) \sim (n-2)^2$ (see Fig.1).

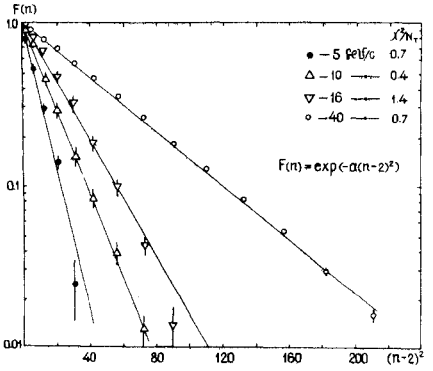

Fig. 1

The multiplicity distribution for the "newly produced" particles $n' = n - \alpha$ (α – the average number of leading particles[4]) in 5–40 GeV interval follows the KNO-scaling (Fig.2). With $\alpha = 2$ the universal function $\psi(z' = n'/\langle n' \rangle)$ has the form $\psi(z') = \frac{\pi}{2} z' \exp\left(-\frac{\pi}{4} z'^2\right)$

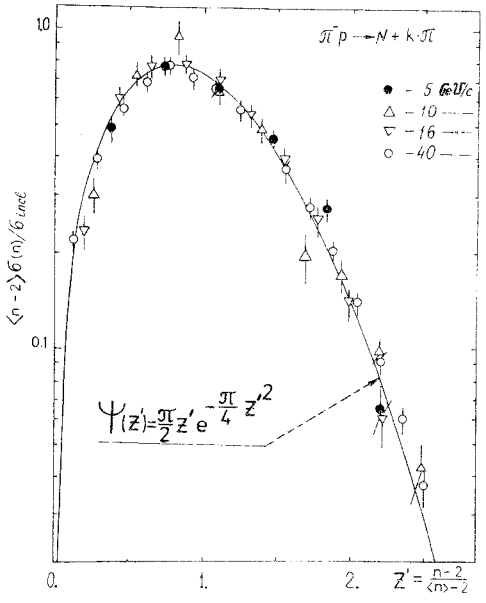

Fig. 2

This function with $\alpha = 0.7$ describes satisfactory also the charged-particle multiplicity distributions for the πp, Kp and pp -interactions above 20 GeV[5].

The analysis of the correlations in the yields of π^0-s and charged secondaries for 5–205 GeV $\pi^- p$ collisions gave the following results[6]. The dependence $\langle n_0 \rangle_{n_-} = f(n_-)$ is satisfactorily described by linear function $f(n_-) = a + b n_-$. The values of the b parameter are the same within error limits for the $\pi^- p$ and pp interactions in the whole energy interval studied.

Fig.3 represents the correlation integrals f_2^{--} and f_2^{0-} as a function of incident momentum. The approximating function $f_2^{--} = 0.86 - 1.15 \ln s + 0.16 (\ln s)^2$ is shown by the full line. The dashed line corresponds to the relation $f^{0-} = f_2^{--} + \frac{1}{2}\langle n_- \rangle$.

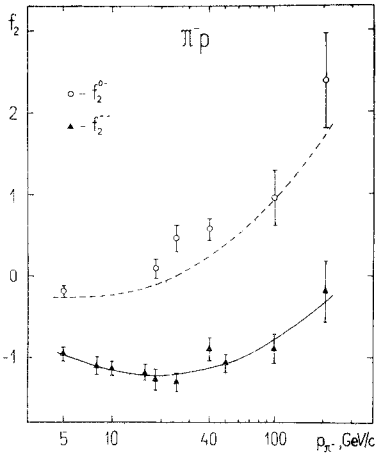

Fig. 3

The deviation from the dependence $f_2 \sim \ln s$ gives evidence to a noticeable contribution of the long-range correlations. The experimental data agree with the relation $f_2^{0-} = f_2^{--} + \frac{1}{2}\langle n_- \rangle$; within the Regge-Mueller approach it shows that the contribution of diagrams with isospin $I \geq 2$ exchange is small.

The study of the scaling properties of the semi-inclusive π^0 cross sections for 5–205 GeV/c $\pi^- p$ scattering[7] shows that for the momentum range $p_{\pi^-} < 40$ GeV/c the Dao-Whitmore relation $\langle n \rangle \sigma_n(\pi^0)/\langle n_0 \rangle \sigma_{in} \to \Phi(z = \frac{n}{\langle n \rangle})$ is not valid (n – the charged-particle multiplicity). At the same time there is an obvious similarity of the $\langle n \rangle \sigma_n(\pi^0)/\langle n_0 \rangle \sigma_{in}$ distributions in the whole energy interval studied. We have noticed that the variety of the experimental data may be regularized if one introduces the scale transformation $z_1 \sim z + \frac{\beta}{\langle n \rangle^2}$ with $\beta = \text{const}$. It gives the universal description for the whole experimental results available.

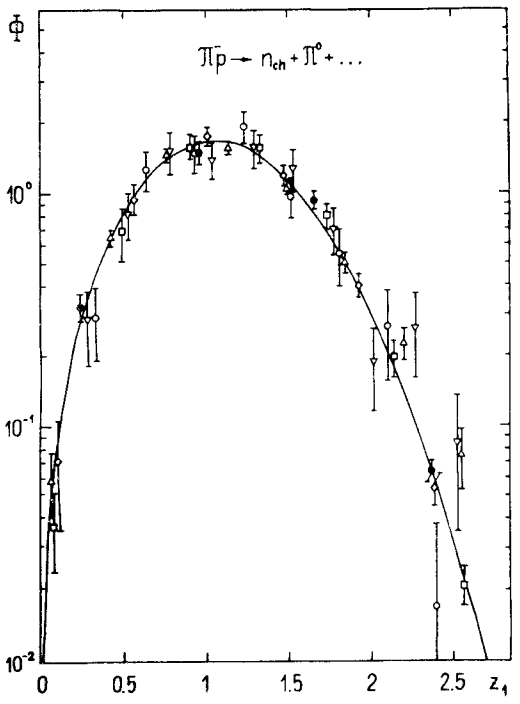

Fig. 4

In Fig.4 the values of $\langle h \rangle \sigma_n(\pi^0)/\langle n_0 \rangle \sigma_{in}$ for 5 GeV - ●, 18.5 GeV - ◇, 25 GeV - □, 40 GeV - △, 100 GeV - ○ and 205 GeV - ▽ $\pi^- p$ collisions as a function of new variable z_1 are plotted. Solid line - approximating function $\varphi(z_1) = a_0 z_1 \exp(a_1 z_1 + a_2 z_1^2)$

If the proposed energy dependence should be valid at higher energies too, the result obtained may be interpreted as the quantitative description of the approach to asymptotics for the $\langle h \rangle \sigma_n(\pi^0)/\langle n_0 \rangle \sigma_{in}$ distribution.

We have measured the differential cross section

$$\frac{E^*}{\pi p^*_{max}} \frac{d^2\sigma}{dx\, dp_\perp^2} = f(x, p_\perp)$$

for the reaction $\pi^- p \to \gamma + \ldots$ at 5 GeV/c in a large range of x and $p_\perp$ using the statistics of ≈ 10000 γ-quanta[8]. The results are given in Fig.5.

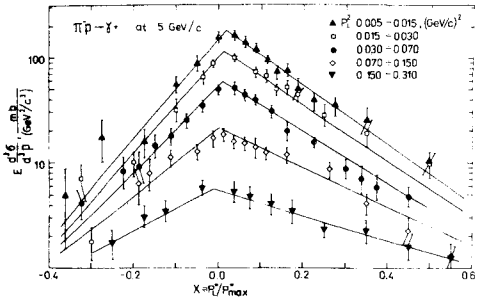

Fig. 5

The experimental data are satisfactorily approximated by the function $f(x,p_\perp) = a_1 \exp(-B|x| + a_4 p_\perp)$, $B = a_2 \exp(-a_3 p_\perp^2)$; where a_i are the free parameters. The function $f(x,p_\perp)$ does not factorize with respect to x and $p_\perp$ at energy of 5 GeV.

We have shown earlier[9] that the differential cross sections $\int E \frac{d^3\sigma}{d^3p} dp_\perp^2$ of the reaction $\pi^- p \to \gamma + \ldots$ are energy independent a) in the central region for 5-100 GeV interval and b) in both fragmentation regions for 5-40 GeV primary energy interval.

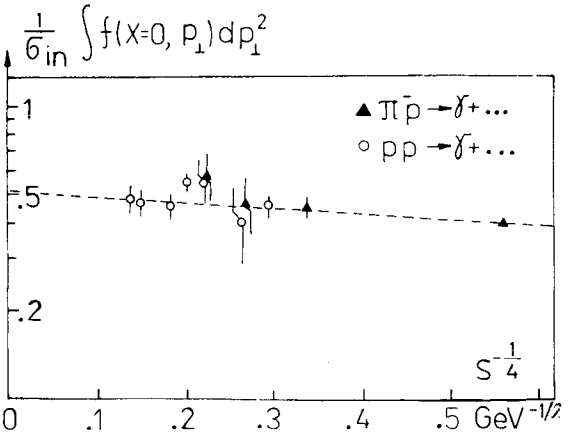

Fig. 6

Fig.6 represents the normalized differential cross sections $\frac{1}{\sigma_{in}} \int f(x=0, p_\perp) dp_\perp^2$ for γ-production in the momentum range of incoming particles (π^- and p) from 5 to 1500 GeV/c. The straight line is a handdrawn one. The essential feature of this picture is a significant difference

from the analogous dependence for charged particle production.

References

1. N.S.Amaglobeli et al. JINR, E1-9817, Dubna, 1976.
2. N.Angelov, V.G.Grishin, P.Kerachev.Yad.Fiz., 21, (1975) 1298.
3. N.S.Amaglobeli et al. JINR, E1-9820, Dubna, 1976.
4. A.J.Buras, J.Dias de Deus, R.Møller. Phys. Lett., 47B (1973) 251; A.Bassetto, J.Dias de Deus. Lett. Nuovo Cim., 9 (1974) 525.
5. N.S.Amaglobeli et al. JINR, P1-9847, Dubna, 1976.
6. Yu.A.Budagov et al. Paper 810/A2-110 presented to this Conference; to be published in Czech.Journ.Phys.B.
7. Yu.A.Budagov et al.JINR, E1-9501,Dubna,1976.
8. N.S.Amaglobeli et al.JINR,E1-9854,Dubna,1976.
9. N.S.Amaglobeli et al. Yad.Fiz.,22 (1975) 1269.

NET CHARGE DISTRIBUTION IN RAPIDITY AND TRANSVERSE MOMENTUM FOR SEMI-INCLUSIVE π^-P INTERACTIONS AT 11.2 GEV/C

(Bologna, Firenze, Genova, Milano, Oxford, Pavia Collaboration)

S.P.Ratti* - Instituto di Fisica Nucleare and Sezione I.N.F.N. - Pavia (Italy)

We present an analysis of the net charge density distributions in π^-p collisions at 11.2 GeV/c, studying how electric charge gets distributed, for different topologies, as a function of rapidity Y and transverse momentum p_T. Following the notations of previous papers[1,2] we define:

$$\rho_n^{(\vec{p})} = \frac{1}{N^{(n)}}\left\{\frac{dN^{(+)}(\vec{p})}{d\vec{p}} - \frac{dN^{(-)}(\vec{p})}{d\vec{p}}\right\} = \rho_n^{(+)}(\vec{p}) - \rho_n^{(-)}(\vec{p}), \quad (1)$$

where n is the topology, $dN^{(+,-)}(\vec{p})/d\vec{p}$ is the number of positive (negative) particles produced in a given interval of any kinematical variable $\vec{p}$ (in our case; Y and p_T) and N^n is the total number of events of a given topology.

The experimental data have been collected in a~850.000 picture exposure of the CERN 2m HBC exposed at the CERN PS to a π^- beam of 11.2 GeV/c. A total of 49593 two prongs, 107173 four prongs and 36656 six prongs is used. When necessary, proton tracks have been identified with a method developed by our collaboration[3,4].

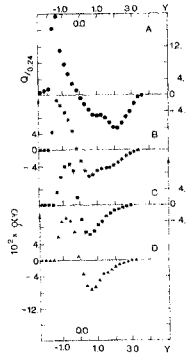

Fig.1. Charge density distributions $\rho(Y)$; A)two prongs; B)four prongs; C) six prongs; D) cut four prongs $t'>0.4$ (GeV/c)^2.

* Co-authors are: R.Attendoli, E.Calligarich, G.Cecchet, R.Dolfini, L.Mapelli (Pavia); A.Quareni-Vignudelli (Bologna); S.Berti, A.M.Cartacci (Firenze); G.Tomasini, U.Trevisan (Genova); G.Costa, L.Perini (Milano); D.Radojicic, G.Thompson (Oxford).

The charge density distributions in rapidity $\rho(Y)$ are shown in figs. 1a,b,c. The data show structures which were not clearly seen in previous similar analyses[1,2,5]. The sharp peak in positive charge excess at $Y \simeq -1.3$ in two prongs becomes, with increasing topology, broader and smaller. For six prongs, the position of the maximum shifts at $Y \simeq -0.7$. In the region of $Y > 0$, an interesting effect is present in two and four prongs but not in six prongs. In figs.1a and 1b, two minima are visible around $Y_1 \simeq 0.8$ and $Y_2 \simeq 2.4$. The contributions to the two accumulations are however of different importance. In fig.1a the excess at Y_1 is $\rho_1 \simeq 5\%$ and at Y_2 is $\rho_2 \simeq 8\%$, while the opposite occurs in fig.1b. The charge excess in six prong at Y_1 (fig.1c) is $\rho_1 \simeq 8\%$. A similar behaviour could be seen in ref.(1) for $\pi^- \bar{p}$ data, but there the topologies were added and, as a result, the effect is smeared out.

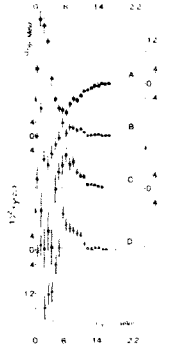

Fig.2. Charge density distributions $\rho(p_T)$; A) two prongs; B) four prongs; C) six prongs; D) cut four prongs $t' > 0.4$ (GeV/c)2.

The distributions of $\rho(p_T)$ are shown in figs.2a,b,c. Again, they display topology dependent structures (positive excess at small p_T in two and four prongs, no positive excess in two prongs for $p_T \geq 0.4$ GeV/c).

In figs.3a,b,c the distributions of the charge density $\rho(Y, p_T)$ are shown by means of equal-level curves: $10^2 \times \rho(Y, p_T) = 0.0; 0.4; 0.8; \ldots$ in units [Q] (0.08 GeV/c x 0.24). The structures, whose presence was detected in figs.1a,b, become clear and separated. On the line of the most probable transverse momentum ($p_T \simeq 0.25$ GeV/c), peaks in charge excess are well visible. The position of the positive charge excess for six prongs at a smaller $|Y|$ (fig.3c) is due to the multiplicity and to the presence of the massive nucleon. The splitting of the accumulation in p_T, is a consequence of the following facts; the p_T distributions are slightly different for protons and for negative pions[6,7]; the total negative charge $Q = -3$ is large in six prongs; the position in Y of the positive excess in six prongs is much nearer to $Y = 0$ than in two and four prongs[6]. In figs. 3a and 3b, the positive excess ($\simeq 0.8\%$) has similar extension and the same position. The relative importance of the two negative excesses for $Y > 0$ (e.g. at the level of $\simeq -0.8\%$) is clearly seen from the figures.

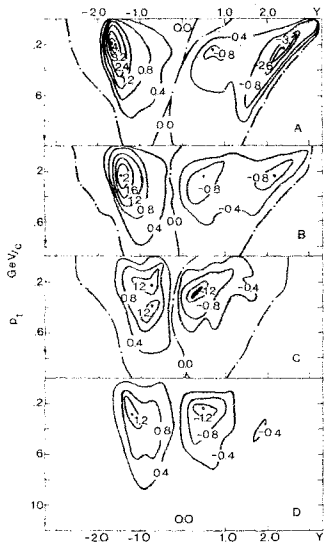

Fig. 3. Charge distributions $\rho(Y, P_T)$. Equal-level curves; A) two prongs; B) four prongs; C) six prongs; D) cut four prongs $t' > 0.4$ (GeV/c)^2.

An appealing explanation of the observed complex structures is the leading particle effect and/or diffraction dissociation, present in two and four prongs, but not in six prongs, at our energy.

To investigate this point we have performed several cuts and selections on both two and four prong events. For the sake of brevity, we show how a very simple cut on four prongs supports this explanation. In fact, by selecting $t' > 0.4$ (GeV/c)^2 (where $t' = t'_{beam,(3\pi)^-}$) all distributions of the four prong events are reduced identically to those of the six prong topology (apart from the splitting in p_T of the positive excess).

For cut four prong events $\rho(Y)$ is shown in fig.1d; $\rho(p_T)$ in fig.2d and $\rho(Y,p_T)$ in fig.3d. The cut antiselects about 40% of the four prongs (61670 events surviving). The negative excess at Y_2 disappears both in fig.1d and in fig.3d; the positive excess at small p_T in fig.2d is absent and the figures can be directly superimposed to figs.1c,3c and 2c respectively. A similar procedure can be applied to the two prong events.

References

1. U.Idschok et al. Nuclear Phys. B67,93(1973).
2. T.Ferbel.U. of R. preprint COO-3065-91 (1974).
3. A.Forino et al.Nuovo Cimento 31A,696(1976).
4. A.Quareni-Vignudelli et al.Paper submitted to this Conference.
5. E.K.Kladnitskaya et al. Paper n.163 to this Conference.
6. P.Borzatta et al. Nuovo Cimento 15A,45(1973).
7. e.g. see R.Slansky. Physics Reports 11C,100 (1974).

A SEARCH FOR NEW NEUTRAL PARTICLES PRODUCED IN HIGHLY INELASTIC π^+ PROTON COLLISIONS AT 10.5 GEV/C

J.R.Elliott, L.R.Fortney, A.T.Goshaw, J.W.Lamsa, J.S.Loos, W.J.Robertson, W.D.Walker, W.M.Yeager
Physics Department, Duke University, Durham, North Carolina 27706

C.R.Sun, S.Dhar
Physics Department, State University of New York, Albany, New York 12222

In recent years, detailed inclusive studies have been made of the charged particle spectrum coming from high energy hadronic interactions. In contrast, many simple but basic properties of the neutral particle spectrum still remain unexplored. We have done an experiment which makes an analysis of the neutral particle spectrum coming from 10.5 GeV/c π^+ proton interactions in which a large fraction of the available energy goes into neutrals. The experiment is designed to determine if all the energy carried away by neutral particles can be accounted for by photons, K^0's, Λ^0's and neutrons. It uses the 4π solid angle detection properties of a bubble chamber and has two distinct advantages over most other neutral particle searches. First, it is sensitive to new neutral particles produced in multineutral final states (in contrast to missing mass experiments). In addition, it does not rely upon any particular decay characteristics of the neutral particle.

The data were taken from an exposure of the SLAC 82'' bubble chamber filled with a hydrogen-neon mixture (30 molar percent neon) and exposed to a 10.5 GeV/c π^+ beam. We select 2 and 4 prong events with one identified proton and net-charge +2. This event sample consists of both neon and hydrogen interactions with about 65% of the events being free proton collisions. These are dominated by the processes

$$\pi^+ p \longrightarrow \pi^+ p + (\text{neutrals})$$
$$\longrightarrow \pi^+ p \pi^+ \pi^- + (\text{neutrals}).$$

The event distribution as a function of the lon-

gitudinal laboratory momentum of the neutrals is shown in Fig.1. Most of this neutral momentum is carried away by gamma rays coming from π^0 and η^0 decays. For the purpose of this study, we will group all short lived sources of gamma rays into one category and measure their total contribution to the neutral momentum spectrum. This is done from the gamma ray pair production in the hydrogen-neon liquid (the average gamma detection efficiency is 25%). The next most important contribution to the neutral momentum comes from K^0 production. We measure this from the $K^0_S \to \pi^+\pi^-$ decay (detection efficiency 75%) properly corrected for neutral and K^0_L decays (3). The average number of gamma rays is 3.79 per event and of $(K^0_S + K^0_L)$'s is 0.18 per event.

The results of a longitudinal momentum balance are plotted in Figure 2 and tabulated in Table 1. The events have been divided into three

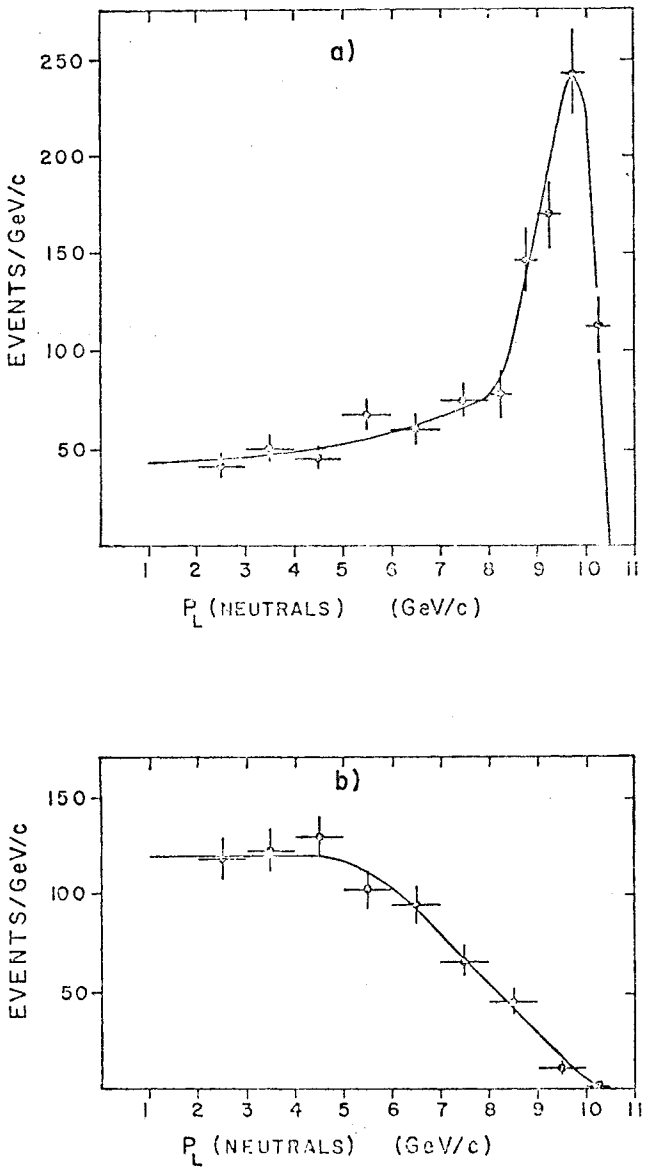

Fig.1. Event distributions as a function of the longitudinal momentum carried by all neutral particles. a) $\pi^+ p \to \pi^+ p$ + (neutrals); b) $\pi^+ p \to \pi^+ p \pi^+ \pi^-$ + (neutrals).

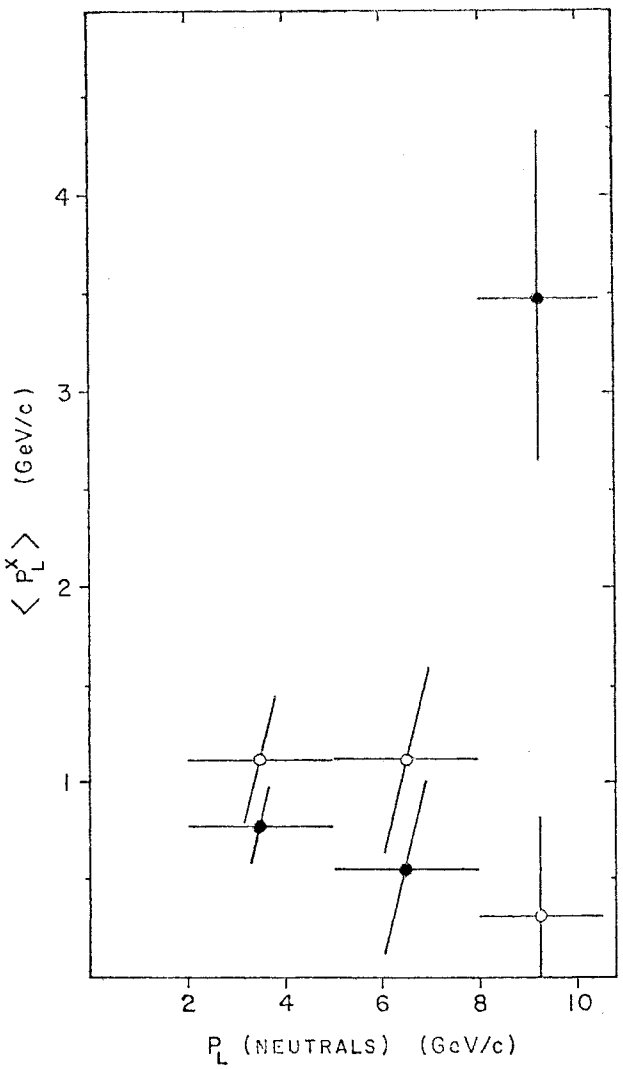

Fig.2. Neutral longitudinal momentum carried by particles other than K^0's and γ's as a function of the longitudinal momentum carried by all neutrals. Open circles $\pi^+ p \to \pi^+ p$ + (neutrals). Solid circles $\pi^+ p \to \pi^+ p \pi^+ \pi^-$ + (neutrals).

neutral momentum regions and the neutral momentum that cannot be accounted for γ's and K^0's, $\langle P_L^X \rangle$, is plotted separately for two prongs (open circles) and four prongs (solid circles). Some structure is indicated and the overall missing neutral momentum is (0.83±0.27) GeV/c per event. This must be accounted for by neutrons unless some unexpected neutral particle is produced.

The requirement of an identified proton eliminates single neutron production from the free proton interactions, but $n\bar{n}$ pair production is possible. The neon interactions included in our event sample can, in addition, produce one or more target fragmentation neutrons. The momentum carried away by neutrons has been measured from their secondary hadronic interactions in the hydrogen-neon liquid. A total of 46 neutral hadronic stars were observed, of which 23 are predicted to come from K^0 interactions as calculated from the measured $K_S^0 \rightarrow \pi^+\pi^-$ spectrum. After subtracting the contribution of the K^0's, and assuming that all the remaining neutral stars are caused by neutrons, we find that the average longitudinal momentum carried by neutrons, $\langle P_L^n \rangle$, is (0.30±0.09) GeV/c per event. Table 1 shows the contribution of neutrons to the neutral momentum in each event category. Finally, the last two columns of the table give the momentum carried away by any neutral particle other than γ's, K^0's, Λ^0's, or neutrons.

Of the six event categories presented in Table 1, only one shows a possibly significant momentum imbalance. The $\pi^+p \rightarrow \pi^+p\,\pi^+\pi^-$ events with neutral momentum over 8 GeV/c have a missing momentum of (2.9±1.0) GeV/c per event. However a significance of 2.9 standard deviations does not establish a new effect although it does define an event category that should be studied further. Averaged over all the events in our data we find that the momentum carried away by any new neutral particle is limited to (0.53±0.28) GeV/c per event. This is within a subset of all π^+p collisions which is especially sensitive to neutral particle production (over 50% of the collision energy goes into neutrals). Expressing this result relative to all inelastic two and four prongs implies that momentum balances to (3±2)%. Therefore, on the level of a few percent, there is no "energy crisis" in these hadronic interactions.

In conclusion, we find that the neutral particle spectrum produced in 10.5 GeV/c π^+p-interactions can be explained in terms of neutrons, Λ^0's, K^0's and photons. Any additional neutral particles produced carry less than 5% of the available momentum.

Table 1

Reaction		$\langle P_L^X \rangle$	$\langle P_L^{neutrals} \rangle$	Missing Neutral Momentum	
Charged Tracks	P_L (neutrals) GeV/c	GeV/c/event	GeV/c/event	GeV/c/event	% of total Momentum
$p\pi^+$	2 to 5	1.11 ± 0.37	0.57 ± 0.23	0.54 ± 0.43	5 ± 4
	5 to 8	1.12 ± 0.52	0.04 ± 0.16	1.08 ± 0.54	10 ± 5
	8 to 11	0.32 ± 0.56	0.02 ± 0.21	0.30 ± 0.60	3 ± 6
$p\pi^+\pi^+\pi^-$	2 to 5	0.78 ± 0.26	0.26 ± 0.10	0.52 ± 0.28	5 ± 3
	5 to 8	0.56 ± 0.51	0.77 ± 0.24	-0.21 ± 0.56	-2 ± 5
	8 to 11	3.48 ± 0.85	0.60 ± 0.56	2.88 ± 1.02	27 ± 10
All data	2 to 11	0.83 ± 0.27	0.30 ± 0.09	0.53 ± 0.28	5 ± 3

P L E N A R Y R E P O R T

MULTIPARTICLE AND INCLUSIVE REACTIONS

P.V. Chliapnikov

Institute for High Energy Physics, Serpukhov, USSR

An enormous amount of experimental and theoretical results have been obtained within the last few years in the field of multiparticle production. Global description of multiparticle final states in terms of only a few variables in the framework of inclusive approach suggested by Logunov and co-workers (1967)[1], the first experimental evidence for scaling in hadron induced reactions (1969)[2,3], the theoretical formulation of the limiting fragmentation hypothesis (LFH) by Yang and co-workers (1969)[4] and of scaling by Feynman (1969)[5] and all subsequent development have been extremely successful in enlarging our knowledge of hadronic processes at high energies.

Detailed discussions of the available data have been the object of many thorough reviews (see, for example[6-11]) where a host of very important results have been collected. Many of the new interesting results have been covered in the invited and mini-rapporteur's talks in the A2-session of this conference. In my embarassing position where I can but describe, with some personal prejudices (and my inability to understand everything), only a small part of the imposing results presented in about 130 submitted contributions, I shall concentrate your attention on the following subjects:

1. Total inclusive cross sections
2. The approach to scaling in the fragmentation and central regions.
3. Inclusive resonance production
   - total cross sections
   - differential cross sections
   - mechanisms.
4. Two-particle correlations
   - angular correlations
   - space structure of events.

1. Total inclusive cross sections

Present results on the energy dependence of the total inclusive π^+, π^- and π° cross sections $\sigma_\pi = \langle n_\pi \rangle \sigma_{inel}$ in inelastic hadron collisions are compiled in fig.1. The increase of the pion cross sections for pp data above 50 GeV/c is compatible with logs dependence. The cross section ratio $\sigma(\pi^-)/\sigma(\pi^+)$ changes slowly from the value of 0.74 ± 0.02 at 69 GeV/c[12] up to 0.80 ± 0.08 at 303 GeV/c[11] (see Table 1). The ratio $\sigma(\pi^\circ)/\sigma(\pi^+)$ is 0.94 ± 0.02 at 69 GeV/c[12] and 1.01 ± 0.10 at 303 GeV/c[11]. It is of interest to note that $\sigma(\pi^+) \approx \sigma(\pi^-) \approx \sigma(\pi^\circ)$ for K^-p interactions up to 32 GeV/c. The energy dependence of the pion cross sections in reactions induced by the different beam particles seems to be similar to that for pp

collisions. The charge conservation, leading particle effect and the contribution of the annihilation channels in $\bar{p}p$ reactions explain some differences observed at low energies.

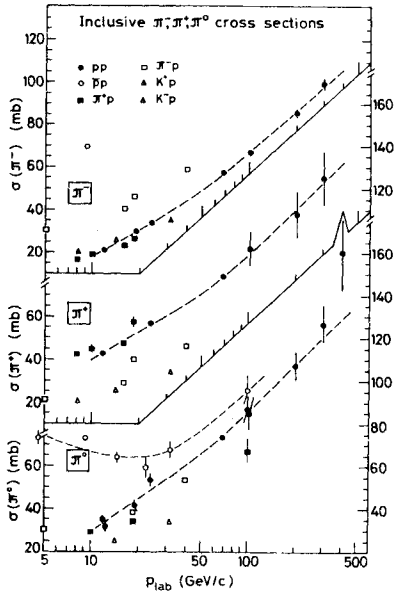

Fig.1. Inclusive π^-, π^+ and π° production cross sections as a function of incident momentum (compilation of published data; new data: K^-p 32 GeV/c[15]; $\bar{p}p$ 32 GeV/c[16], 22.4 GeV/c[17], 9.1 and 4.6 GeV/c[18,19]; π^-p 5 GeV/c[20]); the lines are to guide the eye.

Table 1

Total inclusive cross section (in mb) for π^+, π^- and π° in pp and Kp interactions at highest energies

	pp				K^-p	
P_{LAB} GeV/c	69[12]	100[11]	205[11,14]	303[11,13]	14.3[8]	32[15]
$\sigma(\pi^+)$	78.5±1.3	91.8±9.2	108±11	125±13	25.6±0.8	33.6±1.3
$\sigma(\pi^-)$	57.5±0.6	66.9±1.3	86±2	99.5±3	25.9±1.5	35.3±1.8
$\sigma(\pi^\circ)$	74.0±1.5	85 ±8	107±7	126.5±9	27.2±1.0	35.3±0.8

Neutral strange particle production cross sections are shown in figs.2 and 3 for $K^n(K^\circ/\bar{K}^\circ)$, Λ and $\bar{\Lambda}$. The K^n cross section rises by about a factor of 10 for pp interactions between 12 GeV/c and the highest FNAL energies. For π^-p interactions, the increase of the K^n production is consistent with logs dependence through all energy range up to the highest beam momentum of 205 GeV/c[23]. In $\bar{p}p$ collisions the K^n cross section is systematically higher than in pp interactions and rises as fast as in pp collisions through the Serpukhov-Fermilab energy range[16,17,21].

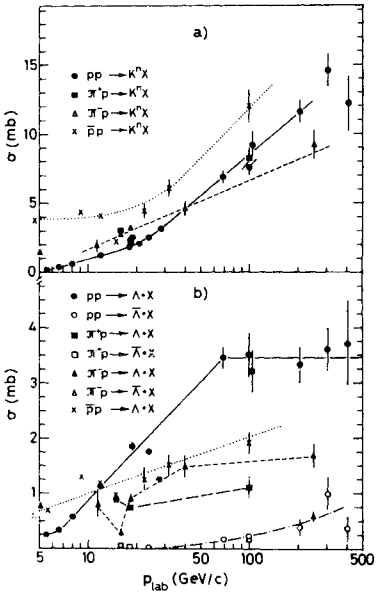

Fig.2. Inclusive K^n, Λ and $\bar{\Lambda}$ production cross sections as a function of incident momentum for $p^\pm p$, $\pi^\pm p$ interactions (compilation of published data; new data: $\bar{p}p$ 32 GeV/c[16], 22.4 GeV/c[17], 12 GeV/c[22], 9.1 and 4.6 GeV/c[18]; π^-p 205 GeV/c[23], 5 GeV/c[24]); the lines are to guide the eye.

The Λ production cross section rises between 5 and 50 GeV/c in pp collisions, but shows little energy dependence above 69 GeV/c. It is about two times higher in pp interactions than in $\bar{p}p$ and $\pi^\pm p$ collisions in the Serpukhov-Fermilab energy range, as it should be expected if the Λ production is dominated by the proton fragmentation. The dominance of the fragmentation process over that of $\Lambda\bar{\Lambda}$ pair production explains also a small energy variation of the

Λ cross section through the FNAL energy range. The $\bar{\Lambda}$ production is small, but exhibits a rapid increase with energy above 69 GeV/c in a striking similarity with $\bar{p}$ production.

In fig.3 the neutral strange particle cross sections for 32 GeV/c $K^{\pm}p$ interactions obtained by the France-USSR and CERN-USSR Collaborations[15,25] are compared with the corresponding data at lower energies.

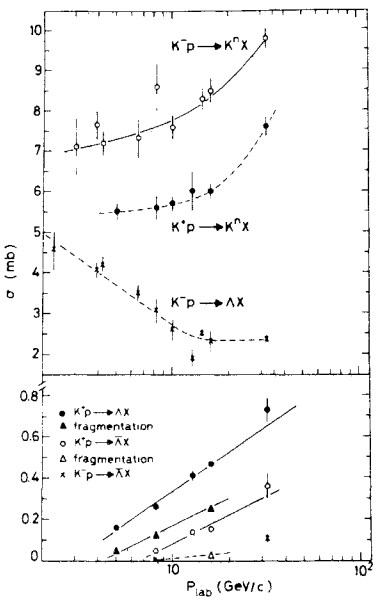

Fig.3. Inclusive K^n, Λ and $\bar{\Lambda}$ production cross sections as a function of incident momentum for $K^{\pm}p$ interactions (compilation of published data; new data: K^+p 32 GeV/c[25], 16, 8.2 and 5 GeV/c[26]; K^-p 32 GeV/c[15], 16 and 10 GeV/c[27], 6.5 GeV/c[28]); also are shown contributions of the Λ and $\bar{\Lambda}$ fragmentation cross sections in K^+p interactions (ref.[26]); the lines are to guide the eye.

One observes a significant rise of the K^n production cross section for both the K^+p and the K^-p interactions ($\Delta\sigma \approx 1.5$ mb) between 16 and 32 GeV/c . This increase may be at least partly attributed to a higher K^nK^n pair production: $\sigma(K^nK^n) = 1.1\pm0.1$ mb and 1.68 ± 0.24 mb in K^+p[25] and K^-p[15] interactions at 32 GeV/c, respectively. It is of interest to note that a significant amount of the K^+K^- pair production has also been observed in the exclusive channels in K^+p interactions at 32 GeV/c[29]. Similar effect was found by the France-USSR and CERN--USSR Collaborations in 32 GeV/c K^-p collisions[30]:

$$\frac{\sigma(K^-p \to K^-pK^+K^-\pi^+\pi^-)}{\sigma(K^-p \to K^-p2\pi^+2\pi^-)} = 0.18\pm0.05;$$

$$\frac{\sigma(K^-p \to K^-pK^+K^-2\pi^+2\pi^-)}{\sigma(K^-p \to K^-p3\pi^+3\pi^-)} = 0.55\pm0.21 .$$

The energy dependence of the Λ and $\bar{\Lambda}$ production in K^+p collisions resembles in character that observed in pp interactions at similar energy range; the data are well described by the logs dependence. In K^-p interactions, the Λ production cross section falls with energy at low incident momenta, but seems to be fairly constant between 10 and 32 GeV/c. The decrease of cross sections at low energies is explained by the falling contribution of the strangeness annihilation process in virtual K^-K^+ scattering in the reaction $K^-p \to \Lambda$+ pions. As energy increases, other mechanisms of the Λ production such as $K^-p \to K\bar{K}$ + pions, become more important (fig.4).

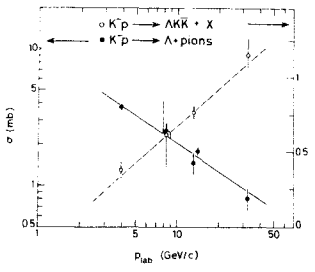

Fig.4. Energy dependence of the Λ production cross sections in the strangeness annihilation process $K^-p \to \Lambda$ + pions (left hand scale) and in the reaction $K^-p \to \Lambda K\bar{K}$ + X (right hand scale)(from ref.[31]).

This results in approximately energy independent cross sections at 10-32 GeV/c incident momentum

range. From the present trend of data, one may expect that Λ production in K^-p interactions will start to increase at higher energies.

2.1 The approach to scaling in the fragmentation region

The approach to scaling in the target fragmentation region has been extensively discussed during the past two years[7,8,32-34]. However the conclusions differ, thus reflecting the lack of the high statistics data in this phase space region at the highest energies. Indeed most of the π data measured at the CERN ISR are confined to $p_T > 0.4$ GeV/c or $y_{LAB} > 0$ while the bubble chamber data are integrated over transverse momenta because of the poor statistics.

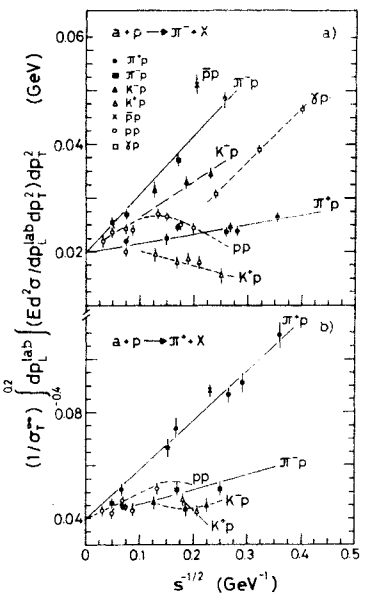

Fig.5. The approach to scaling in the proton fragmentation region for inclusive $\pi^\pm$ production (from ref.[34] with some added published data).

Fig.5 summarizes the present situation with respect to the factorization and the approach to scaling in proton fragmentation into $\pi^\pm$ as measured in the bubble chamber experiments. The hypothesis of limiting fragmentation[4] is not valid in the whole available energy range. However the data at highest energy suggest, that a scaling limit may exist, that it is being approached from above and that the factorization may hold in the limit of infinite energy.

More specifically, for reactions with no exoticity combination (ab, $ab\bar{c}$, $b\bar{c}$, $a\bar{c}$) such as $\pi^\pm p \to \pi^\pm X$, $K^-p \to \pi^-X$, $\gamma p \to \pi^-X$ (and most probably $\bar{p}p \to \pi^\pm X$), one observes a strong energy variation in entire energy range consistent with the Mueller-Regge predictions[35,36] based on the generalized optical theorem[37,38]:

$$E\frac{d^3\sigma}{d^3p} = f(s,p_L,p_T^2) =$$

$$= A(p_L,p_T^2) + \sum_R B_R(p_L,p_T^2)s^{\alpha_R(0)-1} \qquad (2.1.1)$$

where the $\alpha_R(0)$ are the intercepts of the exchange Regge trajectories. For reactions where at least one of the ab, $ab\bar{c}$, or $a\bar{c}$ combinations is exotic (Table 2), the situation is not as straightforward.

Table 2

Exoticity of various combinations for the reaction a + b → c + anything

Reaction	ab	$ab\bar{c}$	$a\bar{c}$	$b\bar{c}$
$pp \to \pi^-X$	Exotic	Exotic		
$\pi^+p \to \pi^-X$		Exotic	Exotic	
$K^+p \to \pi^-X$	Exotic	Exotic	Exotic	
$pp \to \pi^+X$	Exotic	Exotic		
$\pi^-p \to \pi^+X$			Exotic	
$K^+p \to \pi^+X$	Exotic	Exotic		
$K^-p \to \pi^+X$			Exotic	

For these reactions the energy variation is much less pronounced but still exists even in the Serpukhov-Fermilab energy range, where it amounts to 10-20% . It appears[34] that the rise from threshold, which is seen for $pp \to \pi^\pm X$ and $K^+p \to \pi^-X$ reactions and is indicated for $K^+p \to \pi^+X$ reactions, is related to (ab) being an exotic combination. For these reactions, as

cross sections are increasing, the prediction (2.1.1) can not be applied. The reactions $\pi^+p \to \pi^-X$, $\pi^-p \to \pi^+X$ (and perhaps, $K^-p \to \pi^+X$), which show a systematic but small energy variation and which are characterized by having ($a\bar{c}$) exotic, are again consistent with an energy dependence predicted by (2.1.1).

It is of interest to test the above relations between the exoticities of different particle combinations and the energy dependences of the $\pi^\pm$ inclusive cross section in the beam fragmentation region. The study of the reactions $\pi^-p \to \pi^+X$ and $K^-p \to \pi^+X$ with only ($a\bar{c}$) combination being exotic (Table 2) may be of special interest.

The experimental data in the target fragmentation region for heavy particles are quite poor in high energy range. Very qualitative picture of the approach to scaling in proton fragmentation into neutral kaons K^n and Λ is presented in fig.6.

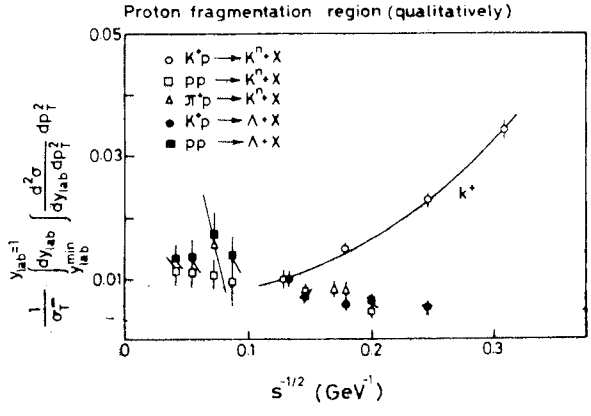

Fig.6. The approach to scaling in the proton fragmentation region for inclusive K^n and Λ production (compilation of published data).

However it is interesting to note that the trend of data is similar to that observed for $\pi^\pm$ production. In particular, the factorization holds in a first approximation, the energy dependence seems to be small in the FNAL energy range and the rise from threshold is observed for all reactions with ab being exotic, apart from $K^+p \to K^n + X$.

The exceptional behaviour of the $K^+p \to K^n + X$ reaction may be related to the presence of the strangeness annihilation process in the virtual K^+Y^{*+} scattering, i.e. the contribution of the f'- Ø exchange, which leads to an s^{-1} behaviour of the structure function (2.1.1)[36,39]. Indeed the data seem to be compatible with such a picture (fig.7(a)) in the target fragmentation region, favouring an s^{-1} dependence.

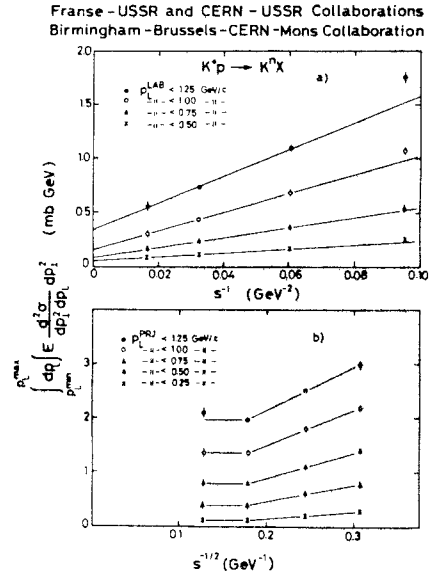

Fig.7. Energy dependence of the structure functions for reaction $K^+p \to K^nX$: (a) in the proton fragmentation region: the lines are fits to the 8.2-32 GeV/c data; (b) in the beam fragmentation region; the lines are to guide the eye (from ref.[25]).

Another interesting experimental observation made by the France-USSR and CERN--USSR Collaboration[25] is the surprising energy dependence of this reaction $K^+p \to K^nX$ in the beam fragmentation and central regions. The cross sections for this reaction in the beam fragmentation region (fig.7(b)) are decreasing with incident momentum between 5

and 16 GeV/c[39] following an $s^{-1/2}$ dependence as predicted by (2.1.1), but practically coincide at 16 and 32 GeV/c. Fig.8 shows this effect in more detail . One indeed observes the scaling of the $d\sigma/d(M^2/s)$ distributions at 16 and 32 GeV/c over the entire range of M^2/s .

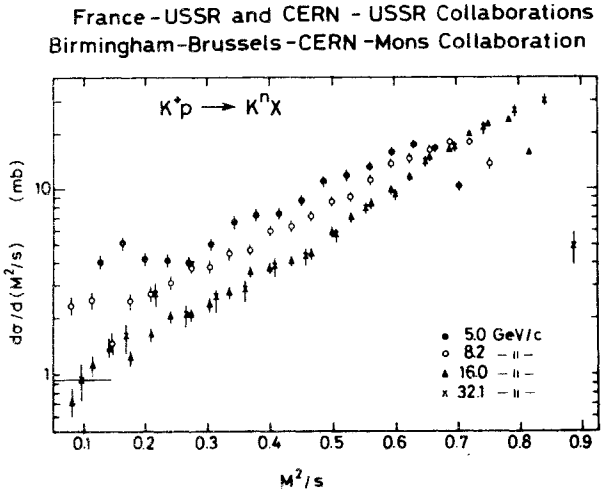

Fig.8. The differential cross section, $d\sigma/d(M^2/s)$, for reaction $K^+p \rightarrow K^nX$ (from ref.[25]).

A similar effect has been found for reaction $K^-p \rightarrow K^nX$ in the same energy range[40]. It is tempting to explain this surprising behaviour by the higher contribution of the K^nK^n pair production at 32 GeV/c (see above section). From this one may expect that, at least in the central region, the observation of the early scaling at 16-32 GeV/c incident momentum range is accidental and the K^n cross section should start to increase at higher energies.

The measurements of the production of $\pi^\pm$, K^+ and protons in $\pi^\pm p$, $K^\pm p$ and $p^\pm p$ interactions from 4 to 250 GeV/c in the target fragmentation region have been made by Pennsylvania group[41], using an electronic detector, in a fixed region of phase space corresponding approximately to $p_T = 0.3$ GeV/c and $y_{LAB} = 0.6$, 0.4 and 0.2 for produced π, K and p, respectively (fig.9).

They have fitted the data to the expression $A + Bs^{-1/2} + Cs^{-1}$ for production of pions in $\pi^\pm p$ and $p^\pm p$ collisions and to the expression $A + Bs^{-1/2}$ for the statistically less significant data.

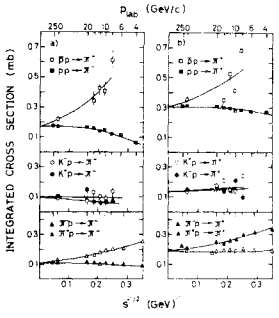

Fig.9. Energy dependence of the invariant cross sections (integrated over the kinematic region $0.3 \leq p^c_{LAB} \leq 0.6$ GeV/c and $60.75° \leq \theta^c_{LAB} + \frac{3.3°}{p^c_{LAB}} \leq 64.25°$) for (a) π^- and (b) π^+ production. The solid lines are fits to $A + Bs^{-1/2}$ and $A + Bs^{-1/2} + Cs^{-1}$.

It seems that at least for the statistically most significant data of the reaction $pp \rightarrow \pi^\pm X$, with ab combination being exotic, the cross sections systematically rise to asymptotic limits in contrast to the bubble chamber data (fig.5), where the cross sections rise slowly and then fall to their asymptotic limit (note, however, that the rapidity ranges are different in these two experiments).

Since in the PS-FNAL energy range the central production may contribute substantially to the fragmentation region, the increased precision of the experiments in different regions of phase space is needed for determination of the actual s-dependence of the invariant cross section in the proton fragmentation region. It is of interest to test in detail whether the s-dependence indeed has a form $A + Bs^{-1/2} + Cs^{-1}$. If it does, we have additional reason to believe (besides the facts that the cross sections are rising in the

central region and for reactions $pp \to \pi^{\pm}$ and $pp \to K^{+}X$ the same is true in the fragmentation region) that we do not understand either the singularity structures in the Regge language or the dual properties of the Regge trajectories (or both) in the scope of the simplest dual Regge approach.

The tests of the factorization of the leading Pomeron singularity

$$\frac{Ed^3\sigma\,(ap \to c)/d^3p}{Ed^3\sigma\,(a'p \to c)/d^3p} \underset{s\to\infty}{=} \frac{\sigma_{tot}(ap)}{\sigma_{tot}(a'p)}$$

made by Pennsylvania group[41] by the extrapolation of the fitted s-dependence to $s \to \infty$ (Table 3) show that the results are within the predictions of the naive quark model ($\sigma(\pi p) = \sigma(Kp) = \frac{2}{3}\sigma(pp)$) or the parametrization[42] of the diffractive part of the total cross sections, evaluated at p_{LAB} = 250 GeV/c.

Table 3

Tests of Pomeron Factorization

Cross section ratio	Asymptotic ratio for produced particle c: c = π^-	c = π^+	c = K^+	c = p	Predicted ratio Ref.[42]	Quark model
$\frac{\pi p \to c}{pp \to c}$	0.63±0.03	0.62±0.03	0.25±0.18	0.62±0.03	0.61±0.02	0.67
$\frac{Kp \to c}{pp \to c}$	0.60±0.06	0.45±0.04		0.61±0.08	0.53±0.02	0.67

A similar conclusion is made by the SLAC group[43] which has measured the ratios R of inclusive particle and antiparticle cross sections in $A^{\pm}p \to A^{\pm}X$ reactions (A = π, K, p) at 10 and 14 GeV/c at $|t| < 0.25$ $(GeV/c)^2$. The integration of R over the whole available missing mass range yields $R = 0.96^{\pm}0.04$, $0.90^{\pm}0.02$ and $1.02^{\pm}0.02$ for $K^{\pm}$, $\pi^{\pm}$ and $p^{\pm}$ inelastic scattering, respectively, at 10.4 GeV/c. This indicates that the C = -1 exchanges are very small for these reactions in contrast to the elastic scattering, where the C = -1 exchanges are quite significant at these energies.

In measurements at the CERN ISR of the diffraction exitation processes, $pp \to (p\pi^+\pi^-)+X$, $pp \to p+X$ and $pp \to (\Lambda K^+)+X$ at $\sqrt{s}$ = 53 GeV[44], factorization is shown to be valid to ≈5% for $|t| < 0.5(GeV/c)^2$. For $0.5 < |t| < 1.1(GeV/c)^2$, a pronounced breakdown in factorization is however observed between the elastic and inelastic diffractive cross sections. This can be seen from fig.10 where the ratios of collinear to non-collinear events are plotted vs. momentum transfer for above three reactions.

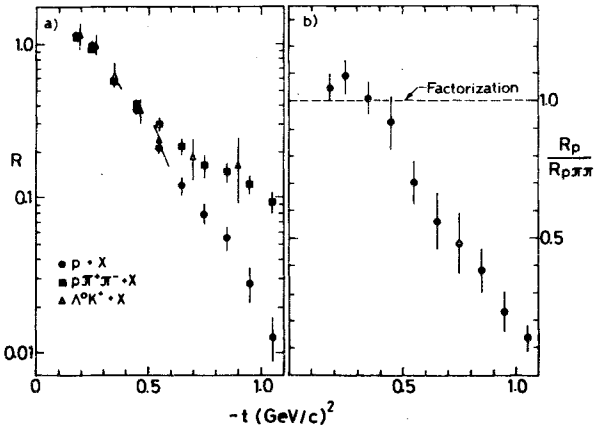

Fig.10. (a) Ratios R_p, $R_{p\pi\pi}$, $R_{\Lambda K}$ of collinear to non-collinear events (corrected for loss of non-collinear events) for reactions $pp \to p + X$, $pp \to p\pi\pi + X$ and $pp \to (\Lambda K^+) + X$ at $\sqrt{s}$ = = 53 GeV vs. momentum transfer; (b) R_p/R_p vs. t (from ref.[44]).

These ratios are related to the differential cross sections of these reactions:

$$R_p = \frac{\varepsilon_p(d\sigma_{el}/dt)}{\varepsilon_p(\frac{1}{2}d\sigma_{SD}/dt)}, \quad R_{p\pi\pi} = \frac{\varepsilon_{p\pi\pi}(\frac{1}{2}d\sigma_{SD}/dt)}{\varepsilon'_{p\pi\pi}(d\sigma_{DD}/dt)},$$

$$R_{\Lambda K} = \frac{\varepsilon_{\Lambda K}(\frac{1}{2}d\sigma_{SD}/dt)}{\varepsilon'_{\Lambda K}(d\sigma_{DD}/dt)}.$$

Factorization requires $\varepsilon_{p\pi\pi} = \varepsilon'_{p\pi\pi}$ and $\varepsilon_{\Lambda K} = \varepsilon'_{\Lambda K}$. All these R parameters are seen to agree with each other for $|t| < 0.5(GeV/c)^2$, but at $|t| > 0.5$ the parameter R_p departs

sharply, demonstrating a breakdown in Pomeron factorization for elastic scattering. The apparently different energy behaviour of the inelastic cross section for reactions $pp \to p(n\pi^+)$ and $pn \to p(p\pi^-)$ as compared to the elastic ones over a broad energy range from 24 GeV up to the ISR energies is also related[125] to the breakdown of a single factorisable t-channel model, which predicts that the elastic and inelastic diffractive amplitudes should have the same energy behaviour $\sim s^{\alpha_P}$.

The experimental values of R_p and $R_{p\pi\pi}$ have been used to extract the absolute differential and total cross sections for single and double diffractive excitation at $\sqrt{s}$ = 53 GeV[44]. They were found to be 8.6 ± 0.7 mb and 5.0 ± 0.8 mb, yielding a total elastic and inelastic diffractive cross section of

$$\sigma_{el} + \sigma_{SD} + \sigma_{DD} = 21.3 \pm 1.1 \text{ mb},$$

or $(49.4 \pm 2.5)\%$ of the total cross section at $\sqrt{s}$ = 53 GeV. The value of $\sigma_{SD} + \sigma_{DD} = 13.6 \pm 1.1$ mb is considerably larger than it is usually assumed and, in fact, is compatible with saturation of the Pumplin bound[45]

$$\sigma_{diff} \leq \frac{1}{2}\sigma_{tot} - \sigma_{el} .$$

The interesting approach to the behaviour of inclusive cross section in the fragmentation region has been suggested by Logunov and co-workers[46]. Using the Jost-Lehmann-Dyson representation of the spectral function they have shown that the inclusive cross section may be written in the form

$$E\frac{d^3\sigma}{d^3p} = \gamma^{a(q^2,\nu)} F(q^2,\nu) \qquad (2.1.2)$$

with $q^2=(p_a-p_c)^2$, $\nu = 2p_b(p_a-p_c)$ and $\gamma = 2p_b(p_a+p_c)/\nu$. If the spectral function has no singularities, then $a(q^2,\nu) < 0$, otherwise $a(q^2,\nu) > 0$. Fig.11 taken from ref.[47] shows that the function (2.1.2) indeed describes the data, with very small dependence of $a(q^2,\nu)$ and $F(q^2,\nu)$ on ν.

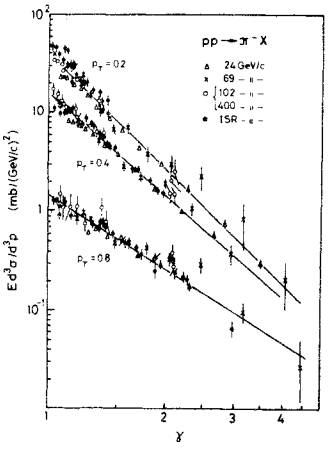

Fig.11. Inclusive cross sections for reaction $pp \to \pi^- X$ as a function of the variable γ; the straight lines are to guide the eye (from ref.[47]).

Besides, $a(q^2,\nu) < 0$ for reactions $pp \to \pi^{\pm} X$ and $a(q^2,\nu) > 0$ for reactions $pp \to pX$[47] and $K^+p \to K^0X$[48] with the strong leading particle effects. For p_T = 0.4 GeV/c $\approx \langle p_T \rangle$, $a \approx 3$. This gives $Ed^3\sigma/d^3p \sim (1-x)^3$. The similar x dependence is observed for the structure function $\nu W_2(x)$ for deep inelastic scattering at x=1, thus suggesting an interesting relationship between the behaviour of inclusive reactions in hadron-hadron collisions and the deep inelastic scattering (see also[49]).

Moreover it seems[47] that the invariant cross section is factorisable in the variables γ_1 and γ_2, pertaining to the beam and target fragmentation regions. In the usual variables

$$x_1 = \frac{E + p_L}{\sqrt{s}} = \frac{m_T e^y}{\sqrt{s}}, \quad x_2 = \frac{E - p_L}{\sqrt{s}} = \frac{m_T e^{-y}}{\sqrt{s}}$$

this implies

$$E\frac{d^3\sigma}{d^3p} \approx \varphi(m_T) f(x_1) f(x_2) \qquad (2.1.3)$$

where the function $f(x) \sim (1-x)^3$ in pp collisions at $x \to 1$. One of the possible manifestations of eq.(2.1.3), related to the

deep inelastic scattering, is the mechanism of the amalgamation of quarks from the colliding hadrons[50].

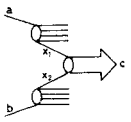

Fig.12. Mechanism of particle production resulting from the amalgamation of quarks from the colliding hadrons.

This analog of the familiar Drell-Yan mechanism for production of lepton pairs in hadron-hadron collisions (fig.12) gives

$$E\frac{d^3\sigma}{d^3p} \approx \frac{A}{m^2} f_q(x_1) f_{\bar{q}}(x_2) \qquad (2.1.4)$$

with $f(x) = \nu W_2(x)$ and

$$x_{1,2} = 1/2((x^2 + 4m^2/s)^{1/2} \pm x) \qquad (2.1.5)$$

From eq.(2.1.4) and (2.1.5) it follows that

$$E\frac{d^3\sigma}{d^3p}_{x\to 1} \approx \frac{A}{m^2} f_q(x) f_{\bar{q}}(\frac{m^2}{sx}) \qquad (2.1.6)$$

$$E\frac{d^3\sigma}{d^3p}_{x\to 0} \approx \frac{A}{m^2} f_q(\frac{m}{\sqrt{s}}) f_{\bar{q}}(\frac{m}{\sqrt{s}}) \qquad (2.1.7)$$

Thus this mechanism predicts the different approaches to scaling in the fragmentation and central regions (the energy dependence is defined by the variables m^2/s and $m/\sqrt{s}$ in (2.1.6) and (2.1.7), respectively). Besides, we see that the scale of energy is measured in units of the mass m of the produced particle (or in units of the transverse mass m_T if the transverse momentum is taken into account). Consequently the average multiplicities of the different particles produced in hadron-hadron interactions may follow[51] some universal curve $(1/m_c^2)\varphi(\langle m_T^2\rangle/s)$ as seems to be the case (fig.13), at least in a first approximation. This has also important implications for the yield of particles in the hadron-hadron collisions, since the factor A/m^2 in the eq.(2.1.4) may distort the simple quark counting rules in the naive quark models (see section 3). It is of interest that similar conclusions have been reached in quite different approaches[52,53].

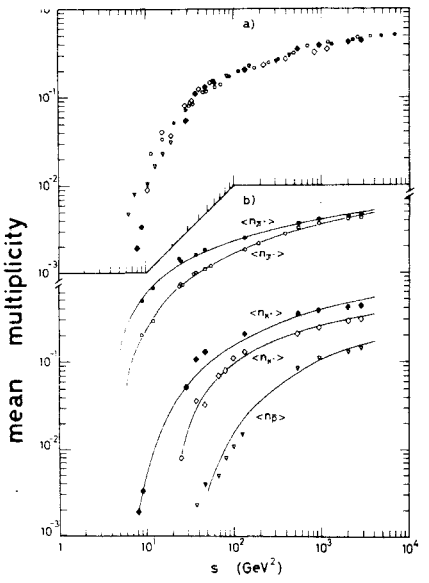

Fig.13. (b) Average multiplicity of $\pi^{\pm}$, $K^{\pm}$ and $\bar{p}$ as a function of s; (a) the same data as in (b) obtained by the simple shifts of the $\pi^{\pm}$, K^- and $\bar{p}$ data to the average multiplicity of the K^{+}'s; the shifts along the $\langle n\rangle$ axis are in the ratios of the corresponding masses squared (for details see ref.[51]; the data from ref.[54]).

2.2 Triple-Regge region

The inelastic hadron diffraction at high energy has been discussed by Kaidalov in his rapporteur's talk at this Conference. I shall concentrate on some specific reactions in the triple-Regge region.

The inclusive production of $\Lambda, \bar{\Lambda}, \Xi^-$ and $\Sigma^+(1385)$ in the fragmentation regions has been studied in several experiments[26,55-58]. Target fragmentation $p \to \Lambda$ can be associated with the diagram in fig.14 with the exchange Reggeon R represented by the K and $K^*(890)$ trajectories. It has been shown that the triple-Regge model yields an approximate description of fragmentation processes even

when extrapolated to cms energies of a few GeV. Resonances in the M_X^2 channels for nonexotic ($ab\bar{c}$) reactions can be accounted for in the sense of semi-local duality[59]. An interesting attempt to explore more directly a dual description of the reggeon-particle scattering in $K^-p \to \Lambda X$ (and $K^-p \to \Sigma^+ + X$) reaction at 4.2 GeV/c is made by the Amsterdam-CERN-Nijmegen-Oxford Collaboration[55]. They use the usual Regge formula

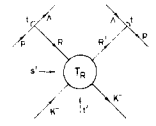

$T_R = T_R^0 + T_R^1$

$\mathrm{Im}\, T_R^0 = 2K^{-1}s^{\alpha_R}\sigma_R$

$T_{K^-}^1 = \beta_K^{p\Phi}(V_{p\Phi} + V_{\bar{p}\Phi}) + \beta_K^{n\Phi}(V_{n\Phi} + V_{\bar{n}\Phi})$

$T_{K^{*-}}^1 = \beta_{K^*}^{p\Phi}(V_{p\Phi} + V_{\bar{p}\Phi}) + \beta_{K^*}^{n\Phi}(V_{n\Phi} + V_{\bar{n}\Phi}) + \beta_{K^*}^{X\Phi}V_{X\Phi} + \beta_{K^*}^{n\Pi}V_{n\Pi} + \beta_{K^*}^{X\Phi}V_{X\Phi}$

σ_R and β_R are the adjustable parameters

V is the Veneziano function

Fig.14. Regge diagram for $p \xrightarrow{K^-} \Lambda$ fragmentation.

$$\frac{d^2\sigma}{ds'dt'} = \frac{1}{16k^2s}\sum_R \frac{\gamma^2_{R\Lambda}}{4\pi}\,\mathrm{Im}\,T_R(s',0,t)\left(\frac{s-u}{2s'}\right)^{2\alpha_R(t)} \qquad (2.2.1)$$

where $\gamma^2_{R\Lambda}$ is the residual factor, but instead of taking the triple-Regge limit, they describe the RK scattering (fig.14) by introducing four-point function $T_R(s',t',t)$. The amplitude T_R is written as a sum of two terms $T_R = T_R^0 + T_R^1$. The diffractive term T_R^0, which according to two-component duality may be extrapolated to low s', describes a non-resonance background in inclusive distribution. The non-diffractive amplitude T_R^1, which is applied as Veneziano amplitude, explicitly reproduces M_X^2 channel resonances.

Fig.15 shows the experimental $d^2\sigma/dtdM$ distributions for reaction $K^-p \to \Lambda + X$, together with the absolute predictions of the above model. The overall agreement is very good, although one observes a discrepancy in the ρ-ω mass region for the two smallest |t|-bins. Similar results were obtained for reaction $K^-p \to \Sigma^+X$. The relative contributions to the integrated cross section evaluated separatly for K and K* exchange are summarized in Table 4.

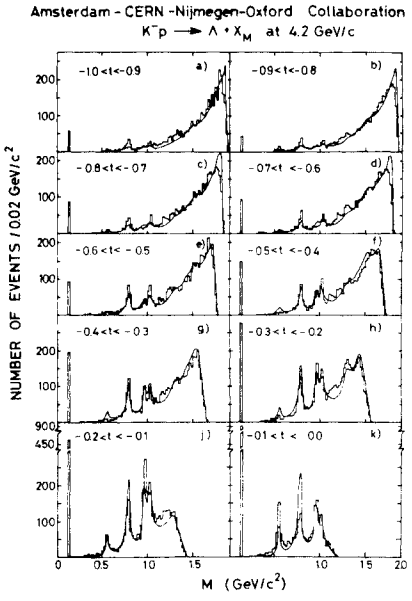

Fig.15. Missing mass distributions in reaction $K^-p \to \Lambda X$ at 4.2 GeV/c for different t-intervals with the absolute predictions of the model (from ref.[55]).

Table 4

Relative contributions of K and K* exchange in the reactions $K^-p \to \Lambda X$ and $K^-p \to \Sigma^+X$ at 4.2 GeV/c for $-t_{p,\Lambda(\Sigma)} < 1\,(\mathrm{GeV/c})^2$

Type of exchange	$K^-p \to \Lambda + X$		$K^-p \to \Sigma^+ + X$	
	σ (mb)	%	σ (mb)	%
Dual part of K exchange	0.11	9	0.01	3
Diffractive part of K exchange	0.33	28	0.16	40
Dual part of K* exchange	0.51	43	0.08	20
Diffractive part of K* exchange	0.23	20	0.15	37

One observes that the ratio of K* exchange to K exchange is 1.7:1 for $K^-p \to \Lambda X$ and 1.3:1 for $K^-p \to \Sigma^+X$, while the ratio of the total contributions from the diffractive and non-diffractive terms is close to unity for $K^-p \to \Lambda X$ and is 3.5 for $K^-p \to \Sigma^+X$.

Similar results were obtained by the Birmingham-Brussels-CERN-MONS Collaboration[26] in the triple-Regge analysis of the reaction $K^+p \to \Lambda X$ at 8.2 and 16 GeV/c in the proton fragmentation region. Here the exoticity of ($ab\bar{c}$) implies the early scaling behaviour which is indeed observed when the threshold effects

are accounted for by introduction of the variable $(M^2 - M_{th}^2)/s$ instead of M^2/s ($M_{th} = 2m_K$ for reaction $K^+p \to \Lambda X$ and $2m_p$ for reaction $K^+p \to \bar{\Lambda} X$). The fit to the triple-Regge formula

$$\frac{d^2\sigma}{d(M^2/s)dt} = \frac{s}{(2p^*)^2} C\exp(-bt)\left(\frac{M^2-M_{th}^2}{s}\right)^{1-2\alpha(t)} \qquad (2.2.2)$$

yields the trajectory $\alpha(t)$ (fig.16) passing close to the mass squared values of the K, Q and L mesons lying between K and K* trajectories.

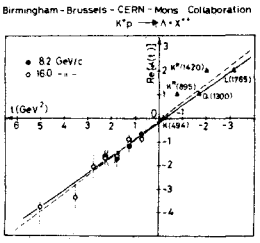

Fig.16. The effective trajectory $\alpha(t)$ resulting from the triple-Regge fit of the reaction $K^+p \to \Lambda X$ at 8.2 and 16 GeV/c; the dashed line corresponds to a simultaneous fit of expression $\alpha(t) = \alpha_0 - \alpha' t$ to combined 8.2 and 16 GeV/c trajectory points; the solid line results from a simultaneous fit of the triple-Regge formula (2.2.2) to the 8.2 and 16 GeV/c data (from ref.[26]).

The beam fragmentation in the reactions $K^+p \to \bar{\Lambda} X$ and $K^+p \to \Lambda X$ is shown to be present although small at the energies of this experiment. Its contribution is evaluated by setting the trajectory parameters in (2.2.2) to the values of N_α and Ξ_α trajectories. Thus one is able to estimate a complete fragmentation contributions to these reactions by integrating distribution functions (2.2.2) over the whole Chew-Low plots. The fragmentation contributions do not account for all of the data. If central production is defined as non-fragmentation production, it can be evaluated by subtracting the distributions predicted by (2.2.2) from the observed distributions. The residual distributions (fig.17) have indeed the characteristics of the central component. It is of interest to apply a similar procedure for other inclusive reactions in order to analyse in detail the central region as it pertains to different incident and inclusive particles.

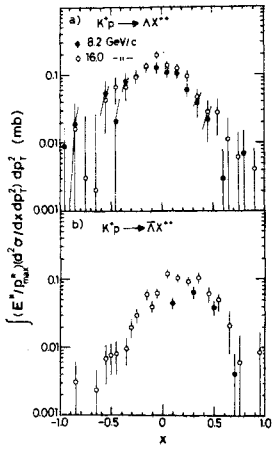

Fig.17. Inclusive distributions for reactions $K^+p \to \Lambda X$ and $K^+p \to \bar{\Lambda} X$ pertaining to the central production (from ref.[26]).

The triple-Regge analysis has also been applied for description of inclusive production of Λ, K^o and $\bar{\Lambda}$ at small angles in pBe interactions at 300 GeV/c[58]. The results show that the nuclear effects can be ignored in a first approximation and confirm the relevance of the triple-Regge parametrization to inclusive production on the nucleus.

Thus the triple-Regge parametrization successfully describes a large variety of inclusive reactions in a wide energy range. However, the parameters of leading singularities obtained in TR fits should be treated with caution, especially in the cases when the inclusive particle can be the decay product of the resonances. This has been beautifully demonstrated by the Birmingham-Brussels-CERN-Mons-Serpukhov Collaboration[60] in the study of the slow protons in the reaction $K^+p \to pX$ at 16 GeV/c. Fig.18(a) shows that the substantial $\Delta^{++}(1236)$ production strongly

affects the shape of the inclusive spectra and consequently the results of the triple-Regge fit (fig.18(b)). It is seen that after removal of events associated with $\Delta^{++}(1236)$ production, the data are consistent with the dominance of an ffR coupling, although this is not the case for total sample of inclusive protons.

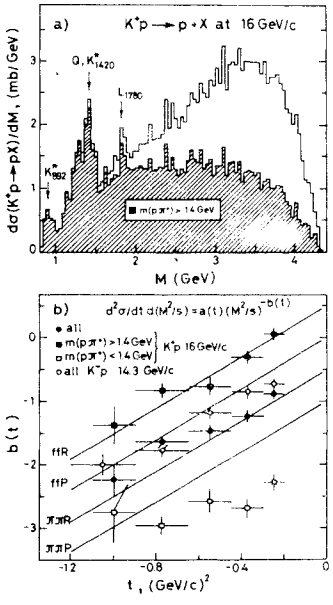

Fig.18. (a) Distribution of the missing mass M to the proton in the reaction $K^+p \rightarrow pX$ at 16 GeV/c. The events with the $\Delta^{++}(1236)$ antiselection ($m(p\pi^+) > 1.4$ GeV) are shaded. (b) The fitted values of b(t) in the triple-Regge fit for reaction $K^+p \rightarrow pX$ at 16 GeV/c for all events, for events with $m(p\pi^+) > 1.4$ GeV and $m(p\pi^+) < 1.4$ GeV. Expected variations of b(t) for several possible triple-Regge couplings are shown as straight lines (from ref./60/.

2.3 The approach to scaling in the central region

The British-Scandinavian-MIT Collaboration (BSM)/61,62/ has extended the measurement of the inclusive $\pi^\pm$, $K^\pm$ and $p^\pm$ production at x=0 over the ISR energy range ($23 \leq \sqrt{s} \leq 63$ GeV) to the small p_T regions: $0.04 \leq p_T \leq 0.4$ GeV/c for $\pi^\pm$, $0.1 \leq p_T \leq 0.3$ GeV/c for $K^\pm$ and $0.1 \leq p_T \leq 0.5$ GeV/c for $p^\pm$. These data together with those at higher values of p_T /63/ are shown in fig.19. The scaling limit is not reached in the central region even at the ISR energies. The average increase of the differential cross section over the ISR energy range amounts to $36\pm2\%$ and $41\pm2\%$ for π^+ and π^-, $52\pm8\%$ and $69\pm8\%$ for K^+ and K^-, $8\pm5\%$ and $84\pm6\%$ for p and $\bar{p}$ in the kinematical region covered by the BSM experiments.

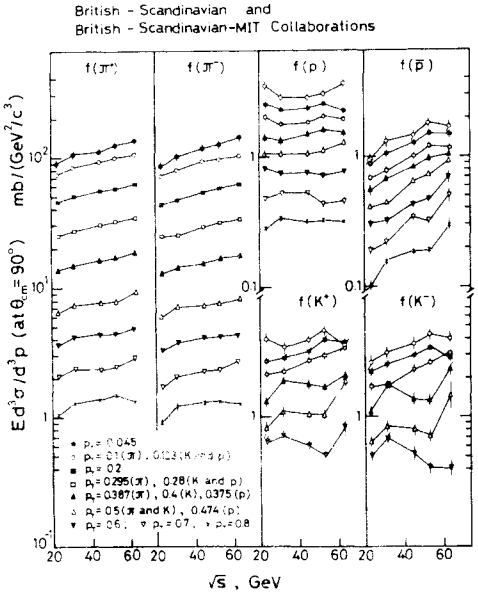

Fig.19. Energy dependence of the invariant inclusive cross section of $\pi^\pm$, $p^\pm$, $K^\pm$ at $\Theta_{cm} = 90°$ for different p_T values at ISR energies ($\sqrt{s}$=23,31,45,53 and 63 GeV) (the data from ref./61-63/).

The particle flux at small p_T is dominated by pions but the fraction of heavier particles, kaons and nucleons, is growing almost linearly with p_T. There is a more pronounces increase with energy in the differential cross sections for $K^\pm$ and $p^\pm$ at higher p_T(fig.20) . However the very low p_T pion cross sections seem to increase more at small values of p_T .

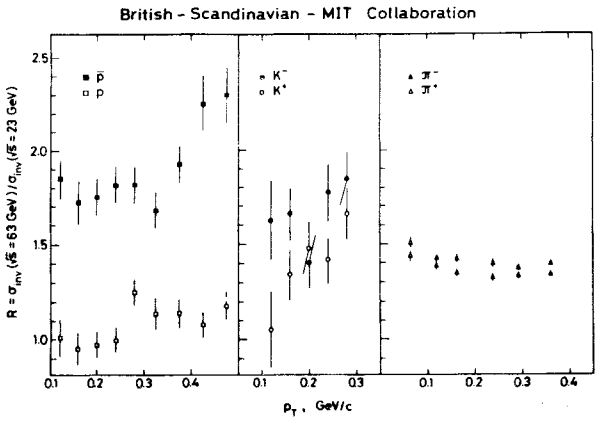

Fig.20. The cross section ratio, $R = \sigma_{inv}(63\ GeV)/\sigma_{inv}(23\ GeV)$, between the invariant differential cross sections of $\pi^{\pm}$, $K^{\pm}$ and $p^{\pm}$ at $\sqrt{s}$ = 63 and 23 GeV as a function of p_T (from ref./61,62/).

It is tempting to explain the latter effect by the increase of the resonance production with energy which leads to higher proportion of pions produced from resonance decays at low p_T values (see section 3). The ratio of particle to antiparticle cross sections (fig.21) shows the strongest variation with p_T and s for protons and antiprotons. A large fraction of

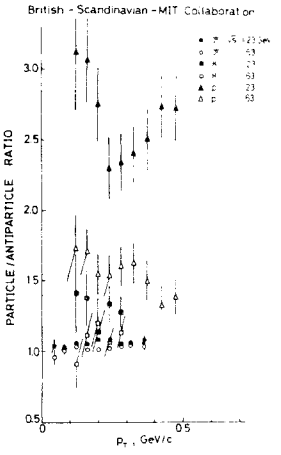

Fig.21. Particle/antiparticle ratio as a function of p_T at $\sqrt{s}$ = 23 and 63 GeV (from ref./62/).

protons at the lowest ISR energy and low p_T appears to result from the fragmentation of incoming particles, whereas at larger s and p_T, p and $\bar{p}$ tend to be produced in equal numbers as expected in the central collisions.

A turnover is observed in the invariant inclusive p_T-distributions at low p_T for pions which is consistent with a p_T dependence proportional to $\exp(-Bm_T)$ with B=7.1 GeV^{-1} for π^+ and B=7.2 GeV^{-1} for π^-, where m_T is transverse mass ($m_T^2 = p_T^2 + m^2$). The same tendency to flatten off is found for K^+(B=6.6 GeV^{-1}) and K^-(B=7.09 GeV^{-1}), but it is not apparent for p and $\bar{p}$ data.

The significant violation of scaling at x=0 in available energy range may imply either an unlimited increase of invariant inclusive cross section with s as predicted by some theoretical models/64/, or an asymptotically constant cross section. The latter alternative is advocated in the framework of the double-Regge expansion/65,66/, represented graphically in fig.22,

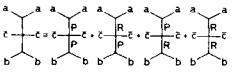

Fig.22. The double-Regge expansion diagram for inclusive reaction a+b → c+X in the central region. P and R are usual singularities with effective intercepts α_P=1 and α_R=1/2 .

which predicts

$$E\frac{d^3\sigma}{d^3p} = \beta_{PP}(m_T)+s^{-1/4}(\sum_R \beta_{RP}(m_T)e^{y/2} +$$

$$+\sum_R \beta_{PR}(m_T)e^{-y/2})+s^{-1/2}\sum_R \beta_{RR}(m_T) \qquad (2.3.1)$$

The assumption that the separate vertices $\beta_{ij}(m_T)$ are factorizeable gives

$$\beta_{ij}(m_T) = (-1)^{2(\alpha_i+\alpha_j)}\,\delta^a_i\,\delta^b_j\,\phi_{ij}(m_T), \qquad (2.3.2)$$

where the term $(-1)^{2(\alpha_i+\alpha_j)}$ is a conjecture, inspired by the rising cross sections in the central region/66/ (α_i, α_j are the intercepts

$\alpha_P(0)=1$ and $\alpha_R(0)=1/2$ of the Pomeron and Reggeon trajectories). The formulae (2.3.1) and (2.3.2) have several important implications. In particular they predict

i) the existence of the asymptotic plateau in rapidity distribution with the same height $(1/\sigma_T)Ed^3\sigma/d^3p = \phi_{pp}(m_T)$ for particle c and antiparticle $\bar{c}$;

ii) an energy dependence of the average multiplicity for the particles of type c

$$\langle n_c\rangle_{central} = a_c + b_c \ln s + \frac{c_c}{\sqrt{s}} + \frac{d_c \ln s}{\sqrt{s}} \qquad (2.3.3)$$

$$\text{with} \quad b_c = \frac{1}{\sigma_T^{\infty}} \int E^* \frac{d^2\sigma}{dp_L^* dp_T^2} dp_T^2 \Big|_{p_L^*=0} = \pi \int \phi_{pp}(m_T) dm_T^2 \qquad (2.3.4)$$

Besides, the expression (2.3.1) relates the energy dependence of inclusive cross section to the shape of rapidity distributions at different energies and through the expression (2.3.2) one is able to relate the inclusive spectra of particle c produced by different incident particles. It has been shown[66-68] that this approach describes the energy dependence of inclusive cross sections and the shape of rapidity distributions in the central region for a number of inclusive reactions. The important result is that the values of the vertex functions β_{RR} and β_{PP} in (2.3.1) are about the same. Therefore one can not neglect the last term when the low energy data are included in the analysis of the energy dependence of inclusive cross sections in the central region.

The compilation of the available high energy data pertaining to the energy dependence of $\pi^{\pm}$ production in the central region is presented in fig.23. The present situation is somewhat different from that expected several years ago[70] (dashed line in fig.23 with b_c = =0.78). The scaling is not yet reached at highest ISR energies. But the data suggest that a scaling limit may exist, that it is being approached from below and that factorization may eventually hold. The double-Regge formalism reproduces the trend of the data up to the highest ISR energies.

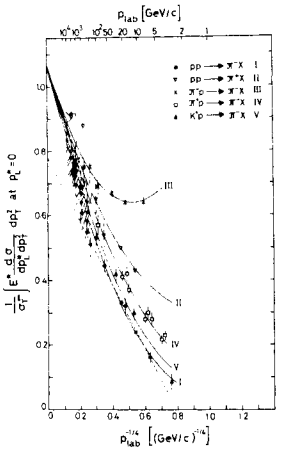

Fig.23. Energy dependence of the invariant inclusive cross sections of $\pi^{\pm}$ in the central region (compilation of published data; new data: $pp \to \pi^{\pm}$ at $\sqrt{s}$=23,31,45,53 and 63 GeV[61]). The curves are the results of the double-Regge fit[66] in (s,m_T,y) space to $pp \to \pi^{\pm}$ data at 12 and 24 GeV/c[69].

The curves I and II in fig.23 represent the results of the fit[66] of formula (2.3.1) to the $pp \to \pi^{\pm}X$ data at 12 and 24 GeV/c in (s,y,m_T) space. The curves IV and V are obtained by using relation (2.3.2) with the values of $\delta_i^{\pi^+}$ and $\delta_i^{K^+}$ known from the analyses of the total cross sections. It is quite surprising that the double-Regge analysis at such low energies (which was made before the high energy data above 100 GeV/c were obtained) provides such promising description of data, apart from some discrepancies for $pp \to \pi^+X$ reaction. For reaction $\pi^-p \to \pi^-X$ with the strong leading particle effect the similar trend is obvious with increasing energy. The energy dependence is quite consistent with that predicted by the formula (2.3.1) when the value of b_c is fixed to be the same as for $pp \to \pi^{\pm}$ reactions (curve III in fig.23).

The situation with respect to an approach to scaling in the central region for $pp \to K_S^0X$ and $K^+p \to K_S^0X$ reactions is summarized in fig.24 .

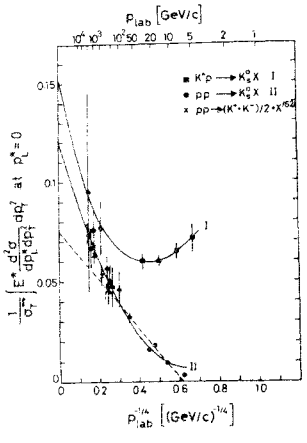

Fig.24.

Energy dependence of the invariant inclusive cross sections of K_s^o for pp and K^+p interactions in the central region (compilation of published data; new data: K^+p 32 GeV/c[25]; pp $\sqrt{s}$ = 23,31,45,53, 63 GeV[62]).

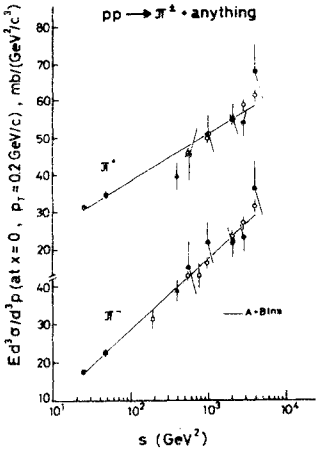

Fig.25.

Energy dependence of the invariant cross section for pp→π±X reactions at x=0 and p_T=0.2 GeV/c (from ref.[61]).

Again the energy dependence of inclusive cross sections for reaction pp → K_s^oX is consistent with the double-Regge picture. The same, with some reservation, can be said about K^+p → K_s^oX reaction, where the RR-term in (2.3.1) is responsible for the falling cross sections in the 5-16 GeV/c incident momentum range[68]. The cross section does not decrease any more between 16 and 32 GeV/c and the double-Regge fit made by the France-USSR and CERN-USSR Collaborations[25] for 5-32 GeV/c data predicts that the cross section should start rising at higher energies. The value of b_c = 0.152 ± 0.030 for this reaction is quite compatible with that for reaction pp → K_s^oX (fig.24). Therefore kaon production in the central region is also consistent with the factorization hypothesis.

Thus, although scaling in the central region is strongly violated at present energies, the available data seem to be consistent with the existence of the asymptotic limit as suggested in the framework of the double-Regge approach. However the compilation made by the British-Scandinavian-MIT Collaboration[61] warns us against possible preconception. The invariant cross sections for pp → π±X reactions at x=0 and p_T=0.2 GeV/c plotted versus s (fig.25), although consistent with double-Regge predictions, are compatible also with logs or A + Bs^{α} (α > 0) dependences, i.e with no scaling limit. More precise data are needed to clarify this picture.

In this respect, it is also of great interest to measure the multiplicity moments in the restricted region of the phase space and particularly in the pionization region. According to the theoretical predictions[71], the rise with energy of the moment $\langle n_c n_d \rangle$ for inclusive reaction a+b → c+d + anything may be as fast as $s/\ln^{\alpha} s$ (α > 0) in the pionization region. The studies of the associated multiplicities $\langle n(M_X^2) \rangle$ for a number of inclusive reactions a+b → c+X_M have shown that they behave differently in the fragmentation and central regions, exhibiting much steeper M_X^2-dependence in the central region[72-74].

The energy dependence of the inclusive cross sections in the central region (fig.23,24) and relations (2.3.3), (2.3.4) have very important implications for the energy dependence of total charged multiplicity, which should have the same form as (2.3.3) with the coefficient of the logs term entirely determined*)

---

*) The contribution of the fragmentation processes to the average charged particle multiplicity is $\langle n \rangle_{fragm.} = a + \frac{b}{\sqrt{s}}$.

by the central production. From the trend of the data (figs.23,24) it follows that the coefficient of the logs term in (2.3.3) for the average charged multiplicity $\langle n_{ch} \rangle$ is of the order 2.5, i.e higher than usually assumed. Therefore one should be careful in comparing the cosmic ray data on the multiplicities of secondary particles at 10^{12}- 10^{16} eV with the extrapolation of data at lower energies.

However, the data on extensive air showers seem to indicate even much faster growth of the multiplicities of secondary particles at cosmic ray energies[75]. Other data on cosmic rays presented at this conference[76-78] also indicate the deviation from scaling (for details, see ref.[79]). The evidence for deviation from scaling at cosmic ray energies is not, of course, surprising since the strong violation of scaling is already apparent at accelerator energies (figs.23-25). What is important is the degree of scaling violation which may be either compatible with the asymptotically constant cross-sections or imply an unlimited increase of cross sections. We wish to remind that the scale of energy in the central region is $\sqrt{s}$ as compared with s in the fragmentation region. Therefore one may expect quite new phenomena at much higher energies than available at present accelerators. The analysis of secondary cosmic ray propagation in the atmosphere indicates that this indeed happens at 10^{14}- 10^{16} eV. It is clear that the accelerators of new generation with energies $\gtrsim 2$ TeV and with the ISR's are very much needed for quantitative studies of all these interesting phenomena.

3. Inclusive resonance production

At present much attention is given to the study of inclusive resonance production. There are several reasons for this. The main one is the abundant production of resonances, which may account for a considerable fraction of the observed final state particles. Correlation effects in multipion production suggest that many pions result from the decay of higher mass clusters. There is increasing evidence that the observed short range correlations may in fact be due to the resonance production. Moreover the resonances, being the "parent particles", represent more of the primary production features than do the observed particles in which they decay. This is important for the test of various symmetry models and production models. The study of the spin density matrix of the resonance decay provides a unique information on the dynamics of production process. Finally, unexpectedly large direct lepton production measured in nucleon-nucleon interactions adds further interest to the study of meson resonances, which may account for at least a part of the observed effect.

3.1 Inclusive production of meson resonances

The energy dependence of the inclusive ρ^0 and f cross sections in hadron-hadron collisions is summarized in fig.26. Average multiplicity of the ρ^0 and the ratio $\langle n(\rho^0) \rangle / \langle n(\pi_c) \rangle$ are also shown. Following ref.[83] we define $\langle n(\pi_c) \rangle$ as the mean number of the "created π^-'s", in order to take into account the strong leading particle effect and the influence of the charge conservation: $\langle n(\pi_c) \rangle = \langle n(\pi^-) \rangle - 1$ for $\pi^- p$ interactions and $\langle n(\pi_c) \rangle = \langle n(\pi^-) \rangle$ for other interactions. The data show a clear rise of the $\sigma(\rho^0)$, $\sigma(f)$ and $\langle n(\rho^0) \rangle$ with increasing energy which is consistent with the ln s dependence. The lines drawn in fig.26 (a) and (b) through the experimental points

give

$\sigma(\rho^0)_{pp} \sim 2.41$ ns $\langle n(\rho^0)\rangle_{pp} \sim 0.081$ ns

$\sigma(\rho^0)_{\pi p} \sim 1.11$ ns $\langle n(\rho^0)\rangle_{\pi p} \sim 0.041$ ns

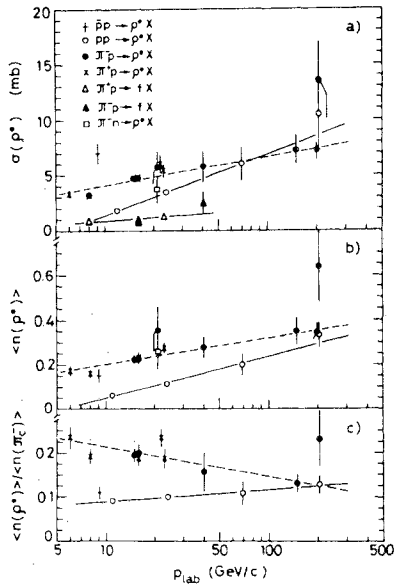

Fig.26. Energy dependence of the ρ^0 and f production (a) inclusive cross section of the ρ^0 and f as a function of p_{LAB}; (b) average multiplicity of the ρ^0 as a function of p_{LAB}; (c) ratio $\langle n(\rho^0)\rangle/\langle n(\pi_c^-)\rangle$ as a function of p_{LAB}; the lines are drown to guide the eye (the compilation of published data; new data: π^-p 200 GeV/c[80], 40 GeV/c[81], 21 GeV/c (π^-p and π^-n from π^-d data)[82], 16 GeV/c[83]; $\bar{p}$p 9.1 GeV/c[19]).

Thus there is a strong indication that the energy dependence of the ρ^0 production is about twice stronger for pp interactions in the energy range now available. We may attribute this feature to the strong leading particle effect in the charge exchange reactions $\pi^{\pm}p \to \rho^0 X$ (fig.27).

From the empirical fact that in the region of $x > 0.4$ the x-distributions for reactions $K^-p \to \bar{K}^{*0}(890)X$ and $\pi^-p \to \rho^0 X$ at 16 GeV/c almost coincide[83], it is reasonable to assume that the fragmentation component

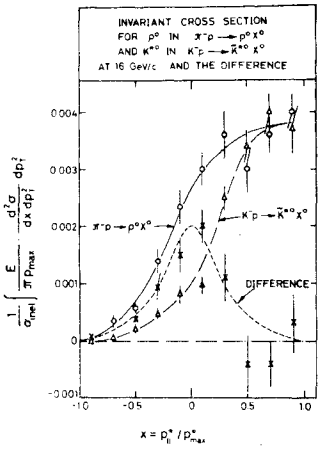

Fig.27. The invariant x distributions of ρ^0 in π^-p interactions and of $\bar{K}^{*0}(890)$ in K^-p interactions at 16 GeV/c and their difference (from ref.[83]).

of the ρ^0 production is equal to the total inclusive $\bar{K}^{*0}(890)$ cross section, since the $\bar{K}^{*0}(890)$ production is dominated by the beam fragmentation. Thus the central ρ^0 production can be evaluated by subtracting the $K^{*0}(890)$ distribution from that of ρ^0. The residual distribution (fig.27) has indeed the characteristics of the central component. From this procedure one may conclude that the fragmentation component of the ρ^0 production in π^-p interactions is dominant at low energies:

$\sigma_{fragm.}(\rho^0) = 3.1 \pm 0.3$ mb,

$\sigma_{centr.}(\rho^0) = 1.6 \pm 0.5$ mb[83]

We have seen earlier that for reactions $\pi^-p \to \pi^-X$ and $K^+p \to K^nX$ where the beam fragmentation is dominant, the energy dependence of the cross sections in the central region is quite different from other reactions (figs.23,24), although it tends to approach the same behaviour as the energy increases. There is a strong reason to believe that the same mechanism is responsible for energy dependence of the ρ^0 production observed in π^-p interactions. Moreover, one may assume that asymptotically, when $\sigma_{centr.}(\rho^0) \gg \sigma_{fragm.}(\rho^0)$ the energy dependence of the $\sigma(\rho^0)$ and $\langle n(\rho^0)\rangle$ in $\pi^{\pm}p$ interactions is the same as in pp interactions.

From these considerations it follows that the ratio $R = \langle n(\rho^0)\rangle / \langle n(\pi)\rangle$ should asymptotically be the same for pp and π^-p interactions and independent of energy. The accuracy of the data does not allow to decide, whether this asymptotic trend is established at present energies (fig.26(c)). The investigation of the energy dependence of the ratio R is crucial for the test of the quark models[84,85]. Anisovich and Shekter predict[84] that asymptotically $R_{\pi p} = R_{pp} = 0.18$ when the main contribution to the meson production comes from the central region. The data at low energies disagree with the equal values of $R_{\pi p}$ and R_{pp}, presumably due to the dominance of the beam fragmentation for reactions $\pi^{\pm}p \to \rho^0 X$. At the highest energies now available, $R_{\pi p} \approx R_{pp}$, but are smaller than predicted. To reduce the value of R in the above quark model one may introduce the short range correlations between constituent quarks (or partons). If the mesonic state of mass M is formed as a bound state of quark and antiquark (with masses m_1 and m_2), then the rapidity difference between them $\Delta y \sim \ln(M^2/(m_1 m_2))$. The probability to find such pair vanishes with the rapidity difference Δy as $\exp(-\alpha \Delta y)$, thus giving the factor $(M^2)^{-\alpha}$ of the SU(6) symmetry breaking. Such considerations[86] lead to the ratios $\rho/\pi = 0.07$, $K/\pi = 0.09$ and $K^*/\pi = 0.10$, if one assumes that $\alpha = 1$, as seems to follow from several theoretical considerations[52,53] (for details see section 2.1).

Fig.28 presents the compilation of data pertaining to the K*(890) production. The K*(890) cross section exhibits a significant rise for pp and πp interactions, but small variation, if any, in $K^{\pm}p$ interactions up to 32 GeV/c. The bulk of the K*(890) production in $K^{\pm}p$ collisions takes place at low

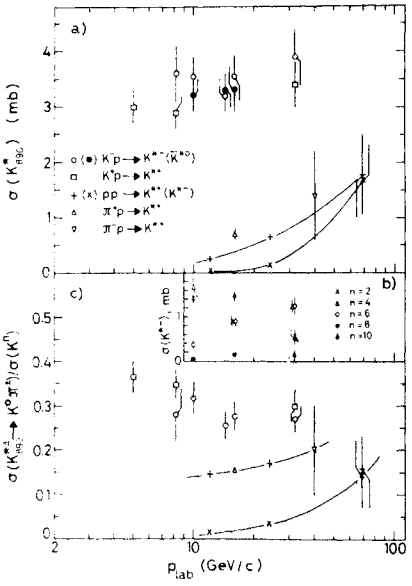

Fig.28. Energy dependence of the $K^*(890)$ production (a) inclusive cross section of the $K^*(890)$ as a function of p_{LAB} ; (c) fraction of the K^n mesons ($K^0 + \bar{K}^0$) coming from the $K^{*+}(890)$ or $\bar{K}^{*-}(890)$ decays in $K^{\pm}p$ interactions as a function of p_{LAB} ; insert (b) shows the p_{LAB} dependence of the $\bar{K}^{*-}(890)$ production in K^-p interactions for different final state multiplicities[87] (compilation of published data; new data: K^-p 32 GeV/c[87], 16 and 10 GeV/c[27]; K^+p 32, 8.2 and 5 GeV/c[88]; π^-p 40 GeV/c[81]).

multiplicity events, but the contribution of higher multiplicities increases with energy[27,87]. The $K^*(1420)$ production is small, amounting to about 10% of that of $K^*(890)$. About 50% of all neutral kaons are produced via the decays of $K^*(890)$'s. The K^n and $K^*(890)$ cross sections are larger in K^-p than in K^+p interactions, but their average multiplicities per inelastic event are approximately the same for K^+p and K^-p interactions (fig.29).

Basically the energy behaviour of the K^* cross sections and average multiplicities in $K^{\pm}p$ interactions is quite similar to that of the ρ^0 in $\pi^{\pm}p$ interactions in the same energy range, because masses of these mesons are

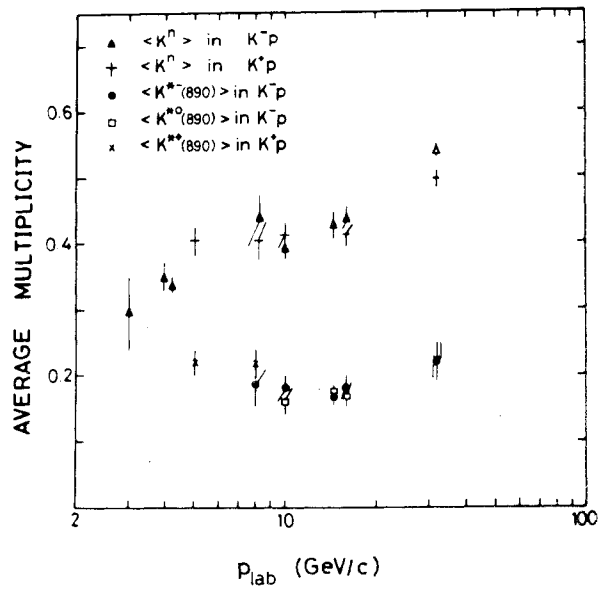

Fig.29. Average multiplicity of the K^n and $K^*(890)$ per inelastic event in K^+p and K^-p interactions (compilation of published data; new data: the same as in fig.28).

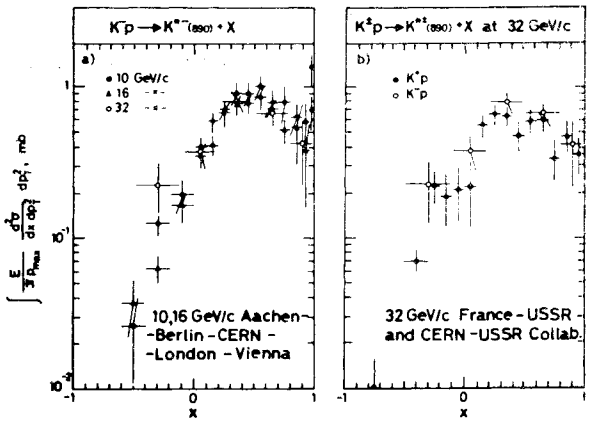

Fig.30. The invariant x distributions for $K^*(890)$ mesons produced in K^-p and K^+p interactions: (a) for reactions $K^-p \to \bar{K}^{*-}(890)X$ at 10, 16[27] and 32 GeV/c[87]; (b) for reactions $K^+p \to K^{*+}(890)X$ and $K^-p \to \bar{K}^{*-}(890)$ at 32 GeV/c[88,87].

comparable and both of them originate dominantly from the beam fragmentation. Indeed most of K^*'s are produced in the forward direction (fig.30), with no evidence for any significant production in the proton fragmentation region and presumably small central production. However, the data of the France-USSR and CERN-USSR Collaborations at 32 GeV/c suggest that the central $K^*(890)$ production has started to increase and would be much higher at the energies of the future BEBC experiments.

We may now compare the average ρ° and K^* multiplicities with the predictions of a "non-asymptotic" quark model[89], where an attempt has been made to improve the original quark model predictions[84], using the experimental information on the average particle multiplicities. The model predictions $\langle n(\rho^\circ)\rangle_{pp} = 0.30+0.15\ln(s/s_0)$, $\langle n(\rho^\circ)\rangle_{\pi p} = 0.45+0.15\ln(s/s_0)$ ($s_0 \approx 55$ GeV^2) are compared with the experimental data in Table 5.

Table 5

The comparison of the measured vector meson multiplicities in inelastic hadron collisions with the predictions of a "non-asymptotic" quark model[89]

Reaction	P_{LAB} GeV/c	Average multiplicity	
		experiment	prediction
$\pi^-p \to \rho^\circ X$	40[81]	0.25 ± 0.06	0.45
	147[90]	0.35 ± 0.06	0.67
	200[80]	0.35 ± 0.04	0.75
$pp \to \rho^\circ X$	69[12]	0.20 ± 0.05	0.30
	205[91]	0.33 ± 0.06	0.60
$K^+p \to K^{*+}_{890}X$	32[88]	0.224±0.026	0.41
$K^-p \to \bar{K}^{*-}_{890}X$	32[87]	0.22 ± 0.03	0.41

Since the $K^*(890)$ mesons in $K^\pm p$ interactions are dominantly produced in the fragmentation region, we compare their average multiplicities with the model predictions[89] in the fragmentation region. From Table 5 it is clear that the quark model disagrees with the experimental data at the highest available energies by a factor of 2.

The reaction $K^+p \to K^{*+}(890)$ and $K^-p \to \bar{K}^{*-}(890)X$ may proceed via I=0 and I=1 exchanges with both exchange particles π- B,

ρ - A_2 and ω - f. The spin density matrix elements of the K^* decay (Table 6) show an important contribution of pion exchange at 32 GeV/c, a fact already known at lower energies[92,93].

Table 6

K^*_{890} spin density matrix elements in $K^{\pm}p$ reactions at 32 GeV/c for $|t_{KK^*}| < 1 (GeV/c)^2$ and $(M_X^2/s) < 0.5$[87,88]

Reaction	ρ_{00}	ρ_{1-1}	$Re\rho_{10}$	$\frac{\rho_{00}+\rho_{11}-\rho_{1-1}}{\rho_{11}+\rho_{1-1}}$
$K^+p \to K^{*+}_{890} X$	0.45±0.08	-0.02±0.08	-0.03±0.07	2.9 ± 1.1
$K^-p \to K^{*-}_{890} X$	0.42±0.10	0.07±0.08	-0.07±0.06	1.8 ± 0.6

The ratio of unnatural $\sigma^- = \rho_{00} + \rho_{11} - \rho_{1-1}$ to natural $\sigma^+ = \rho_{11} + \rho_{1-1}$ parity exchange for both K^* helicities ($\lambda = 0$ and 1) implies a higher contribution of the unnatural parity exchange in the region of $|t_{KK^*}| < 1 (GeV/c)^2$ and $(M^2/s) < 0.5$, although an important part of the K^* production in both reactions proceeds through the natural parity exchange. Within the present accuracy, the inclusive x-distributions of K^*-mesons in K^+p and K^-p interactions are about the same in the shape (fig.30(b) and roughly are in the ratio of the total inelastic K^+p and K^-p cross sections.

In fig.31 and 32 the transverse momentum distributions of $\bar{K}^{*-}(890)$ produced in K^-p interactions and of ρ° and f mesons produced in $\pi^{\pm}p$ interactions are compared with the corresponding p_T^2-distributions of the neutral kaons and pions. We observe a well known fact that the p_T^2-distributions of meson resonances are roughly exponential in shape and have approximately equal slopes at similar energies. The low p_T steep peak for ρ° production in π^-p[83,94] and π^+p[95] interactions comes from the contributions of the quasi-two-body processes (it is not seen for ρ°'s produced

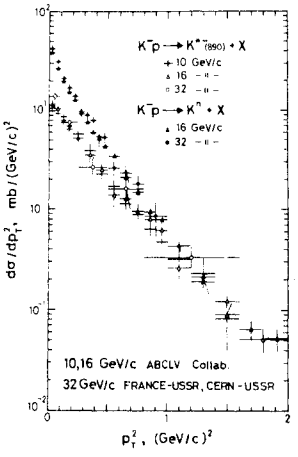

Fig.31. Inclusive p_T^2-distributions for neutral kaons in reaction $K^-p \to K^nX$ and for $\bar{K}^{*-}$'s in reaction $K^-p \to \bar{K}^{*-}(890)+X$ (data from refs.[27,87]).

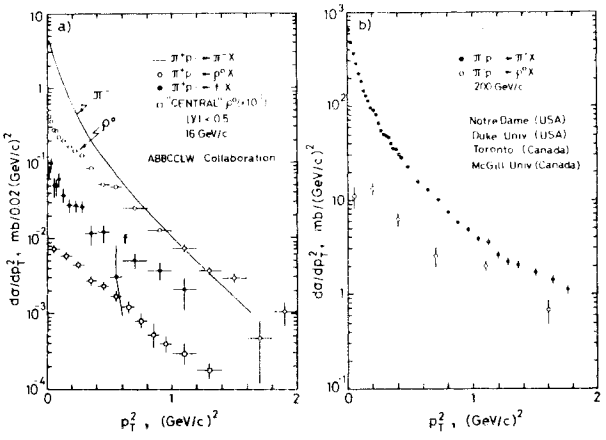

Fig.32. Inclusive p_T^2-distributions (a) for π^-'s, ρ°'s and f's in π^+p interactions at 16 GeV/c[94] and (b) for π^+'s and ρ°'s in π^-p interactions at 200 GeV/c[80].

in central region fig.32(a)) and disappears with the increasing energy (fig.32(b)). The ρ°/π and $K^*(890)/K^n$ ratios are quite small at low p_T^2 region but they are increasing to near unity as p_T^2 increases. This tendency is quite striking for 200 GeV/c where the ρ°/π^+ ratio is about 0.02 for the smallest values of p_T^2. This difference between the meson resonance transverse momentum spectrum and that of pions may be considered as a consequence of the decay kinematics, since many pions are likely to originate from the decays of resonances. It is beautifully demonstrated by the

ABBCCHW Collaboration[96]. The daughter pions originating from the decay of the ω and η resonances produced in a quasi-inclusive reactions

$$\pi^+p \rightarrow \omega + \text{charged particles} \qquad (3.1.1)$$

$$\pi^+p \rightarrow \eta + \text{charged particles} \qquad (3.1.2)$$

have much steeper p_T^2-distributions than the corresponding parents, while the p_T^2-distribution of π^-'s from the f decay is very similar to that of the f. The values of the exponential slopes of p_T^2-distributions for η, ω and ρ° in quasi-inclusive reactions are the same within errors, and the x-distributions for η and ω in reactions (3.1.1) and (3.1.2) are quite similar to the fully inclusive distributions for ρ°.

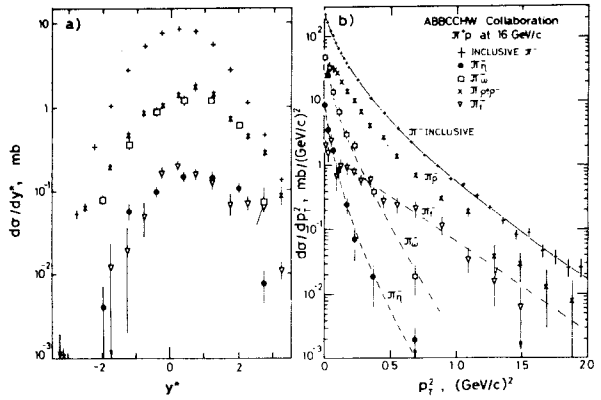

Fig.33. Comparison (a) of the c.m. rapidity distributions of π^-'s from the decays of the η, ω, ρ° and f and (b) of the p_T^2-distributions of π^-'s from the decays of the η, ω, $\rho^\circ+\rho^-$ and f with the corresponding distributions of the inclusive π^-'s in π^+p interactions at 16 GeV/c. The data are normalized to $\sigma(\eta)$ = 1.5 mb, $\sigma(\omega)$ = 4.0 mb, $\sigma(\rho^\circ)$ = 4.8 mb, $\sigma(\rho^-)$ = 1.6 mb and $\sigma(f)$ = 0.63 mb (from ref.[96]).

In fig.33 the c.m. rapidity distributions and p_T^2-distributions of the daughter pions from the η, ω, ρ and f decays are compared with one another and with that of the inclusive π^-'s.

From the comparison of the rapidity distributions one sees that the indirect pions account for a larger fraction of the inclusive pions in the beam fragmentation region than elsewhere. In the very low p_T^2 region the contribution of the pions from the ω decay seems to be dominant, while at the high p_T region the π^-'s from the ρ and f decay give the most important contribution.

These experimental observations and the analysis of the exclusive channels with η, ω and ρ° production have permitted to evaluate the inclusive yields of η, ω and ρ° in $\pi^\pm p$ interactions at 16 GeV/c[97]:

$$\eta : \omega : \rho^\circ = 0.34 : 0.9 : 1$$

with $\sigma(\rho^\circ) = 4.8 \pm 0.4$ mb, $\sigma(\omega) = 4.0 \pm 0.6$ mb and $\sigma(\eta) = 1.5 \pm 0.3$ mb. These estimates are in agreement with the values of $\omega/\rho^\circ = 1.0 \pm 0.2$ and 1.1 ± 0.2 obtained in pp interactions at 12 and 24 GeV/c[98] and the new results from the CERN ISR[99] for reaction pp → ppX (X = ρ, ω, f, A_2) in the restricted region of momentum transfers t_{pp1}, t_{pp2} and the rapidity of the central cluster $y_X < 0.8$:

$\sqrt{s}$ (GeV)	(ω/ρ)	$(\omega+\rho)/f$	(A_2/f)	$\langle -t \rangle$ (GeV^2)
4.9[98]	0.78 ± 0.13	3.3 ± 1.0	–	
6.9[98]	0.66 ± 0.13	0.89 ± 0.15	–	
23.5[99]	0.5 ± 0.25	1.1 ± 0.3	0.7 ± 0.2	0.22 ± 0.05
30.5[99]	0.8 ± 0.5	0.7 ± 0.3	0.8 ± 0.3	0.30 ± 0.07

The ABBCCLVW data[97] also support the results from the CERN ISR, showing the substantial amount of the η production at large transverse momenta[100]. Thus pions from the decays of ρ, ω, η and f alone ($\sigma(f)$=0.63 mb) account for nearly 46% of all pions produced in $\pi^\pm p$ interactions at 16 GeV/c and this fraction is consistent with being stable in a broad energy range.

The η', ϕ production is suppressed at least at low energy experiments. The inclusive ϕ production amounts to $\sigma(\phi) = 158 \pm 35\,\mu$b with $\phi/\rho^\circ = 0.045 \pm 0.012$ in pp interactions at

24 GeV/c[8,10]. In π^+p interactions at 16 GeV/c, $\phi/\rho^\circ \lesssim 2.5\%$ and $\eta'/\eta \approx (5\text{-}10)\%$[97]. The measurement of the ϕ production in π^-Be and K$^-$Be experiments at 43 GeV/c in Serpukhov[102] by the studying of dimuon $\mu^+\mu^-$ spectra has revealed no ϕ signal in π^-Be interactions, but a very clean ϕ meson signal in K$^-$Be interactions (fig.34) with $\sigma(K^-Be \to \phi X) = 2.0 \pm 0.5$ mb/nucleus for $x \geq 0.4$. This gives $\sigma(K^-N \to \phi X) = 0.43 \pm 0.11$ mb for $x \geq 0.4$, if one assumes the $A^{2/3}$ dependence of the ϕ production on nucleus. The ratio of the cross sections for ϕ meson production in π^-Be and K$^-$Be interactions is $(2.1 \pm 1.1)10^{-2}$ for $x \geq 0.4$.

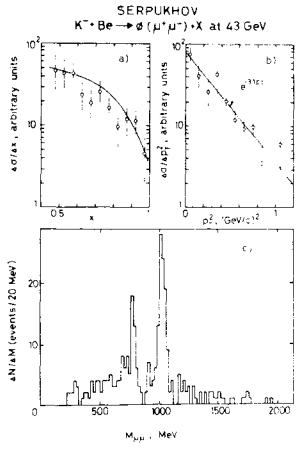

Fig.34. Mass spectrum for dimuons produced in K$^-$Be interactions at 43 GeV/c and the x and p_T^2-distributions of the ϕ meson (from ref.[101]); the lines in (a) and (b) represent the fits to the (1-x) and $\exp(-Bp_T^2)$ dependences, respectively.

The x-distribution of ϕ-meson (fig.34(a)) is well described by the 1-x dependence as it follows from the Drell-Yan mechanism described above and the dimensional counting[103]. The similar $(1-x)^n$ dependence for spectra of the ρ, ω and ψ is observed by the Boston group[104] in πFe and pFe interactions at 200 and 240 GeV/c. As expected, n=3 and n=1 for $x > 0.5$ in pFe and πFe collisions, respectively.

The suppression of the ϕ production in πp and pp collisions may be a consequence of Zweig's rule, which states that the two quarks in a meson do not annihilate and the production and decay take place by connected quark diagrams. The applicability of Zweig's rule has been established in a study of the ϕ production in reactions $\bar{p}p \to K^+K^-K^+K^-$ and $\bar{p}p \to K^+K^-\pi^+\pi^-$ at 3.6 GeV/c[105]. In reactions $K^-p \to K^-\omega p$ and $K^-p \to K^-\phi p$ at 14.3 GeV/c[106], the absence of events with low $p\phi$ masses in comparison with low mass enhancement in the $p\omega$ mass spectrum is also a direct consequence of Zweig's rule. The similar conclusion has been made in the study of ϕ and ω production in exclusive reactions in πp, Kp and pp interactions at 10 GeV/c[107]. Thus there is a peculiar situation when the Zweig rule is operative in exclusive reactions, but does not hold good in the case of inclusive ϕ production in pp collisions at 24 GeV/c[101]. In the latter experiment the ϕ production in association with an additional pair of strange particles is found to be less strong than the production via the nonstrange component. An interesting suggestion to explain this descrepancy has been made in two papers contributed to this conference[108,109], where one uses a simple ϕ-ψ analogy to postulate a possible existence of the new excited state $P_\lambda^* \to \phi_\chi$.

The suppression of the ϕ and η' production represents still another serious problem for the simple quark models[84,85] as seen from the the comparison of the model predictions with the results of the π^+p experiments at 16 GeV/c[94] (Table 7).

Table 7

Ratios of the inclusive cross sections of non-strange mesons in π^+p interactions at 16 GeV/c[94] and the predictions of a simple quark model[84]

Ratio	Prediction	Experiment
ω/ρ°	1	1
η/ω	11/81	0.39 ± 0.03
ϕ/ρ°	1/9	0.025
η'/η	19/11	0.05 - 0.10
π_{DIR}/π_{ALL}	1/14	0.5

If one takes into account the suppression factor $(M^2)^{-1}$ for the meson of the mass M, discussed earlier with respect to analogy with the Drell-Yan mechanism, the situation improves, but only slightly.

Since the pions are frequently produced as the resonance decay products one should make a distinction between directly produced pions and those from the decay of other particles. The evaluation of fraction of the directly produced pions, π_{DIR}/π_{ALL}, obtained in above experiment[94] by summing up all the contributions to the total inclusive cross section for $\pi^+p \to \pi^- + X$ from the decays of the various known resonances (Table 7), is also incompatible with the quark model prediction. Another approach to evaluate the π_{DIR}/π_{ALL} ratio uses the fact, that the high p_T^2 region is dominated by the direct pion component. The data indicate that a ρ°/π_{DIR} ratio is about unity at $p_T > 1$ GeV/c for πp interactions at 16 GeV/c and slightly lower at 200 GeV/c (fig.32), thus leading to $\pi_{DIR}/\pi_{ALL} \approx 0.2\text{-}0.3$. The ratio $\rho^\circ/\pi_{DIR} \approx 3$ expected from the number of spin polarization states in quark models seems to be ruled out by the present data within a factor of 3-4. However, if the above ratio π_{DIR}/π_{ALL} is corrected for the contribution of π_{ρ° and π_f in the high p_T -region[96], then we obtain $\pi_{DIR}/\pi_{ALL} \approx 0.15$. This result is still incompatible with quark model predictions. It is also difficult to reconcile this very rough estimate with the value of $\pi_{DIR}/\pi_{ALL} \lesssim 0.5$ obtained by summing up the resonance contributions, if the baryon resonance production is not responsible for an appreciable fraction of indirect pions.

3.2 Inclusive production of baryon resonances

Most of available information on baryon resonance inclusive cross sections comes from the studies of the Δ^{++} and Δ° resonance production in bubble chamber experiments . Therefore the data are confined to the target fragmentation region, where the slow protons can be identified by ionization. The measurement of the inclusive $\Delta^{++}(1236)$ cross section is somewhat arbitrary since the Δ^{++} is a wide resonance and the different procedures are used for evaluation of the background. The overall features of the cross section dependence on energy are summarized in fig.35 .

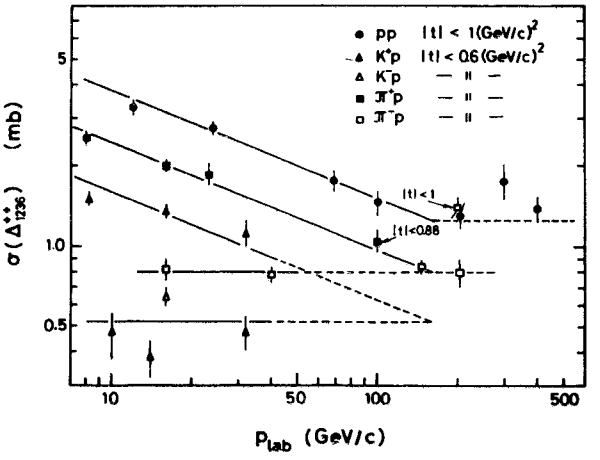

Fig.35. Inclusive $\Delta^{++}(1236)$ production cross section as a function of incident momentum. The Δ^{++} is defined in the $1.12 < M(p\pi^+) < 1.32$ GeV mass band (with some small deviations for some of the data) and for $|t|$-cuts indicated in the fig. The background is, however, evaluated by different methods in different experiments. The Breit-Wigner procedure is used to extract the Δ^{++} cross section in some experiments (compilation of published data; new data: π^-p 200 GeV/c[80], 147 GeV/c[110], 40 GeV/c[81], 16 GeV/c[111]; π^+p 16 GeV/c[111], K^-p 32 GeV/c[87], 16 GeV/c[111]).

For nonexotic ($ab\bar{c}$) pp, π^+p and K^+p reactions, cross sections fall at low incident momenta with about the same rate. The ratios of the inclusive

cross sections for these reactions are compatible with the ratio of the corresponding total inelastic pp, π^+p and K^+p cross sections, thus supporting the factorization.

For pp collisions above 100 GeV/c, the energy dependence of the Δ^{++} production levels off at the value of $\sigma(\Delta^{++}) \approx 1.5$ mb. The study of the Δ^{++} production at the CERN ISR in the range $0 < p_T < 0.7$ GeV/c and $x > 0.6$ has shown[112] that the Δ^{++} cross section is essentially s-independent, $\sigma(\sqrt{s}=23\ \text{GeV})/\sigma(\sqrt{s} = 35\ \text{GeV}) = 1.03 \pm 0.03$, between center of mass energies $\sqrt{s}$ = 23 GeV and 35 GeV. In the restricted range of variables $(1.16 < M(p\pi^+) < 1.32$ GeV, $0.86 < x < 0.92$, $0.1 < -t < 0.5\ (\text{GeV/c})^2)$, the Δ^{++} production at $\sqrt{s}$ = 30.4 GeV in the same experiment is found to be consistent with the dominance of one--pion-exchange and particularly with the Chew--Low equation modified by the Dürr-Pilkuhn form factor. The integration of this equation over all variables yields an s-independent cross section $\sigma(\Delta^{++})$ = 4.5mb for production in both hemispheres. This result is not incompatible with the bubble chamber data above 100 GeV/c, where the application of t-cuts leads to underestimation of real cross sections.

For exotic π^-p and K^-p reactions one expects no energy dependence even at low energies. Within limited statistics the data are consistent with this assumption. This trend is clearly seen for π^-p collisions in a broad energy range (fig.35), where the data are obtained with a similar experimental technique. From the very rough comparison between the trend of data for nonexotic K^+p and π^+p reactions and approximately constant cross sections for exotic K^-p and π^-p reactions, it follows that the energy dependence for K^+p and π^+p reactions should start to level off at FNAL energies above 100 GeV/c, as it does for pp collisions. Of course, the real energy dependence of the Δ^{++} production in reactions initiated by different incident particles at high energy range may be quite different from that obtained by a simple extrapolation of the low energy data. It depends upon the leading exchange mechanisms.

The analyses of the Δ^{++} decay angular distributions and of the Δ^{++} spin matrix elements in a number of experiments have established a strong dominance of one-pion-exchange at low $|t|$-values even at the CERN-ISR energies. Extrapolation to the pion pole using the Chew-Low formula, applied to the reaction $pp \rightarrow \Delta^{++}(1236)X$ at $\sqrt{s}$=30.4 GeV[112], yields $\sigma_{tot}(\pi^-p)$ in the range between 21.1 ± 1.3 mb and 23.7 ± 0.5 mb which is in good agreement with the true value of 24.3 mb. The Chew-Low extrapolation to the pion pole or the application of the Reggeized one-pion-exchange model has permitted to obtain the total $K^\pm\pi^-$ and $\pi^+\pi^-$ cross sections (fig.36) from the studies of reactions $K^\pm p \rightarrow \Delta^{++}X$[113-115], $\pi^-p \rightarrow nX$[116] and $\pi^+n \rightarrow pX$[117].

The $\pi^+\pi^-$ total cross section is observed to fall rapidly from the resonance region to an asymptotic value of about 14-16 mb. The data are consistent with the factorization prediction $\sigma_t(\pi^+\pi^-) = \sigma_t(\pi^+p)\sigma_t(\pi^-p)/\sigma_t(pp)$. The $K^+\pi^-$ total cross section measured up to the c.m.energy 3.5 GeV seem to follow the same trend but still exceed slightly the factorization prediction in the energy range available. One may speculate that this is due to the existence of the numerous resonance states in the nonexotic $(K^+\pi^-)$ channel. The $K^-\pi^-$ total cross section, in the exotic $K^-\pi^-$ channel, is much smaller than the $K^+\pi^-$ cross section and tends to the asymptotic limit from below. If this trend of the data indicated in fig.36 will persist at higher energies one may expect that the Δ^{++} production cross sections in the target fragmentation region will be

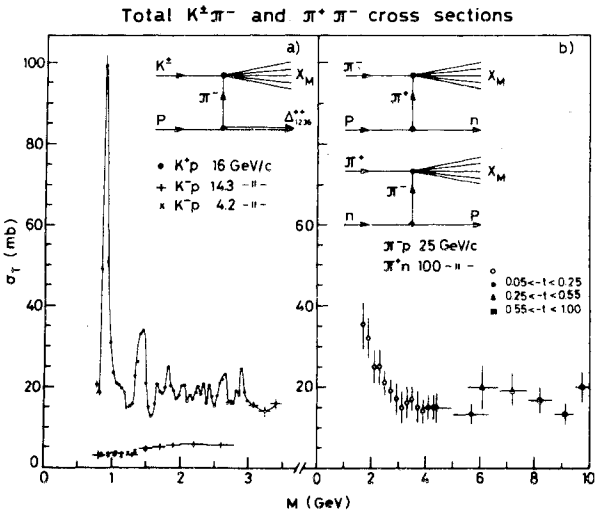

Fig.36. Total $K^+\pi^-$, $K^-\pi^-$ and $\pi^+\pi^-$ cross sections obtained from the analysis of the reactions $K^\pm p \to \Delta^{++}X$, $\pi^- p \to nX$ and $\pi^+ n \to pX$ as a function of X mass (i.e.energy of $K\pi$, $\pi\pi$ systems in their rest frame); the data from ref./113-117/.

equal for K^+p and K^-p and for π^+p and π^-p interactions, respectively, with

$$\sigma_{\Delta^{++}}(pp):\sigma_{\Delta^{++}}(\pi p):\sigma_{\Delta^{++}}(Kp)=\sigma_t(\pi p):\sigma_t(\pi\pi):\sigma_t(K\pi)$$

However the contribution of other isotopic one exchange particles (ϱ,A_2), which could mediate these reactions, and the interference between possible exchanges may eventually lead to a quite different results for all t-region. Besides, the important part of the Δ^{++} cross section comes from the production and subsequent decay of the diffractive systems $p\pi^+\pi^-$ where the triple-Pomeron coupling and factorization of the Pomeron should give somewhat different predictions.

Very little information is available about the Δ° inclusive production. We know that the production of low mass $p\pi^+$ and $p\pi^-$ systems is strongly correlated by the diffractive production of $p\pi^+\pi^-$. Since this diffractive system is generally assumed to be an isospin 1/2 state, there are nine times more $\Delta^{++} \to p\pi^+$ than $\Delta^\circ \to p\pi^-$. This explains the large background under the Δ° peak and makes difficult the study of the Δ° production. However, contrary to what is often stated, I would like to stress that the Δ° inclusive cross section may be quite higher than the value of 1/9 from the Δ^{++} cross section, since the diffractive production of the $p\pi^+\pi^-$ state with I=1/2 is not the unique mechanism of the Δ° production at least at present energies. Specifically in the low |t|-region, where the pion exchange dominates one has the following relations:

$$\frac{\sigma(pp \to \Delta^\circ X)}{\sigma(pp \to \Delta^{++}X)} = \frac{\sigma(\pi^+ p)}{3\sigma(\pi^- p)} \qquad (3.2.1)$$

$$\frac{\sigma(\pi^\pm p \to \Delta^\circ X)}{\sigma(\pi^\pm p \quad \Delta^{++}X)} = \frac{\sigma(\pi^\pm\pi^+)}{3\sigma(\pi^\pm\pi^-)} \qquad (3.2.2)$$

$$\frac{\sigma(K^\pm p \to \Delta^\circ X)}{\sigma(K^\pm p \to \Delta^{++}X)} = \frac{\sigma(K^\pm\pi^+)}{3\sigma(K^\pm\pi^-)} \qquad (3.2.3)$$

Just for example, the Δ inclusive cross sections are found to be equal to $700\pm100\,\mu b$ for reaction $K^-p \to \Delta^{++}X$ and to $985\pm180\,\mu b$ for reaction $K^-p \to \Delta^\circ X$ at 14.3 GeV/c high statistics experiment/118/. In the same experiment the ratio (3.2.3) for K^-p reaction as well as the ratio $\sigma(K^+p \to \Delta^{++}X)/\sigma(K^-p \to \Delta^\circ X)$ which should be equal to 3 for any isospin 1 meson exchange, have been specifically tested and found to be compatible with the K^-p/113,118/ and K^+p/114,119/ data. Thus the production and decay of the Δ^{++} and Δ° resonances may account for considerable fraction of indirect pions produced in hadron-hadron interactions.

An interesting attempt to separate the Δ^{++} production over the entire kinematic region has been made by ABBCCHLVW Collaboration in $\pi^\pm p$ and K^-p experiments at 16 GeV/c/111/. Table 8 shows, that the total inclusive cross sections of $\Delta^{++}(1236)$ are almost twice as high as those obtained with a mass cut $1.12 < M(p\pi^+) < 1.34$GeV and $|t|<0.6(GeV/c)^2$ (shown in fig.35). The fraction of Δ^{++} production increases with increasing charged multiplicity and

Table 8

Δ^{++} production cross sections and the fraction of produced Δ^{++}'s per inelastic collision at 16 GeV/c for different charged multiplicities[111]

Reaction	σ_{inel} (mb)	Fraction (%)				
		inclusive	2prongs	4prongs	6prongs	8prongs
π^+p	3.39	17.2	6.1	19.6	21.9	23.4
π^-p	1.41	6.6	-	7.5	10.5	18.0
K^-p	1.23	4.4	-	7.7	12.0	13.3

a substantial part (45 + 49%) of the Δ^{++} cross section comes from topologies with more than four prongs.

Because of practical difficulties, there is almost no information about inclusive production of heavier N^{*}'s which presumably decay through a 3-body or cascade processes. Some new information is obtained on strange baryon $\Sigma^{\pm}(1385)$ production in K^-p collisions[57,87,120] (fig.37).

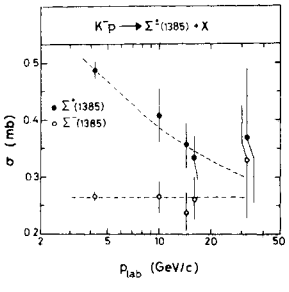

Fig.37. Inclusive $\Sigma^{\pm}(1385)$ production cross sections in K^-p interactions as a function of incident momentum (the data from refs.[57,87,120,121]); the lines are to guide the eye.

The decrease of the $\Sigma^+(1385)$ cross section with energy seems to be similar with that observed earlier for reaction $K^-p \rightarrow \Lambda X$ (fig.3). It is falling between 4.2 and 10 GeV/c but then shows the tendency to level off in the 10-32 GeV/c incident momentum range, where the Σ^+ cross section is quite close to the Σ^- cross section which is essentially energy independent. From the invariant x-distributions (fig.38), one sees that Σ^- is produced symmetrically about x=0, thus suggesting a predominance of the central production.

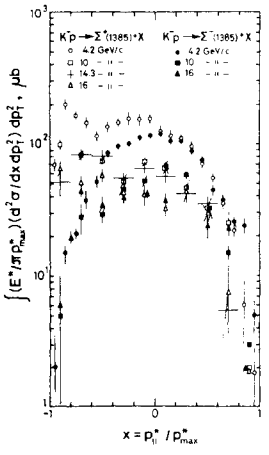

Fig.38 The invariant x-distributions for reaction $K^-p \rightarrow \Sigma^{\pm}(1385)X$ (the data from refs.[57,120,121]).

For each energy the Σ^+ and Σ^- distributions are the same in the forward direction, but there is a strong excess of Σ^+'s in the backward direction, which can be attributed to a quasi-two-body hypercharge exchange processes with a strong energy dependence. Indeed a triple-Regge analysis of the $\Sigma^+(1385)$ production at 4.2 GeV/c in proton fragmentation region, involving strangeness annihilation at the K^- vertex, has shown[57] that the Regge trajectory responsible for the strangeness annihilation process $K\bar{K} \rightarrow$ pions is consistent with the f'- ϕ trajectory.

The information provided by the weak Λ-decay in the two step sequence $\Sigma^+(1385) \rightarrow \pi^+(\Lambda \rightarrow p\pi^-)$ has been used by the Amsterdam-CERN-Nijmegen-Oxford Collaboration[57] for the reconstruction of the complete $\Sigma^+(1385)$ spin density matrix in the reaction $K^-p \rightarrow \Sigma^+(1385)X$ at 4.2 GeV/c. Although the errors in the polarization are large due to the uncertainties introduced by the appreciable amount of background, the conclusion is that the $\Sigma^+(1385)$ polarization in the region $|t'_{p\Sigma}| < 0.5 (GeV/c)^2$ is small and compatible with 0, which is in agreement with the predictions[122] of the additive quark model. These results are in remarkable contrast with the recent studies of the inclusive Λ production in reaction $K^-p \rightarrow \Lambda X$ where the existence of significant

polarization has been established (see[123] and references therein).

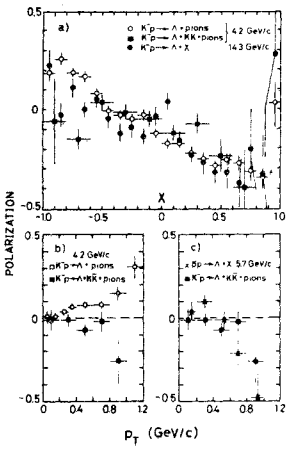

Fig.39. (a) Variation of the Λ polarization $P_\Lambda = \frac{3}{\alpha N} \sum_{i=1}^{N} \vec{q}_i \vec{n}_i$ (usual notations) with x for reactions $K^-p \to \Lambda$ + pions, $K^-p \to \Lambda KK$ + pions at 4.2 GeV/c[123] and $K^-p \to \Lambda$ + anything at 14.3 GeV/c[124]; (b,c) Λ polarization for reactions $K^-p \to \Lambda$ + pions, $K^-p \to \Lambda + K\bar{K}$ + pions at 4.2 GeV/c and for $\bar{p}p \to \Lambda$ + X at 5.7 GeV/c in the region $-1 < x < -0.2$ as a function of p_T.

Fig.39(a) shows that the Λ polarization in the region $x < -0.5$ exhibits different behaviour for the reactions

$$K^-p \to \Lambda + \text{pions} \qquad (3.2.4)$$

$$K^-p \to \Lambda + K\bar{K} + \text{pions} \qquad (3.2.5)$$

It is positive for reaction (3.2.4), while it is slightly negative for reaction (3.2.5). For events in the target fragmentation region ($-1 < x < -0.2$), a striking difference in the P_Λ with increasing p_T is seen for these two reactions in fig.39(b), whereas the P_Λ for strangeness nonannihilation process (3.2.5) and for $\bar{p}p$ reaction $\bar{p}p \to \Lambda$ + X have a similar dependence (fig.39(c)). The small magnitude of the Λ polarization in proton fragmentation region for $\bar{p}p$ interactions and for K^-p interactions with the off-mass-shell strangeness nonannihilation process $K\bar{K} \to K\bar{K}$ + pions might indicate that the above two processes are dominated by the Pomeron exchange.

4. Two-particle correlations

Many conclusions on the status of two-particle correlations in rapidity space are now completely different from those made at the time of the Aix-en-Provence and London conference. The importance of presenting results in terms of semi-inclusive correlations (shown by the bubble chamber experiments in Serpukhov and Fermilab), of discriminating between particles of different charges and of collecting the reasonable statistics is well understood now and it explains the drop in flow of experimental (but not theoretical) information on this subject.

A simple independent cluster emission model still describes the most salient features of the data. But there is increasing evidence that the copious resonance production may explain to a large extent the short-range effects observed in two-particle correlations. From my personal point of view some of the most significant evidence for such interpretation comes from the stable structure of events in a broad energy range.

Thus the Saclay-Ecole Polytechnique--Rutherford Collaboration[125] has found a striking similarity between the diffractive excitation systems $N \to N\pi$, $N \to N\pi\pi$ and $N \to \Lambda K$ induced by K^- mesons at 14.3 GeV/c and protons at ISR energies.

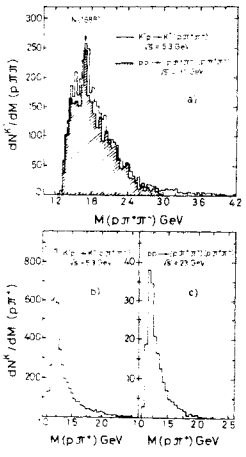

Fig.40. Comparison of $p \to p\pi^+\pi^-$ fragmentation systems in single dissociation process $K^-p \to K^-(p\pi^+\pi^-)$ at 14.3 GeV/c and in double dissociation reaction $pp \to (p\pi^+\pi^-)(p\pi^+\pi^-)$ at ≈500 GeV/c: (a) $p\pi^+\pi^-$ mass spectra; (b) and (c) $p\pi^+$ subsystem mass spectra (arbitrary units in fig.(c)); from ref.[125].

As an example fig.40 shows that the shapes of the $p\pi^+\pi^-$ and $p\pi^+$ effective mass spectra in reactions $K^-p \to K^-(p\pi^+\pi^-)$ at 14.3 GeV/c and $pp \to (p\pi^+\pi^-)(p\pi^+\pi^-)$ at 500 GeV/c are practically the same, both for resonance components and for overall fragmentation background.

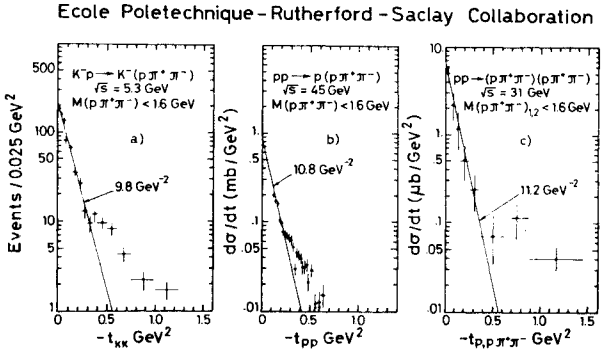

Fig.41. Comparison of production differential cross sections of the low mass diffractive $N\pi\pi$ systems (from re./125/).

The production differential cross sections for three sets of data (fig.41) display a similar behaviour with a break at $|t| \approx 0.3$ GeV^2 and relatively large slopes below the break. The similarities of the invariant mass distributions, decay angular distributions and differential cross sections at c.m.energies differing by an order of magnitude indicate a remarkable energy independence of the diffractive production dynamics over this broad energy range.

The small energy dependence of the correlation function $R(y_1, y_2)$ in the central region over a broad energy range is another important feature of data. The CERN-USSR and France-USSR Collaboration has shown/29/ that the behaviour of the semi-inclusive correlation function

$$G_n^{--}(y_1,y_2) = \left(\frac{d^2\sigma}{dy_1 dy_2}\right)_n - \frac{n-1}{n\sigma_n}\left(\frac{d\sigma}{dy_1}\right)_n\left(\frac{d\sigma}{dy_2}\right)_n$$

for reaction $K^+p \to \pi^-\pi^-X$ is quite similar between 12 and 32 GeV/c. In the study of the energy dependence of two-particle rapidity correlations in the central region for π^-p semi-inclusive reactions between 8 and 360GeV/c the NDDCIMM Collaboration/126/ has presented evidence that the central region correlation maximum grows as logs. The semi-inclusive (--) correlations are smaller and have less s dependence than those for the (+-) pairs, where the logs growth of semi-inclusive correlations is quite strong. The latter fact is consistent with the cluster emission phenomenology, but can be as well explained by the growth of the resonance production.

The only evidence against the resonance interpretation of correlations seems to be a somewhat higher average charged particle multiplicity of "cluster" $\langle k\rangle \approx 2\text{-}3$/127,128/. One should remember, however, that it is a model dependent value and other estimates give $\langle k\rangle \lesssim 2$ (for details see, for example/129/), which is not inconsistent with the resonance interpretation. Besides, the decay of baryon resonances of high masses may result in higher multiplicity of charged particles in a "cluster".

Following is a brief discussion of the experimental data on two-particle correlations presented to this conference, where the main emphasis is made on angular correlations, interference correlations between the like pions and on the spacial structure of interaction region (for more details see the mini-raporteur's talks of Kistenev and Podgoretsky at this conference).

4.1 Angular correlations

Azimuthal correlations are usually studied in terms of the asymmetry parameter $A = (N(\phi_T > \pi/2) - N(\phi_T < \pi/2))/(N(\phi_T > \pi/2) + N(\phi_T < \pi/2))$, where the ϕ_T is the azimuthal angle between the transverse momenta p_{T_1} and p_{T_2} of two particles. In Table 9 the experimental values of A for like and unlike pairs obtained in several experiments/130-133/ are shown.

Table 9

Asymmetry parameters A for like and unlike pion pairs

	$\bar{p}n$ /130/ (1-1.6) GeV/c	π^-p /131/ 11.2 GeV/c	π^-p /132/ 40 GeV/c	pp /133/ 102 GeV/c
$A_{LIKE(L)}$	0.182 ± 0.008	0.1074 ± 0.0008	0.062 ± 0.006	0.040 ± 0.010
$A_{UNLIKE(U)}$	0.335 ± 0.006	0.1764 ± 0.0008	0.106 ± 0.003	0.078 ± 0.010
$A_U - A_L$	0.153 ± 0.009	0.0690 ± 0.0011	0.044 ± 0.007	0.038 ± 0.01
$\frac{A_U - A_L}{A_U + A_L}$	0.296 ± 0.018	0.243 ± 0.004	0.262 ± 0.04	0.322 ± 0.08

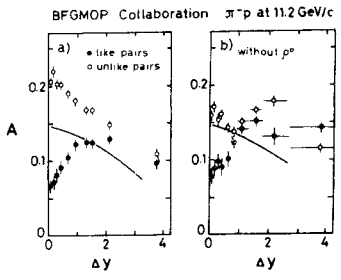

Fig.42. Azimuthal asymmetry parameters for like and unlike pairs in π^-p interactions at 11.2 GeV/c as a function of the rapidity difference $\Delta y = y_1 - y_2$; (a) for all events; (b) after removal of events with a $\pi^+\pi^-$ pair in the ρ° region (from ref./131/).

In fig.42 the parameters A_L, A_U in π^-p experiment at 11.2 GeV/c/131/ are presented as a function of the rapidity difference Δy and compared with the predictions of statistical model. We observe the following important facts. The high multiplicities of neutral particles at higher energies result in decrease of A_L, A_U and $A_U - A_L$ with increasing s, whereas the ratio $(A_U - A_L)/(A_U + A_L)$ is constant within errors. The difference between A_U and A_L is most significant for small rapidity difference. The asymmetry for unlike pairs tends to be compatible with statistical model predictions after removal of events in ρ° mass band, but persists for like pairs. Thus the rise of A_U at small Δy can be interpreted as a consequence of resonance decay, whereas the drop of A_L at small Δy seems to be due to Bose-Einstein symmetrization effect.

Since the resonance production influences the angular asymmetries, it is appropriate to investigate angular correlations between particles in terms of their effective mass M. Indeed, effect of different origins, such as resonances or Bose-Einstein statistics can contribute predominantly at $\Delta y = 0$, while with respect to M these mechanisms could be seperated.

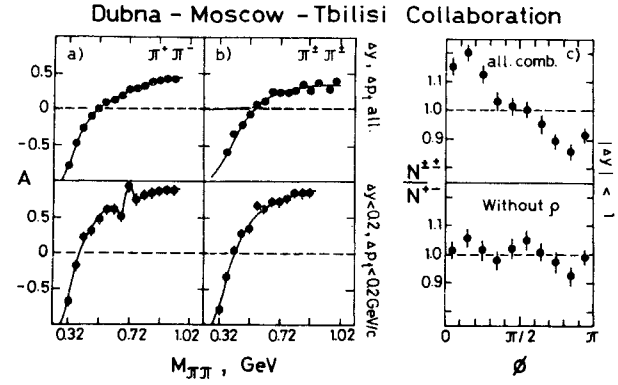

Fig.43. Azimuthal asymmetry parameter A for (a) $\pi^+\pi^-$ and (b) $\pi^\pm\pi^\pm$ pairs as a function of their effective mass M in π^-p interactions at 40 GeV/c; (c) the ratio of the azimuthal distributions for like and unlike pairs for all combinations and after removal of $\pi^+\pi^-$ pairs from the ρ° mass band (from ref./134/).

The Dubna-Moscow-Tbilisi Collaboration/134/ has studied asymmetry parameter A for $\pi^+\pi^-$, $\pi^\pm\pi^\pm$ pairs in π^-p interactions at 40 GeV/c as a function of their mass M (fig.43(a)). A sharp maximum is observed at $M = M_{\rho^\circ}$ for $\pi^+\pi^-$ pairs which is strongest at $\Delta y < 0.2$ and $\Delta p_T^2 < 0.2 (GeV/c)^2$. No difference is seen in the azimuthal distributions for like and unlike pairs (fig.43(c)), when the $\pi^+\pi^-$ pairs from ρ° mass band are removed from the data.

The detailed study of the angular correlations as functions of the effective mass has been made by the Aachen-Berlin-Bonn-CERN-Cracow--Heidelberg-Warsaw Collaboration/135/ in 4 and

6 prong events of π^+p interactions at 16 GeV/c. They present the results in terms of the opening angle ϕ between the three-momenta p_1 and p_2 of particles for pion-pion and proton-pion pairs, which is studied as a function of the two-particle mass M. The mean value of cos ϕ as a function of M for like and unlike charged pions is to a large extent determined by kinematics. However, an influence of the momentum configuration of resonance on the opening angle is striking when for pion pairs the difference

$$d_{\pi\pi}(M) = \langle\cos\phi^{\pi^+\pi^-}\rangle_M - \langle\cos\phi^{\pi^\pm\pi^\pm}\rangle_M$$

and for proton-pion pairs the difference

$$d_{p\pi}(M) = \langle\cos\phi^{p\pi^+}\rangle_M - \langle\cos\phi^{p\pi^-}\rangle_M$$

is studied as a function of M

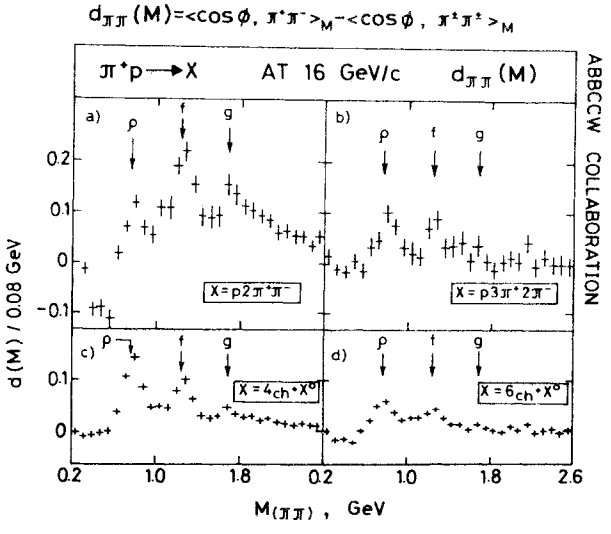

Fig.44. The distribution of the difference in the opening angle ϕ between the three momenta of particles for unlike and like pion pairs as a function of the effective mass M of the pair for (a) $p2\pi^+\pi^-$ final state, (b) $p3\pi^+2\pi^-$ final state, (c) 4-prong events, (d) 6-prong events in π^+p interactions at 16 GeV/c (from ref.[135]).

A clear structures with the resonance signals of ρ^0,f,g mesons (fig.44) and of the $\Delta^{++}(1236)$ and $\Delta^{++}(1890)$ (not shown) are visible. It is of great interest that resonances which are not (or just hardly) seen in the corresponding two-particle mass distributions, such as f,g, and $\Delta^{++}(1890)$, are observed more clearly in d(M) distributions. This is due to an increase of the $\langle\cos\phi\rangle$ caused by resonances, which increase the probability for the longitudinal momenta p_{L1} and p_{L2} to have the same sign and even more so if they are produced peripherally.

Thus it seems reasonable to conclude that the angular correlations are mainly of the kinematical origin. The difference between the like and unlike charged combinations outside the threshold region, where the interference effects could be essential, can be explained by the resonance production.

4.2 Space structure of events

Let us consider now the interference region near the threshold $M \approx 2m_\pi$. The interest to this region is motivated by the possibility to study the dimensions of the region from which pions are emitted. The first indication that it is possible to measure the space-time properties of the interaction region was observed in the angular clustering of identical pions (in terms of the opening angle ϕ) known as GGLP effect[136]. The measurement of the range of the Bose-Einstein correlations in units of pion Compton wave-length as formulated by GGLP has been attempted in π^-p experiment at 200 GeV/c[137]. It was shown that $\pi^+\pi^-$ correlations differ from the $\pi^-\pi^-$ correlations only at small values of $t_{12}=(p_1-p_2)^2$. This difference is accounted for if the range of the Bose-Einstein correlations $R = (1\pm0.25)$ fm.

More recently Kopylov and Podgoretsky[138] (see also[139,140]) have proposed to study the dimensions of the region from which pions are emitted by means of second order interference effects between identical pions. They argue that the interference between identical pions

is constructive at small values of the variables q_o and q_t defined as

$$q_o = E_1 - E_2 \quad \text{and} \quad q_t = \angle(\vec{p}_1 - \vec{p}_2)\times\vec{n},$$

where $\vec{n} = (\vec{p}_1+\vec{p}_2)/|\vec{p}_1+\vec{p}_2|$, ($q_t^2 \to M^2_{\pi\pi} - 4m^2_\pi$ at $q_o \to 0$). The interference effect is measured in terms of ratio

$$\frac{N_L}{N_B} = 1 + \frac{(2J_1(q_tR)/(q_tR))^2}{1 + (\tau q_o)^2}, \qquad (4.2.1)$$

where N_L is the number of pions of equal charge and N_B is background. This expression is obtained[138] in the framework of the statistical Pomeranchuk model, describing the emission of pions from massive point-like centers with the radius of the interaction region R and the lifetime of the pion source τ.

The existence of Kopylov-Podgoretsky effect is firmly established at several experiments[130,141-147]. In all of them (as for example is shown in fig.45) one observes a clear excess of like pion pairs at small values of q_t^2 and q_o, which decreases with increasing q_o and q_t^2 and finally disappears.

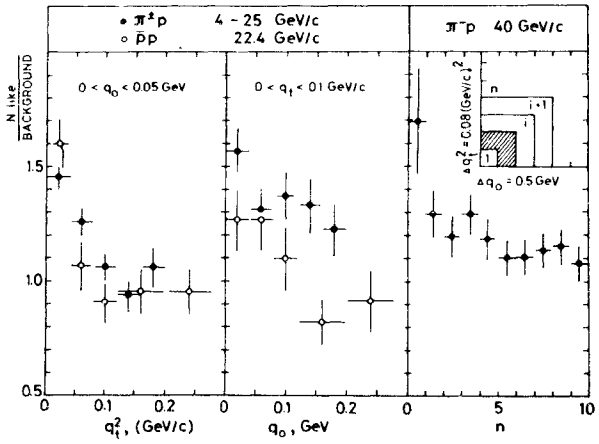

Fig.45. The ratio of the normalized q_t^2 and q_o spectra of like and unlike pions for two intervals of q_o and q_t, respectively, (from ref.[142,145,146]).

The effect of the ρ^o production on the q_t^2 and q_o distributions is negligible in the region of low q_t^2 and q_o, affecting the shape of q_t^2-distribution for unlike pion pairs only around $q_t^2 \approx 0.40(\text{GeV/c})^2$[130]. The estimates of the interaction radius R obtained in several experiments[130,141-147] are compiled in fig.46.

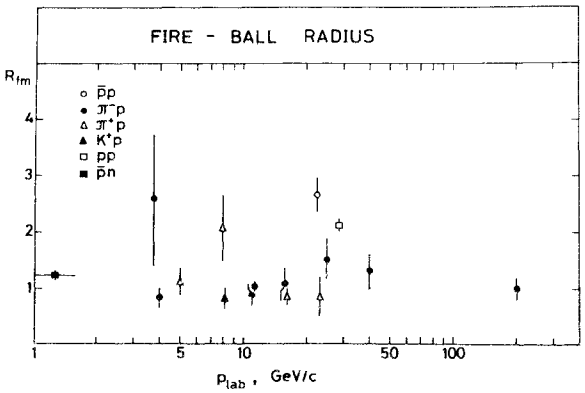

Fig.46. Energy dependence of the interaction (fair-ball) radius; (in refs.[130,141-147] it is obtained from the fits to the Kopylov-Podgoretsky formula (4.2.1), in ref.[137] (π^-p 200 GeV/c) as proposed by GGLP (see text))

R values for meson-proton interactions are all in good agreement, being consistent with the value of $R \approx 1$fm, which is quite close to the proton radius. The energy dependence seems to be small within present accuracy. However there is some indication that interaction radius may be different for different types of interaction. Characteristic emission time of the pion source was found to be small in all experiments. But while in some of them $c\tau < R$[142,144,147], in others $c\tau > R$[130,141,146]. This may suggest different interpretations of the parameter $c\tau$[138,140] (see also[148]).

Another possibility of studying the spacial structure of the interaction region has recently emerged from the impact parameter representation of inelastic reactions[149-152]. In the paper[153] the lower bounds b_L for the

root mean square impact parameters

$$\langle b^2 \rangle \geq b_L^2 = \langle \sum_i^n (x_i^2 - r_i^2)/(2p_i^{max2}) \rangle^2 / \langle \sum_{ij}^n x_i x_j \vec{r}_i \vec{r}_j \rangle$$

have been determined for annihilation, production and coherent $\bar{p}$ induced reactions in the 5-15 GeV/c incident momentum range ($\bar{p}p$ 5.7 GeV/c, $\bar{p}d$ 4.72 - 14.6 GeV/c). Here r_i is the transverse momentum of the i-th final-state particle with $x_i = p_i/p_i^{max}$, where p_i^{max} is the maximum allowed p_i value calculated for each kind of particle emitted in the studied reactions. The results indicate that at a given incident momentum, the b_L decreases with the number of final state particles for annihilation and production processes. For the coherent channel $\bar{p}d \rightarrow \bar{p}d\pi^+\pi^-$ the b_L decreases with increasing incident momentum as has already been observed[154] in the $pp \rightarrow pp\pi^+\pi^-$ and $\pi^-p \rightarrow \pi^-p\pi^+\pi^-$ reactions produced diffractively (fig.47).

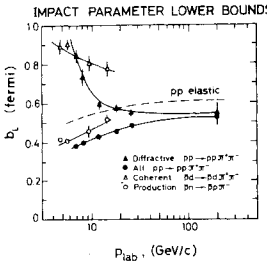

Fig.47. Impact parameter lower bounds b_L for $pp \rightarrow pp\pi^+\pi^-$, $\bar{p}d \rightarrow \bar{p}d\pi^+\pi^-$ and $\bar{p}n \rightarrow \bar{p}p\pi^-$ reactions as a function of incident momentum (data from refs.[153,154]).

The impact parameter bounds for coherent reactions were found to be about 2-3 times larger than for production reactions and even much larger (about 10 times) than for annihilation channels. Thus $\bar{p}p$ annihilation to mesons is more central than the production reactions. This conclusion is in accord with the earlier results[155] and seems to indicate that the simple interpretation of $\bar{p}p$ annihilation as responsible for difference between $\bar{p}p$ and pp interactions has to be abandoned, since elastic scattering data show that this difference is particularly peripheral in impact parameter.

The impact parameter language is intimately connected with the search of the planarity effects in the momentum space, i.e. the alignment of emitted particles in a preferred direction in the transverse plane containing the impact parameter vector. Several methods have been proposed to measure a degree of a possible alignment of the final particles in the transverse plane. In the framework recently developed by Counihan[156] one introduces the principal axis as the direction for which the sum of the squares of the transverse momenta is minimum. The principal axes are defined as the eigenvectors $\vec{z}^{(k)}$ of the matrix

$$Q^{\alpha\beta} = \sum_i^n p_i^\alpha p_i^\beta$$

where the sum includes all final state particles in the event and α and β denote the 3 components of the momentum $\vec{p}_i$. The eigenvalues $\lambda_k = \sum_i (\vec{p}_i \vec{z}^{(k)})^2$ describe the overall shape of the final state in momentum space and are ordered as $\lambda_1 > \lambda_2 > \lambda_3$. Thus defined principal axis system is shown in fig.48.

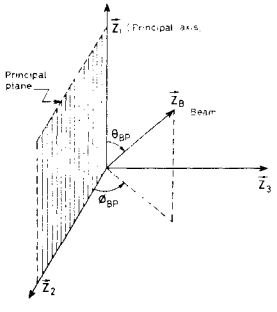

Fig.48. Definition of the principal axis system.

The France-USSR and CERN-USSR Collaborations[157] have indeed observed the alignment of the final state particles and the beam particle in the reactions $K^+p \rightarrow K^+p\pi^+\pi^-$ and $K^+p \rightarrow K^+p2\pi^+2\pi^-$ at 32 GeV/c in thus defined principal plane. The degree of this alignment seems to be higher than can be expected from the ordering relation ($\lambda_1 > \lambda_2 > \lambda_3$). Even more surprising is the

behaviour of the differential cross sections $d\sigma/d\cos\Theta_{BP}$ and $d\sigma/d\cos\alpha$ in these reactions (α is the generalized scattering angle, see [156]). They are consistent with exponential shape (fig.49) for $\cos\Theta_{BP} > 0.98$ and $\cos\alpha > 0.98$ with the values of the slope:

$B_\alpha = 205\pm10$ $B_\Theta = 204\pm10$ for $K^+p \to K^+p\pi^+\pi^-$

$B_\alpha = 175\pm25$ $B_\Theta = 168\pm24$ for $K^+p \to K^+p2\pi^+2\pi^-$

which are quite close to the corresponding value of the slope $B_{el} = 195\pm9$ in the exponential parametrization of the $d\sigma/d\cos\Theta$ distribution of elastic K^+p scattering at the same energy.

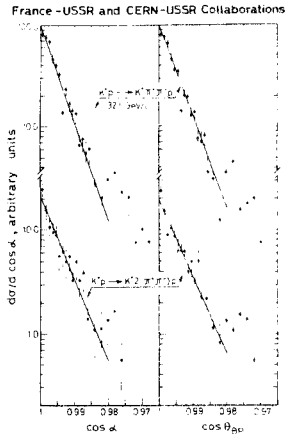

Fig.49. The $d\sigma/d\cos\Theta_{BP}$ and $d\sigma/d\cos\alpha$ distributions in the principal axis system for reactions $K^+p \to K^+p\pi^+\pi^-$ and $K^+p \to K^+p(2\pi^+)(2\pi^-)$ at 32 GeV/c (from ref. [157]. The scattering angle Θ_{BP} is defined in fig.48, the generalized scattering angle α is defined as the angle between the beam direction and the same direction rotated by the matrix $Q^{\alpha\beta}$.

This means that the description of multiparticle final states in principal axis variables is quite similar to that of elastic scattering. One might expect this for $K^+p \to K^+p\pi^+\pi^-$ reaction where the diffractive channels are dominant [158] (indeed, B_α is slightly higher than B_{el}, reflecting the well known fact that the slope of the differential cross section $d\sigma/dt$ is higher for diffractive system than for elastic scattering). However the nearness of B_{el} and B_α for 6 particle state is quite surprising and invites further investigations.

In closing I would like to make a point of some general conclusions which the above presentation leads us to draw.

5. Conclusions

1. Limiting fragmentation hypothesis as formulated by Yang and co-workers is compatible with the present trend of data at the highest accelerator energies within $\approx 10\%$ errors.

2. The Pomeron factorization seems to hold with the same accuracy at low momentum transfers. However for $-t > 0.5\,(GeV/c)^2$ pronounced breakdown in factorization is indicated between the elastic and inelastic diffraction cross sections.

3. The dramatic violation of scaling is firmly established in the central region. The accelerators of new generation with energies $\gtrsim 2$ TeV and with ISR's are very much needed to choose between two very important alternatives: the existence of asymptotic limit or unlimited rise of cross sections with energy.

4. There is a strong evidence that hadron-hadron reactions are dominated by resonance production. As a consequence the cluster and the short range order correlation effects may be to a large extent explained by resonance production.

Aknowledgements

The author is grateful to the organizing committee of the conference and to the scientific secretaries Drs. E.Kistenev, A.Likhoded, N.Melnikova and L.Tikhonova for their efficient help. He thanks in particular Dr.A.Likhoded for many useful discussions and suggestions.

It is a pleasure to aknowledge the help of Drs. L.Gerdyukov, O.Tchikilev and V.Uvarov in the compilation of data. The author would like to thank Mrs.G.Pavlovskay for efficient preparing of the drawings.

REFERENCES

1. A.A.Logunov, M.A.Mestvirishvili, Nguen Van Hieu, Phys.Letters 25B (1967) 611.
2. Yu.B.Bushnin et al, IHEP-CERN Collaboration, Phys.Letters 29B(1969) 506.
3. D.B.Smith, R.J.Sprafka, J.A.Anderson, Phys.Rev.Letters 23 (1969) 1064.
4. J.Benecke, T.T.Chan, C.N.Yang, E.Yen, Phys.Rev. 188 (1969) 2159.
5. R.P.Feynman, Phys.Rev.Letters 23 (1969)1415.
6. L.Foá, Physics Reports 22C (1975) N1.
7. K.Zalewski, Rapporteur's talk at the XVII-th International Conference on High Energy Physics, London (1974).
8. K.Böckmann, Rapporteur's talk at the Intern. Conf. on High Energy Physics, Palermo (1975).
9. N.A.McCubbin, Rapporteur's talk at the Intern. Conf. on High Energy Physics, Palermo (1975).
10. M.Boggild and T.Ferbel, Ann. Reviews of Nucl. Sci. 24 (1974).
11. J.Whitmore, Phys.Reports 10C (1974) 273.
12. V.V.Ammosov et al, IHEP Report M-26 (1976).
13. A.Sheng et al, Phys.Rev. D11 (1975) 17.
14. K.Yaeger et al, Phys.Rev. D11 (1975) 2405.
15. C.Cochet et al, France-USSR and CERN-USSR Collaboration, paper 1034 (A2-89).
16. J.Hanton et al, France-USSR, CERN-USSR Collaborations, paper 1035 (A2-90).
17. B.V.Batyunya et al, Alma-Ata-Dubna-Helsinki--Moscow-Prague-Kosice Collaboration, paper 159 (A2-11).
18. M.T.Regan et al, Liverpool-Stockholm Collaboration, paper 682 (A2-63).
19. P.S.Gregori et al, Liverpool-Stockholm Collaboration, paper 683 (A2-102).
20. N.S.Amaglobeli et al, Tbilisi-Dubna-Minsk Collaboration, paper 1078 (A2-122).
21. W.W.Neale, Invited talk at the Intern. Conference on High Energy Physics, Palermo (1975).
22. D.Bertrand et al, Brussels-CERN-London--Mons-Orsay Collaboration, paper 722(A2-67).
23. D.Bogert et al, FNAL-Florida Collaboration, paper 199(A2-33).
24. Yu.A.Budagov et al, Dubna-Tbilisi-Kosice--Erevan-Minsk Collaboration, paper 811(A2--82).
25. P.V.Chliapnikov et al, France-USSR, CERN--USSR Collaborations, paper 1167(A2-127).
26. P.V.Chliapnikov et al, Birmingham-Brussels--CERN-Mons Collaboration, paper 1060(A2-75).
27. H.G.Kirk et al, Aachen-Berlin-CERN-London--Vienna Collaboration, paper 695(A2-68).
28. B.Musgrave et al, Argonne-Brussels-Kansas--Michigan-Tufts Univ. Collaboration, paper 366(A2-59).
29. P.V.Chliapnikov, invited talk at the Intern. Conference on High Energy Physics, Palermo (1975).
30. A.Givernaud et al, France-USSR, CERN-USSR Collaborations, paper 1161(A1-10).
31. J.I.Arestov et al, France-USSR, CERN-USSR Collaborations, paper 207(A2-37).
32. R.Stroynowski, Rapporteur's talk at the VI Intern.Colloquium on Multiparticle Reactions, Oxford (1975).
33. T.Ferbel, Proceedings of the Summer Institute on Particle Physics, SLAS REPORT 179, v.II(1974),175.
34. J.Whitmore et al, Phys.Letters 60B(1976)211.
35. Chan Hong-Mo et al, Phys.Rev.Letters 26(1971)672.
36. H.I.Miettinen, Phys.Letters 38B(1972)431.
37. A.H.Mueller, Phys.Rev.D2(1970)2963.
38. O.V.Kancheli, JETP Letters 11(1970)397.
39. G.Ciapetti et al, Nucl.Phys. B89(1975)365.
40. R.Barloutaud, Invited talk at this conference.
41. E.W.Beier et al, Pennsylvania, paper 402(A2-58).
42. R.E.Hendrick et al, Phys.Rev. D11(1975)536.

43. R.K.Garnegie et al, SLAC, paper 289(A2-55).
44. W.Lockman et al, California-Saclay Collaboration, paper 1210 (A1-163).
45. J.Pumplin, Phys.Rev. D8(1973)2899.
46. A.A.Logunov et al, IHEP 74-66,Serpukhov (1974).
47. A.N.Tolstenkov, paper 791(A5-2).
48. P.V.Chliapnikov, IV Intern. Seminar on High Energy Physics Problems, Dubna(1975), 32.
49. P.V.Chliapnikov et al, Phys.Letters 60B (1976)218.
50. J.F.Gunion, Phys.Rev. D11(1975)1796; M.B.Green, M.Jacob, P.V.Landshoff, Nuovo Cimento 29A(1975)123.
51. A.K.Likhoded, A.N.Tolstenkov, IHEP 75-88 (1975) Serpukhov.
52. T.K.Gaisser, F.Halzen, Phys.Rev. D11 (1975)3157.
53. D.Silvers, ibid., 3253 and Nucl.Phys. B106 (1976)95.
54. A.M.Rossi et al, Nucl.Phys. B84(1975)269.
55. K.Blokzijl et al, Amsterdam-CERN-Nijmegen--Oxford Collaboration, paper 279(A2-78).
56. Amsterdam-CERN-Nijmegen-Oxford Collaboration, paper 276(A2-51).
57. Amsterdam-CERN-Nijmegen-Oxford Collaboration, paper 278(A2-52).
58. T.J.Devlin, paper 332(A2-57).
59. A.A.Logunov, L.D.Soloviev, A.N.Tavkhelidze, Phys.Letters 24B(1967)181; P.Freund, Phys.Rev.Letters 20(1968)235; H.Harary, Phys.Rev.Letters 20(1968)1395.
60. I.V.Ajinenko et al, Birmingham-Brussels--CERN-Mons-Serpukhov Collaboration, paper 200(A2-34).
61. K.Guettler et al, British-Scandinavian-MIT Collaboration, paper 114(A2-39).
62. K.Guettler et al, British-Scandinavian-MIT Collaboration, paper 1121(A2-113).
63. B.Apel et al, Nucl.Phys. B100(1975)237.
64. H.Cheng, T.T.Wu, Phys.Letters 45B(1973)367.
65. Chan Hong-Mo et al, Phys.Letters 40B(1972) 406.
66. M.N.Kobrinsky, A.K.Likhoded, A.N.Tolstenkov, Yad.Fiz. 20(1974)775; A.K.Likhoded, A.N.Tolstenkov, IHEP Preprint 74-51(1974).
67. R.Windmolders et al, Yad.Fiz. 22(1975)1014.
68. P.V.Chliapnikov et al, Nucl.Phys.B97(1975)1.
69. V.Blobel et al, Nucl.Phys. B69(1974)454.
70. T.Ferbel, Phys.Rev. D8(1973)2321.
71. V.V.Ezhela, A.A.Logunov, M.A.Mestvirishvili, IHEP 72-1(1971) Serpukhov.
72. P.V.Chliapnikov et al, Phys.Letters 52B (1974)375.
73. I.V.Ajinenko et al, IHEP Preprint M-30(1976) Serpukhov.
74. V.V.Babintsev et al, France-Soviet Union and CERN-Soviet Union Collaborations, paper 204 (A2-35).
75. T.Stewart et al, Durham-Lodz Collaboration, paper 194(A2-29).
76. S.N.Vernov et al, paper 778(A2-110).
77. V.P.Pavluchenko et al, paper 169(A2-2).
78. V.K.Budilov et al, "Pamir" Collaboration, paper 169(A2-1).
79. N.N.Roinishvili, minirapporteur's talk at this conference.
80. N.N.Biswas et al, Notre Dame-Duke Univ.--Toronto-McGill Univ. Collaboration, paper 1026(A2-87).
81. N.Angelov et al, Dubna 2 m Propane BC Collaboration, paper 868(A2-86)
82. R.E.Ansorge, Cambridge-Kracow-Warsaw and Davis-Kracow-Seattle-Warsaw Collaborations, paper 1003(A2-73).
83. J.Bartke et al, Aachen-Berlin-Bonn-CERN--Cracow-Heidelberg-Warsaw Collaboration, paper 196(A2-31).
84. V.V.Anisovich, V.M.Shekhter, Nucl.Phys.B55 (1973)455.
85. J.D.Bjorken, G.R.Farrar, Phys.Rev. D9(1974) 1449.
86. A.K.Likhoded et al, IHEP 76-2 Serpukhov (1976).

87. U.Gensch et al, France-USSR, CERN-USSR Collaborations, paper 206(A2-36).
88. M.De Beer et al, France-USSR, CERN-USSR Collaborations, paper 1168(A2-128).
89. V.V.Anisovich, M.N.Kobrinsky, V.I.Povsun, paper 85(A3-5).
90. D.Fong et al, Phys.Letters 60B(1975)124.
91. R.Singer et al, Phys.Letters 60B(1976)385.
92. P.V.Chliapnikov et al, Nucl.Phys. B37(1972) 336.
93. K.Paler et al, Nucl.Phys. B96(1975)1.
94. Aachen-Berlin-Bonn-CERN-Cracow-London--Vienna-Warsaw Collaboration, paper 663 (A2-105).
95. M.Deutschmann et al, Nucl.Phys.B103(1976)426
96. Aachen-Berlin-Bonn-CERN-Cracow-Heidelberg--Warsaw Collaboration, paper 664(A2-104).
97. Aachen-Berlin-Bonn-CERN-Cracow-London--Vienna-Warsaw Collaboration, paper 186 (A2-27).
98. V.Blobel et al, Phys.Letters 48B(1974)73; Nucl.Phys. B69(1974)237; Preprint Bonn HE 76-9(1976).
99. J.C.M.Armitage et al, CHM Collaboration, paper 347(A2-72).
100. F.W.Büsser et al, Phys.Letters 55B(1975)232
101. V.Blobel et al, Phys.Letters 59B (1975)88.
102. Yu.M.Antipov et al, IHEP 76-42 Serpukhov (1976).
103. V.Matveev, R.Muradyan, A.Tavkhelidze, Lett.Nuovo Cimento 7(1973)719.
104. M.L.Mallary et al, Northeastern Univ., paper 138(N1-18).
105. R.A.Donald et al, Phys.Letters 61B(1976)210
106. Rutherford-Ecole Polytechnique-Saclay Collaboration, paper 71(A1-70).
107. R.Baldi et al, Geneva Univ., paper 728 (A1-135).
108. V.G.Kartvelishvili et al, paper 631(N3-14)
109. S.D.Ellis, M.B.Einhorn, C.Quigg, paper 953 (N3-35).
110. D.Brick et al, 30-inch-bubble chamber--proportional-wire-chamber hybrid spectrometer Collaboration, paper 1050 (A2-88).
111. Aachen-Berlin-Bonn-CERN-Cracow-Heidelberg--London-Vienna-Warsaw Collaboration, paper 198(A2-32).
112. W.Lockman et al, Univ.California-Aachen--CERN Collaboration, paper 1201(A2-108).
113. M.Bardadin-Otwinowska et al, Nucl.Phys.B72 (1974)1.
114. P.V.Chliapnikov et al, Nucl.Phys. B91 (1975)413; Phys.Letters 55B(1975)237.
115. H.Voorthuis et al, Amsterdam-CERN-Nijmegen--Oxford Collaboration, paper 277(C3-24).
116. W.J.Robertson et al, Phys.Rev.D7(1973)2554.
117. J.Hanlon et al, FERMILAB-PUB-76/28-EXP (1976).
118. M.Bardadin-Otwinowska et al, paper submitted to the International Conf. on Elementary Particles, Palermo (Italy)1975.
119. P.V.Chliapnikov et al, Nucl.Phys. B105 (1976)510.
120. Aachen-Berlin-CERN-London-Vienna Collaboration, paper 144(A2-111).
121. M.Bardadin-Otwinowska et al, Nucl.Phys. B98(1975)418.
122. P.Gizbert-Studnicki, A.Golemo, Lett.al Nuovo Cimento IV(1970)473.
123. Amsterdam-CERN-Nijmegen-Oxford Collaboration, paper 272(A2-50).
124. H.Abramowicz et al, Nucl.Phys.B105(1976) 222.
125. D.Denegri et al, Saclay-Ecole Polytechnique--Rutherford Collaboration, paper 73(A1-72).
126. V.P.Kenney et al, Notre Dame-Durham-Canada--Iowa-Maryland-Michigan Collaboration, paper 1023(A2-103).
127. C.B.Chiu, K.-H.Wang, papers 357(A3-24) and 358(A3-25).
128. A.M.Gershkovich, I.M.Dremin, Reports on Physics, FIAN N1(1976)1.
129. P.Darriulat, Rapporteur's talk at the VI Intern. Colloquim on Multiparticle Reactions, Oxford(1975).

130. G.Borreani et al, Torino, paper 112(A2-66).
131. A.Quareni-Vigundelli et al, Bologna-Firenze-Genova-Milano-Oxford-Pavia Collaboration, paper 1202(A2-117).
132. Alma-Ata-Bucharest-Budapest-Cracow-Dubna-Hanoi-Moscow-Sofia-Tashkent-Tbilisi--Ulan Bator-Warsaw Collaboration, Phys. Letters 48B(1974)277; G.Ranft et al, Nucl.Phys. B86(1975)63.
133. G.Bromberg et al, Phys.Rev. D9(1974)3100.
134. N.Angelov et al, Dubna-Moscow-Tbilisi Collaboration, paper 205 (A2-6)
135. Aachen-Barlin-Bonn-CERN-Cracow-Heidelberg--Warsaw Collaboration, paper 1070(C2-53).
136. G.Goldhaber, S.Goldhaber, W.Lee, A.Pais. Phys.Rev.120(1960)300.
137. N.N.Biswas et al, Notre Dame-Duke Univ.--Toronto-Monreal Collaboration paper 1022 (A2-107).
138. G.I.Kopylov and M.I.Podgoretsky, Yad.Phys. 15(1972)392; 18(1973)656; 19(1974)434; G.I.Kopylov, Phys.Letters 50B(1974)472.
139. E.V.Shuryak, Phys.Letters 44B(1973)387.
140. G.Cocconi, Phys.Letters 49B(1974)459.
141. F.Grard et al, Nucl.Phys. B102(1976)221.
142. M.Deutschmann et al, Nucl.Phys.B103(1976) 198 and paper 197(A2-24).
143. J.Canter et al, Preprint BNL-20516(1975).
144. Y.D.Bayukov et al, Preprint ITEP(1976) Moscow.
145. N.Angelov et al, Dubna-Moscow-Tbilisi Collaboration, paper 205(A2-106).
146. V.V.Filippova et al, Alma Ata-Dubna--Helsinki-Kosice-Moscow-Prague Collaboration, paper 160(A2-10).
147. A.Calligarich et al, Pavia-Bologna-Firenze--Genova-Milano-Oxford Collaboration, paper 1090(A2-114).
148. G.I.Kopylov and M.I.Podgoretsky, paper 1007(A2-120).
149. V.G.Grishin, V.I.Ogievetski, Nucl.Phys.18 (1960)516.
150. M.I.Shirokov, JETP 42(1962)173.
151. A.A.Logunov, Nguen Van Hieu, Theor.Mat. Phys. 1(1969)375.
152. B.R.Webber, Phys.Letters 49B(1974)474.
153. H.Braun et al, Strasbourg, paper 377 (A2-109).
154. B.R.Webber, D.M.Chew, M.J.Counihan, H.Yuta, Nucl.Phys. B97(1975)317.
155. G.Warren et al, Nucl.Phys.B97(1975)381.
156. M.J.Counihan, Phys.Letters 59B(1975)367.
157. I.V.Ajinenko et al, France-USSR and CERN-USSR Collaborations, paper 1162 (A1-49).
158. J.Saudraix et al, France-USSR and CERN-USSR Collaborations, paper 1165 (A1-120).